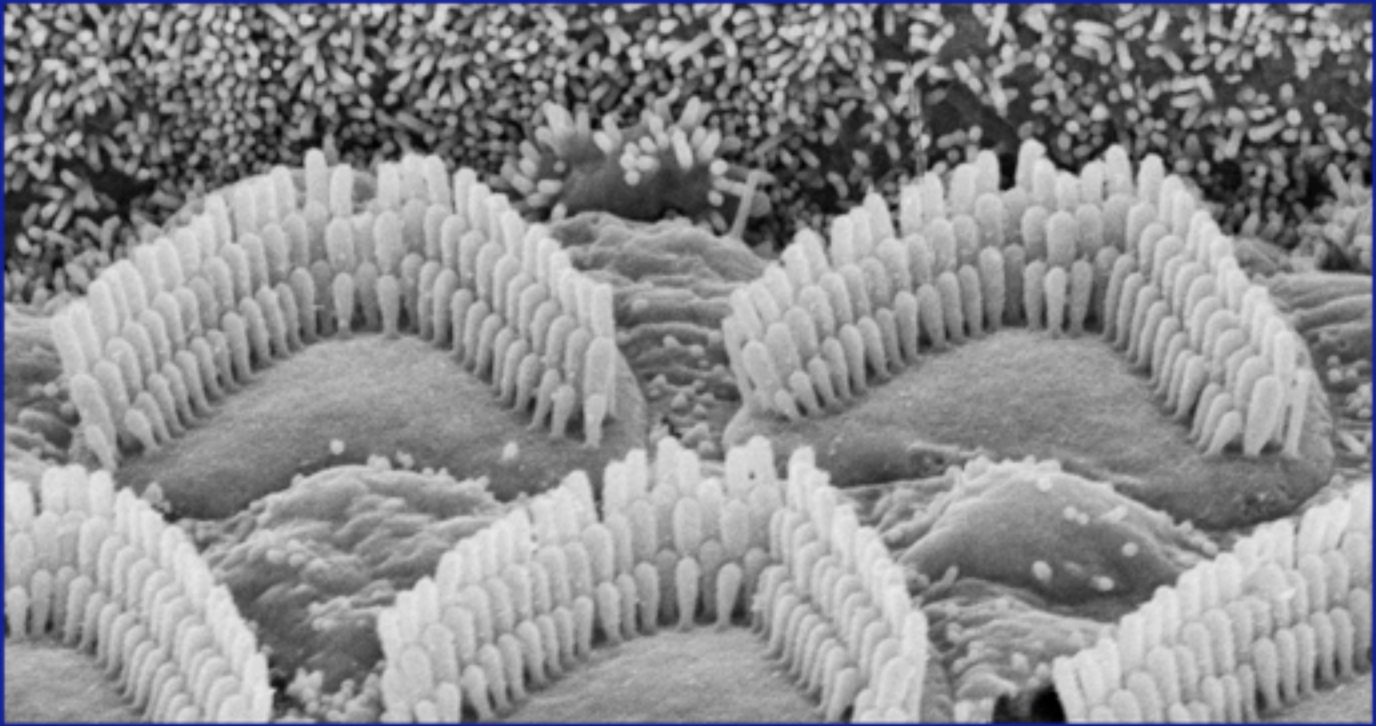

THE TRANSDUCTION CHANNEL

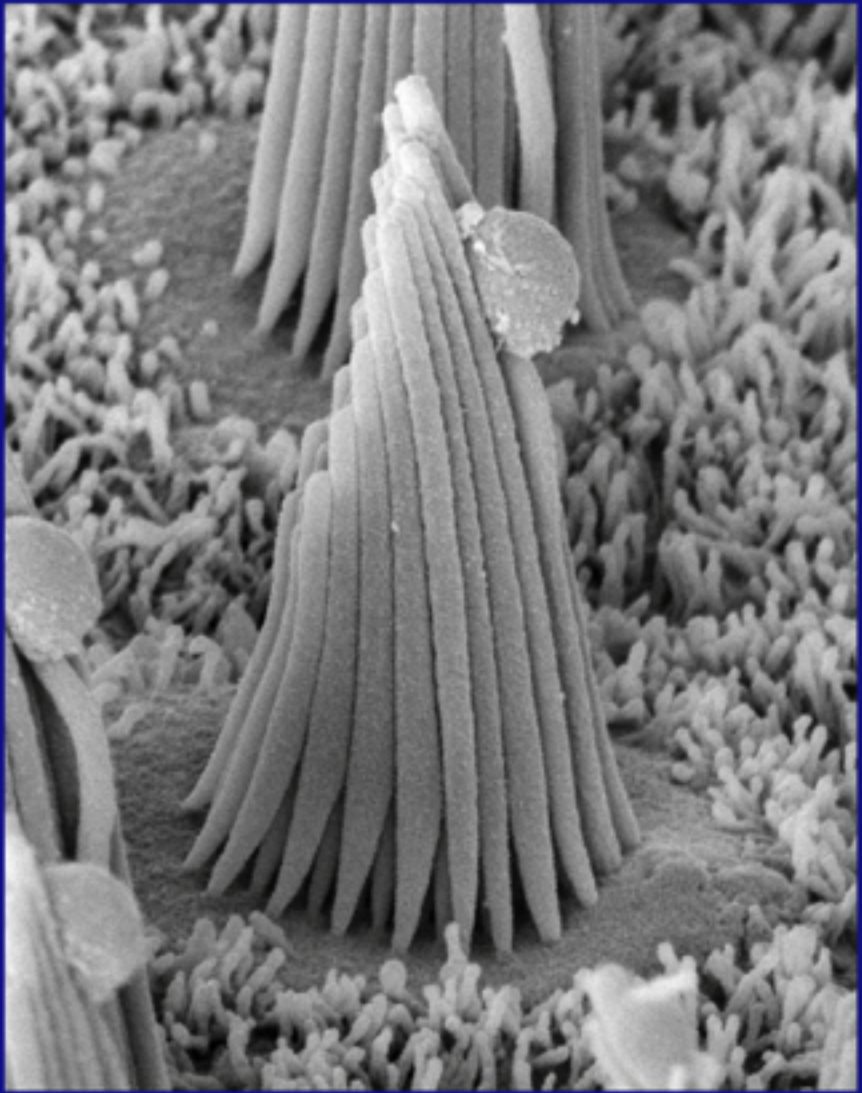

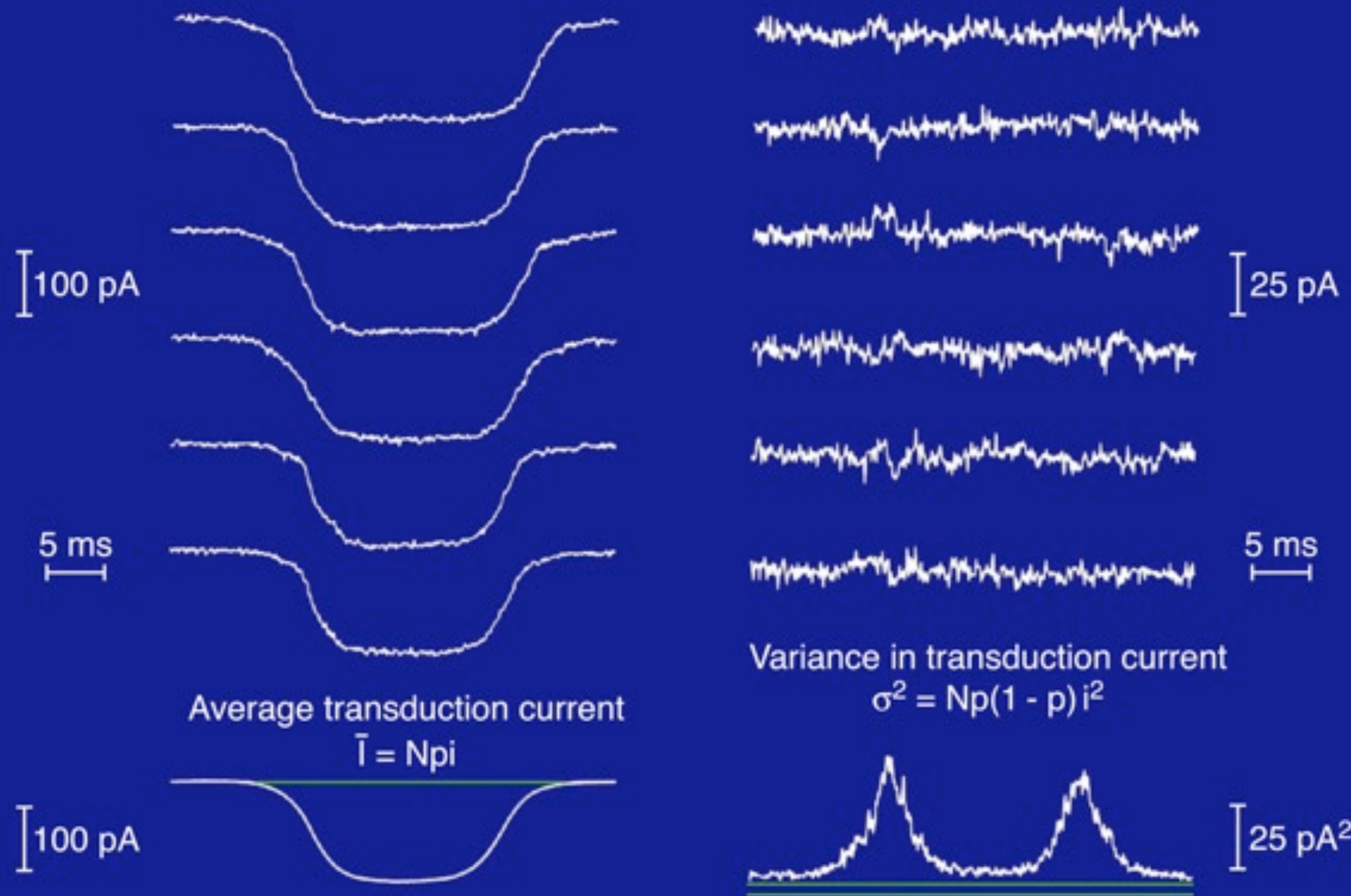

100 pA
5 ms
Average transduction current
$\bar{I} = Npi$
100 pA
25 pA
5 ms
Variance in transduction current
$\sigma^2 = Np(1 - p)\,i^2$
25 pA^2

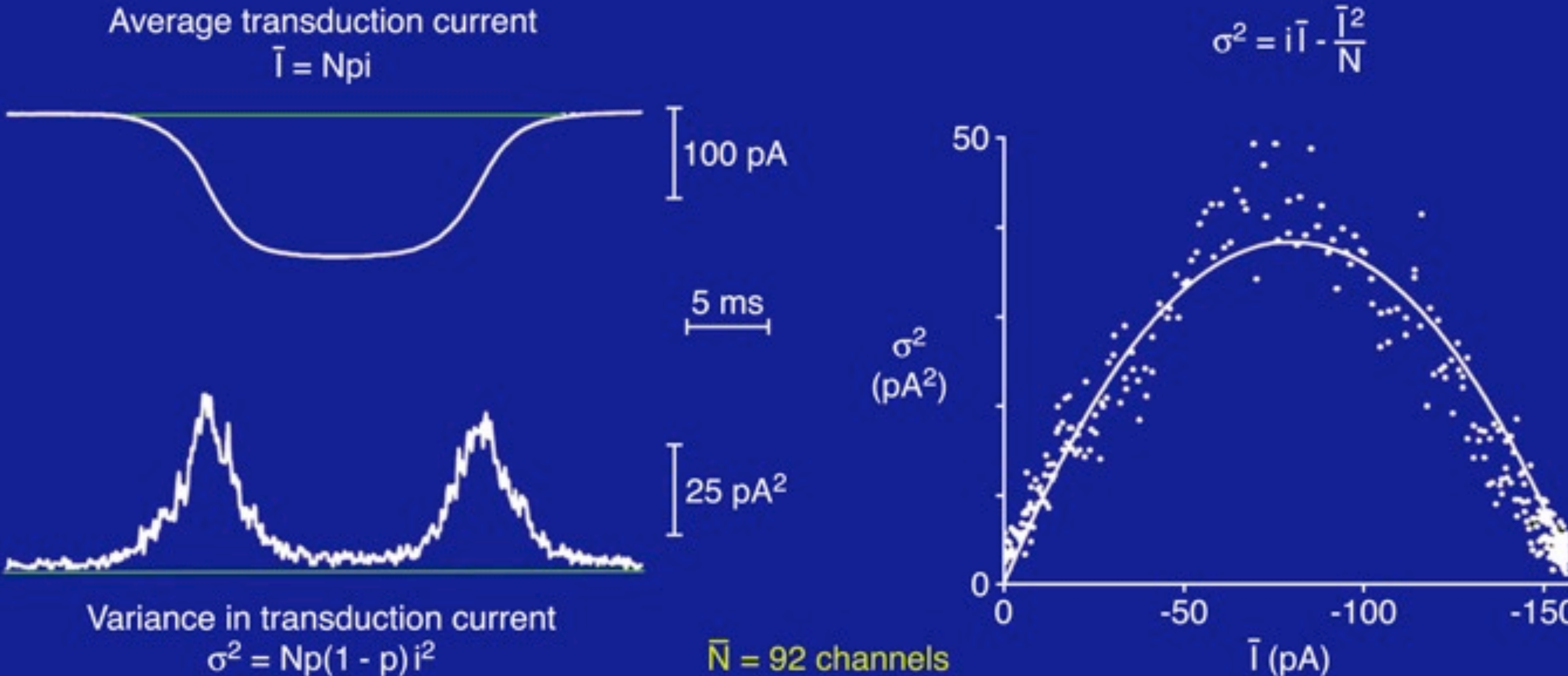
Average transduction current
$\bar{I} = Npi$
100 pA
5 ms
25 pA^2
Variance in transduction current
$\sigma^2 = Np(1 - p)\, i^2$
$\bar{N}$ = 92 channels
$\sigma^2 = i\bar{I} - \frac{\bar{I}^2}{N}$
50
0
σ^2
(pA^2)
0
-50
-100
-150
$\bar{I}$ (pA)

TONOTOPIC VARIATION IN SINGLE – CHANNEL CONDUCTANCE OF MECHANOELECTRICAL – TRANSDUCTION CHANNELS

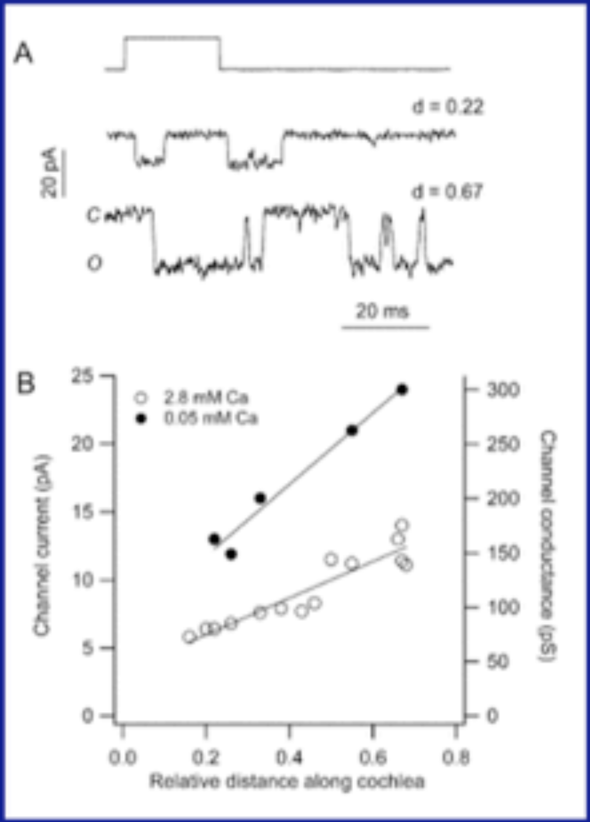

After Ricci *et al.*, 2003

Range of single-channel conductances
in immature mutant and wild-type murine inner hair cells

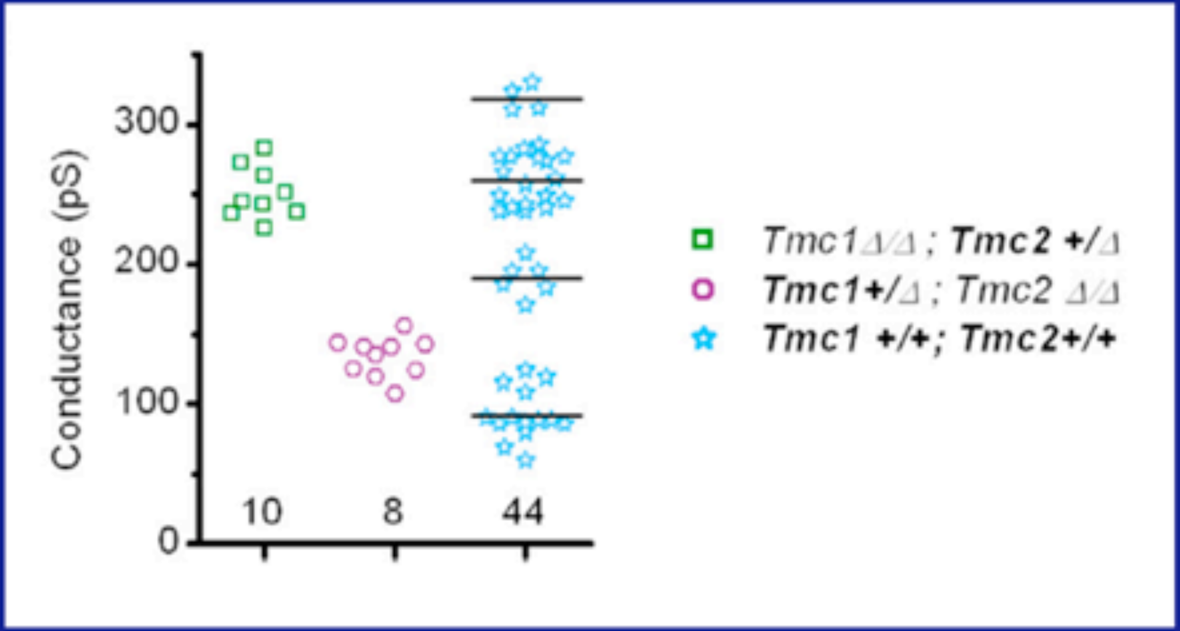

After Pan *et al.*, 2013

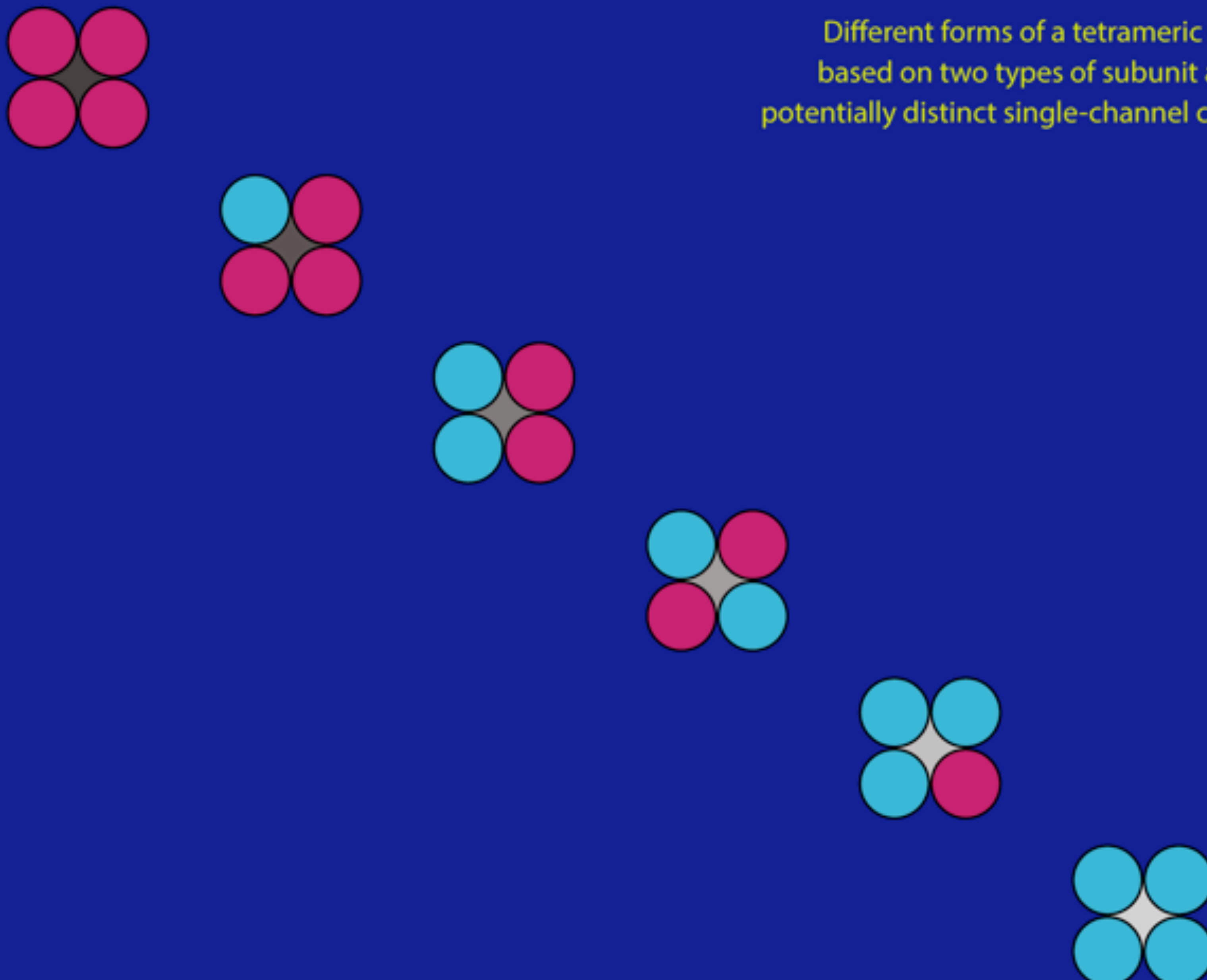

Different forms of a tetrameric channel
based on two types of subunit and with
potentially distinct single-channel conductances

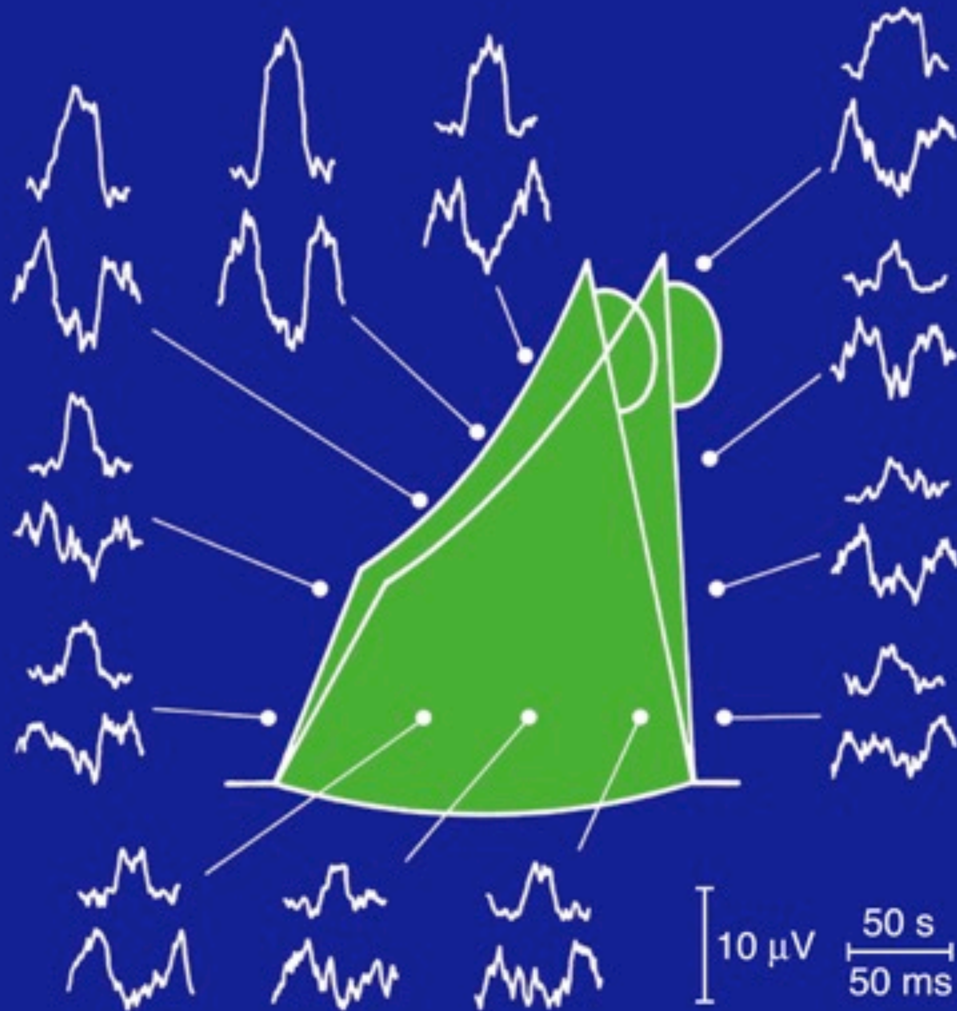
10 µV
50 s
50 ms

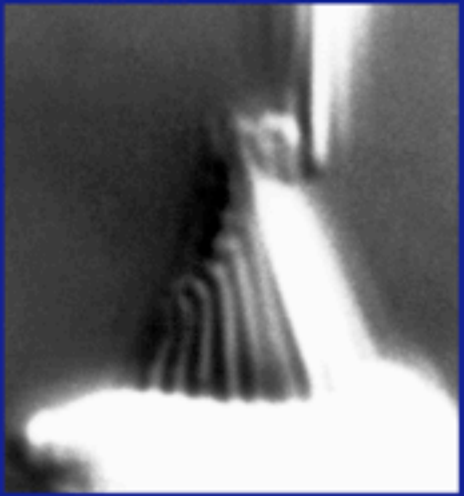

Hair bundle and stimulus probe

Iontophoretic pipette

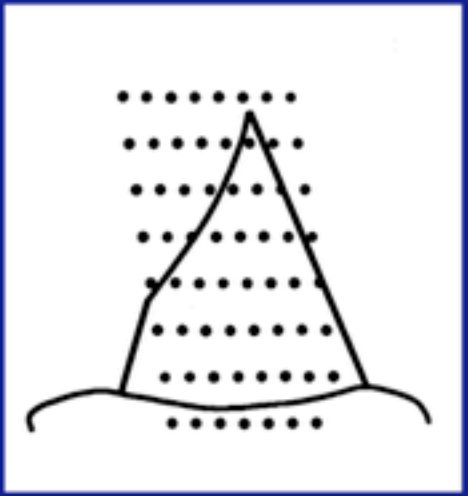

63 sites of iontophoresis

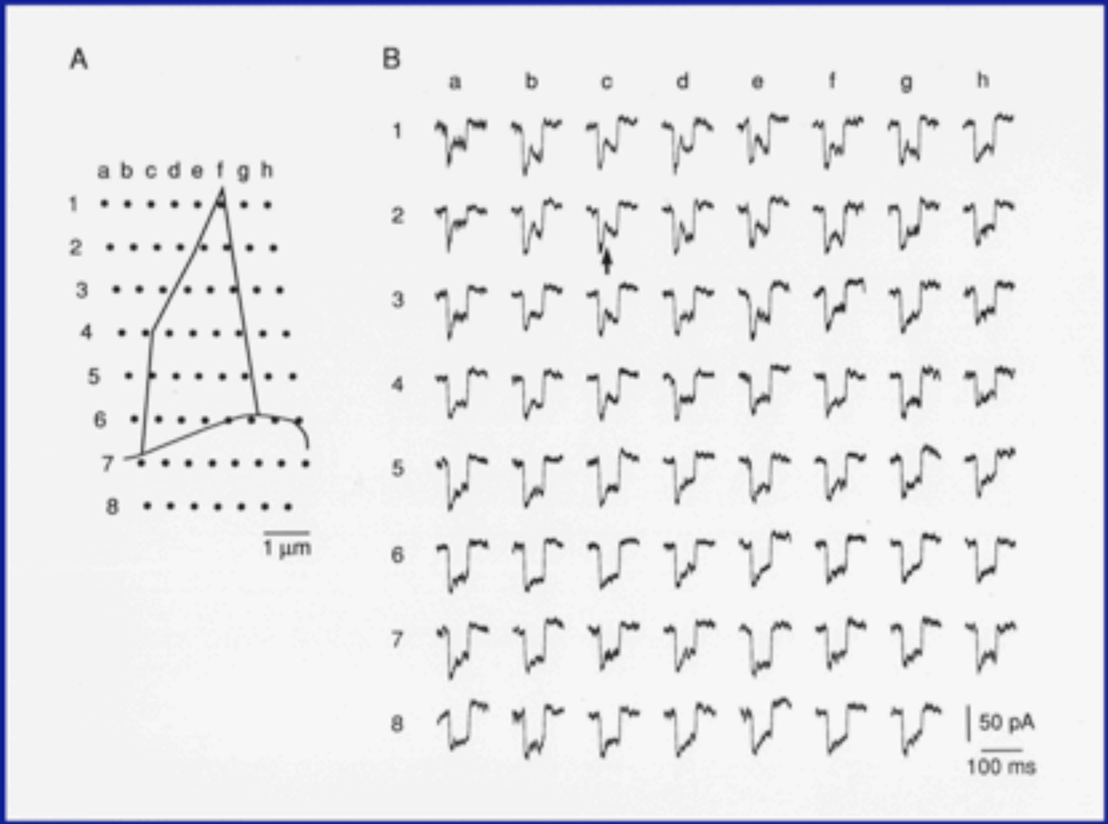
A
B
a b c d e f g h
1 2 3 4 5 6 7 8
1 µm
50 pA
100 ms

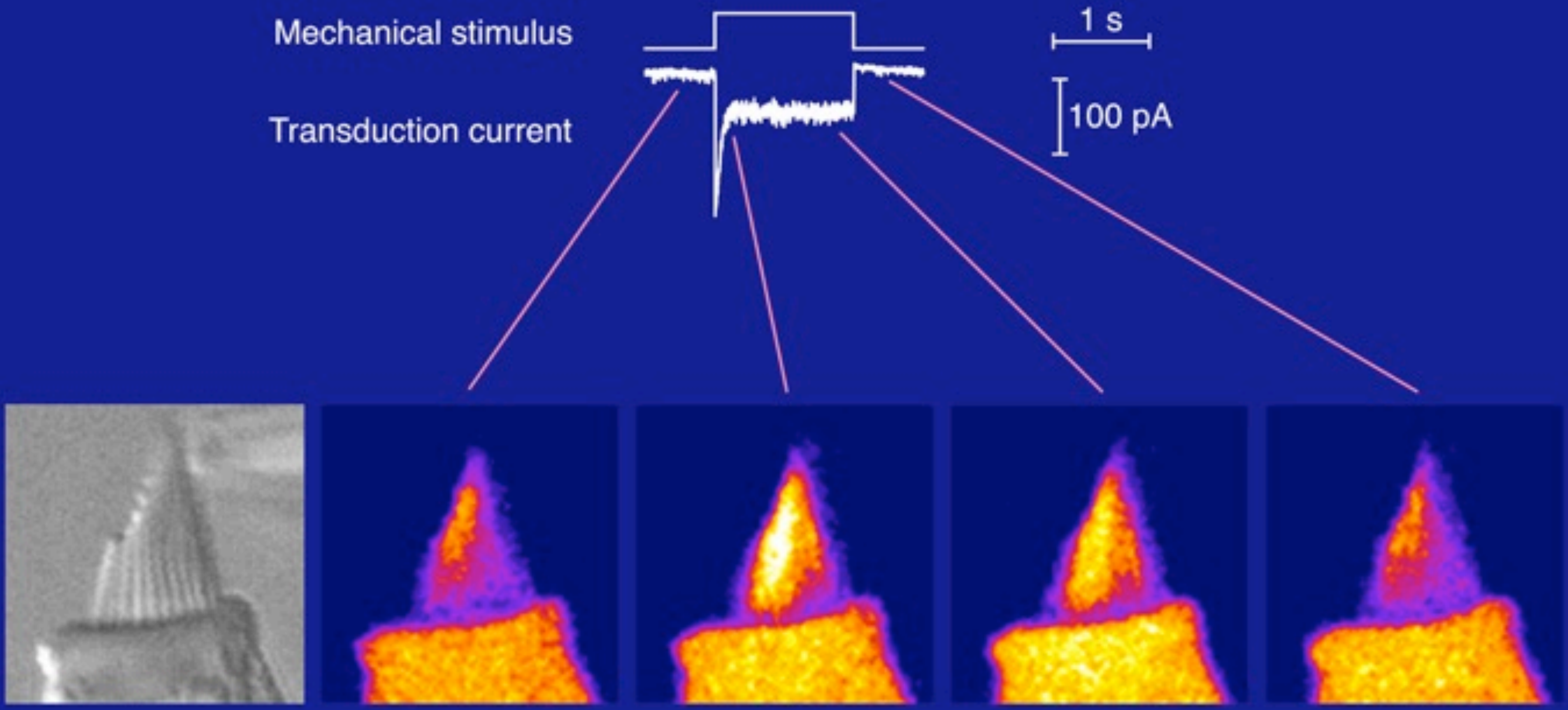

Mechanical stimulus
Transduction current
1 s
100 pA

Transduction-channel localization in rat inner hair cells with Fluo-4FF

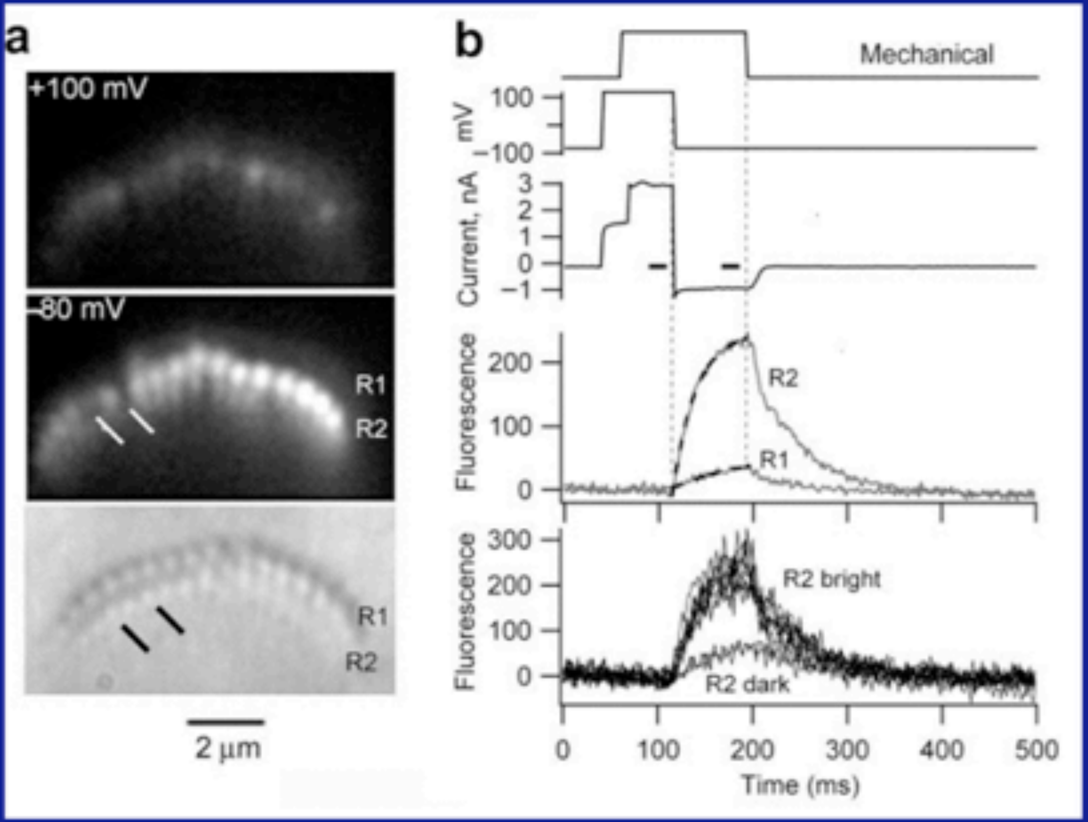

After Beurg *et al.*, 2009

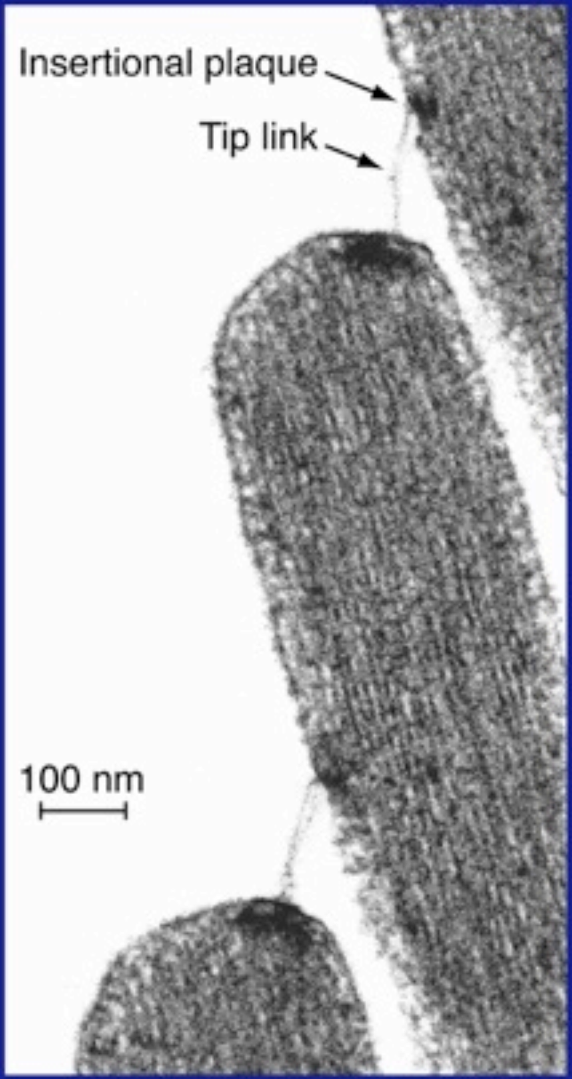
Insertional plaque
Tip link
100 nm

THE GATING–SPRING MODEL

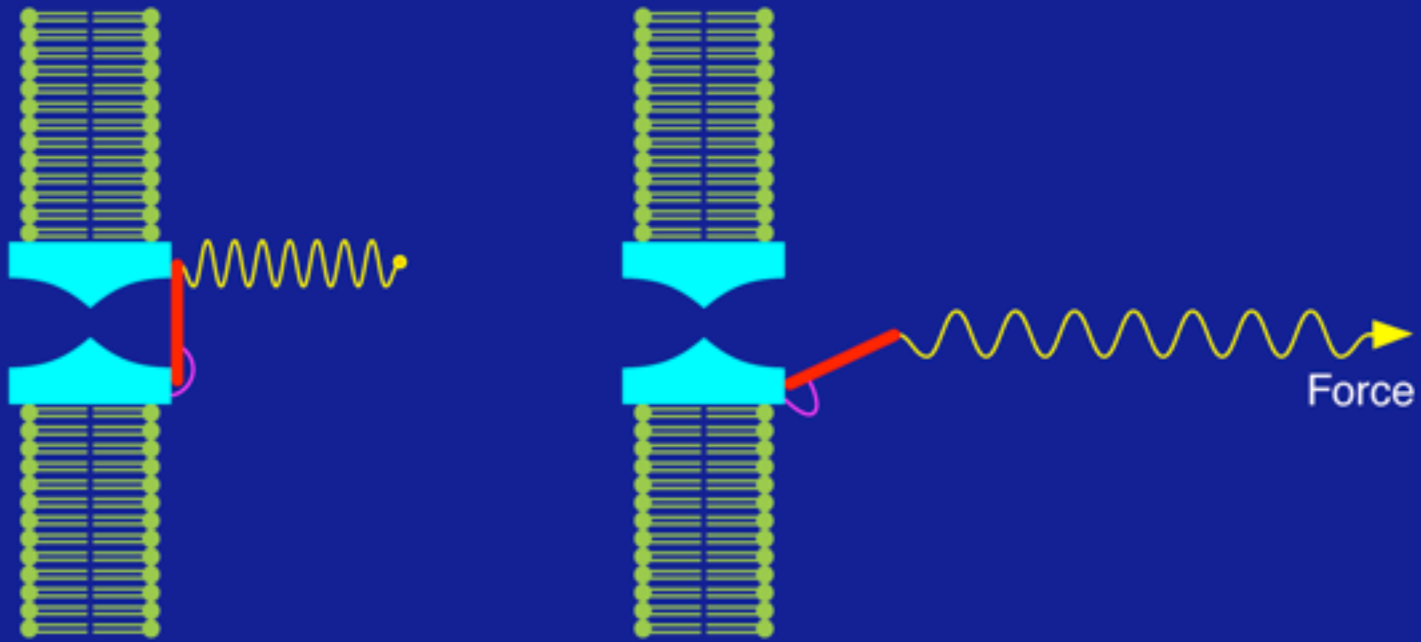
Force

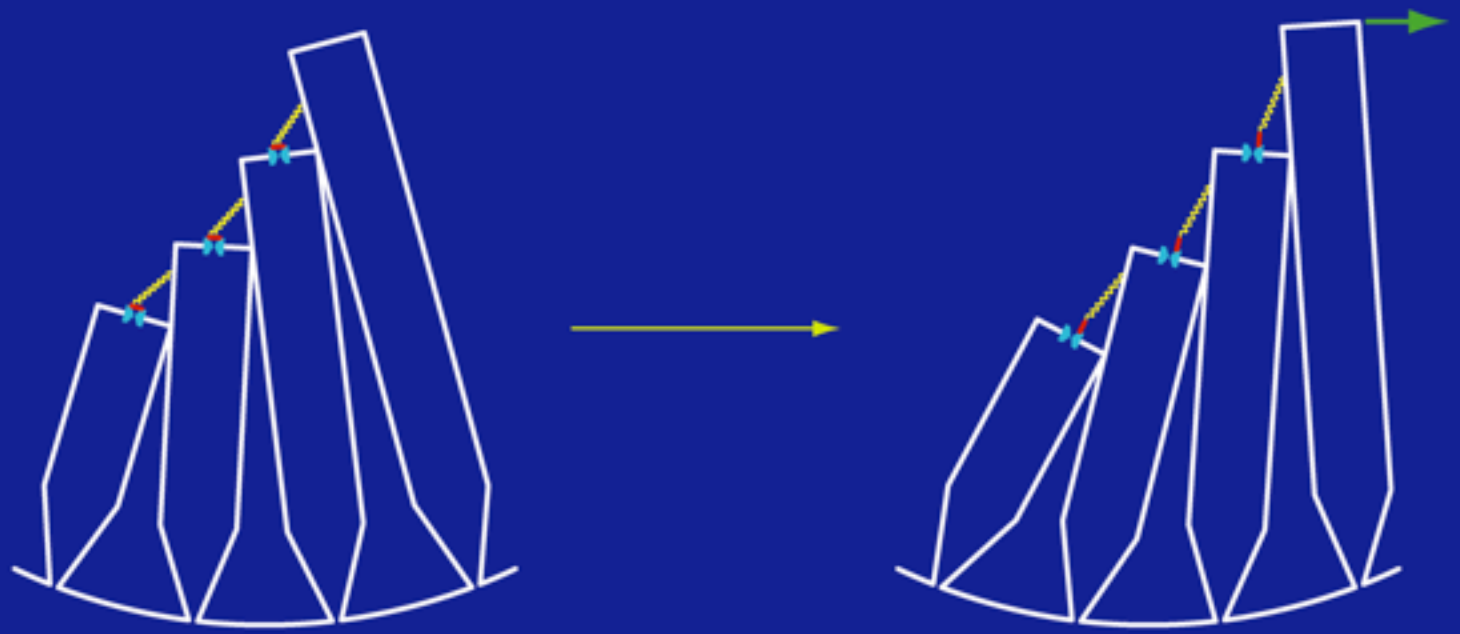

THE GEOMETRICAL GAIN FACTOR γ

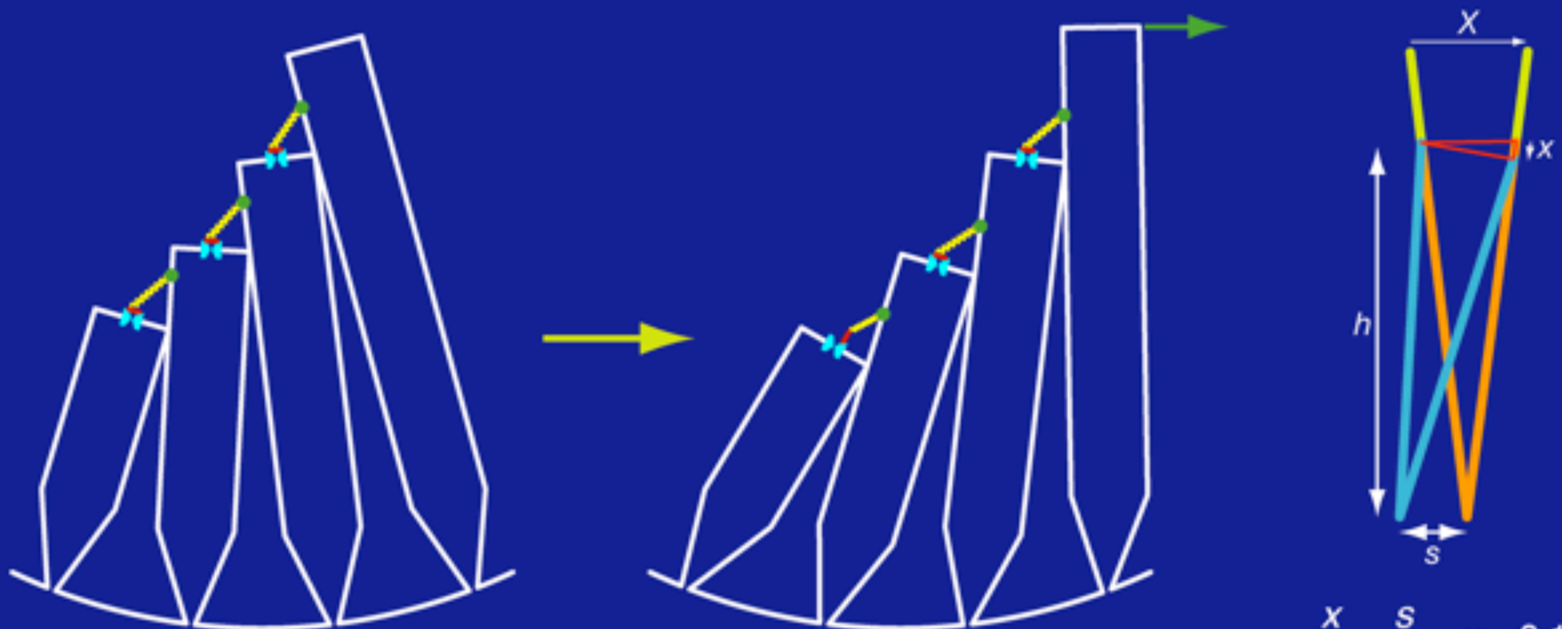

$$\frac{x}{X} \approx \frac{s}{h} = \gamma \approx 0.14$$

For displacements: $X = x/\gamma$
For forces: $F = N\gamma f$
For stiffnesses: $\mathrm{K} = N\gamma^2\kappa$

THE GATING – SPRING MODEL

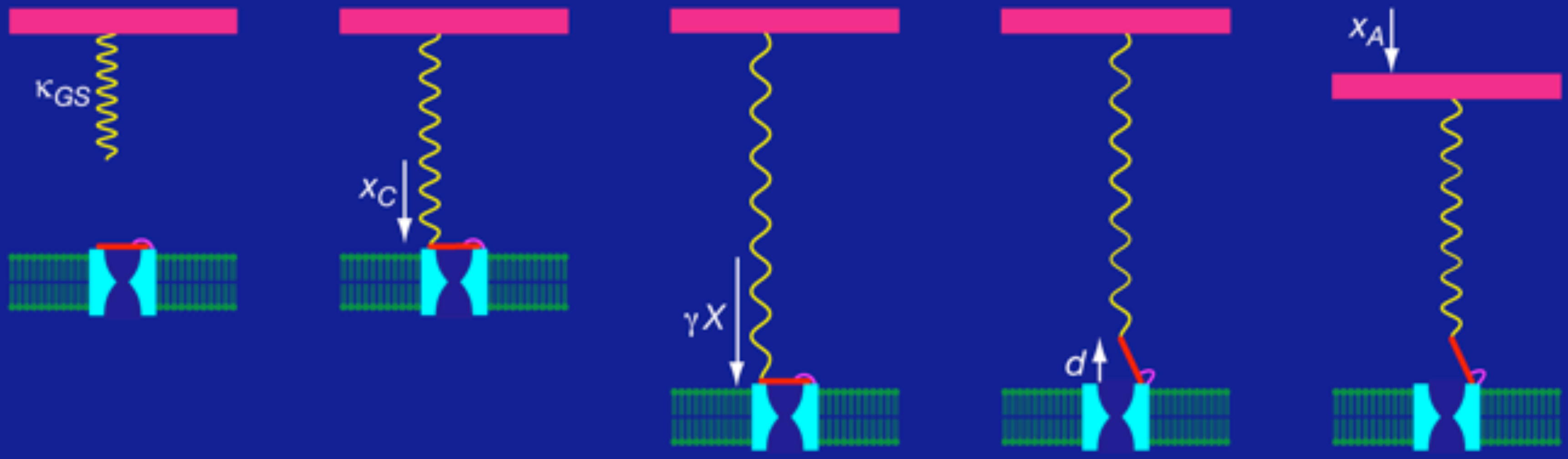

Force produced by a single gating spring: $f = \kappa_{GS}(\gamma X + x_C - x_A)$
(as measured locally; channel closed)

Force produced by a single gating spring: $f = \kappa_{GS}(\gamma X + x_C - x_A - d)$
(as measured locally; channel open)

Force produced by N gating springs in parallel: $F = N\gamma\kappa_{GS}(\gamma X + x_C - x_A - P_O d)$
(as measured at hair bundle's top)

Force produced by an entire hair bundle: $F_{HB} = N\gamma\kappa_{GS}(\gamma X + x_C - x_A - P_O d) + K_{SP}(X - X_{SP})$
(as measured at hair bundle's top)

GATING – SPRING MODEL

Channel open probability

$$P_O = \frac{1}{1+e^{-Z(X-X_0)/kT}}$$

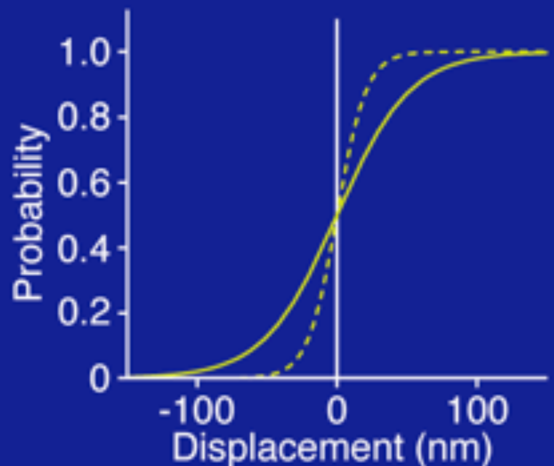

Hair-bundle force

$$F_{HB} = N\gamma\kappa_{GS}(\gamma X + x_C - x_A - P_O d) + K_{SP}(X - X_{SP})$$

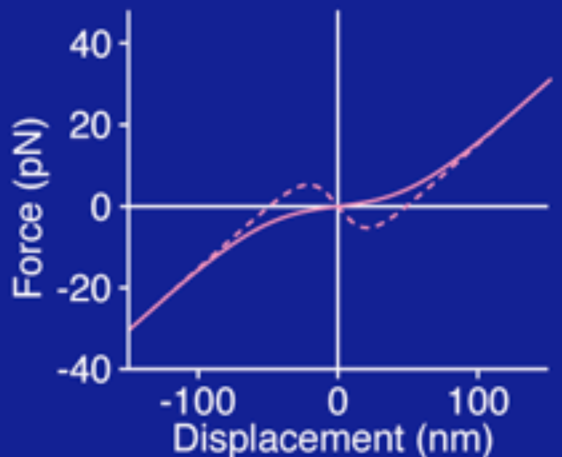

GATING – SPRING MODEL
(Gating compliance)

Hair-bundle stiffness

$$K_{HB} = N\gamma^2\kappa_{GS} + K_{SP} - \left(\frac{NZ^2}{kT}\right)P_O(1-P_O) = K_\infty - \left(\frac{NZ^2}{kT}\right)P_O(1-P_O)$$

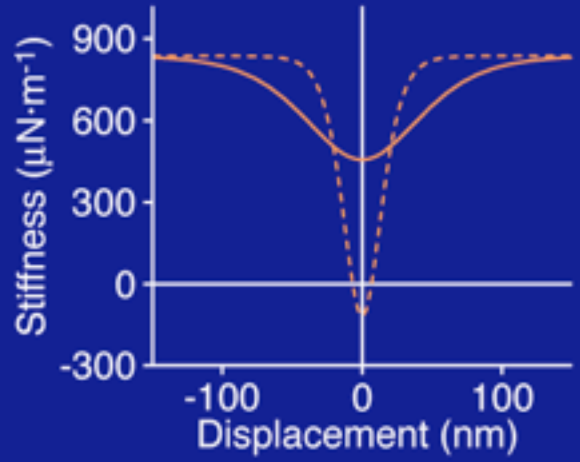

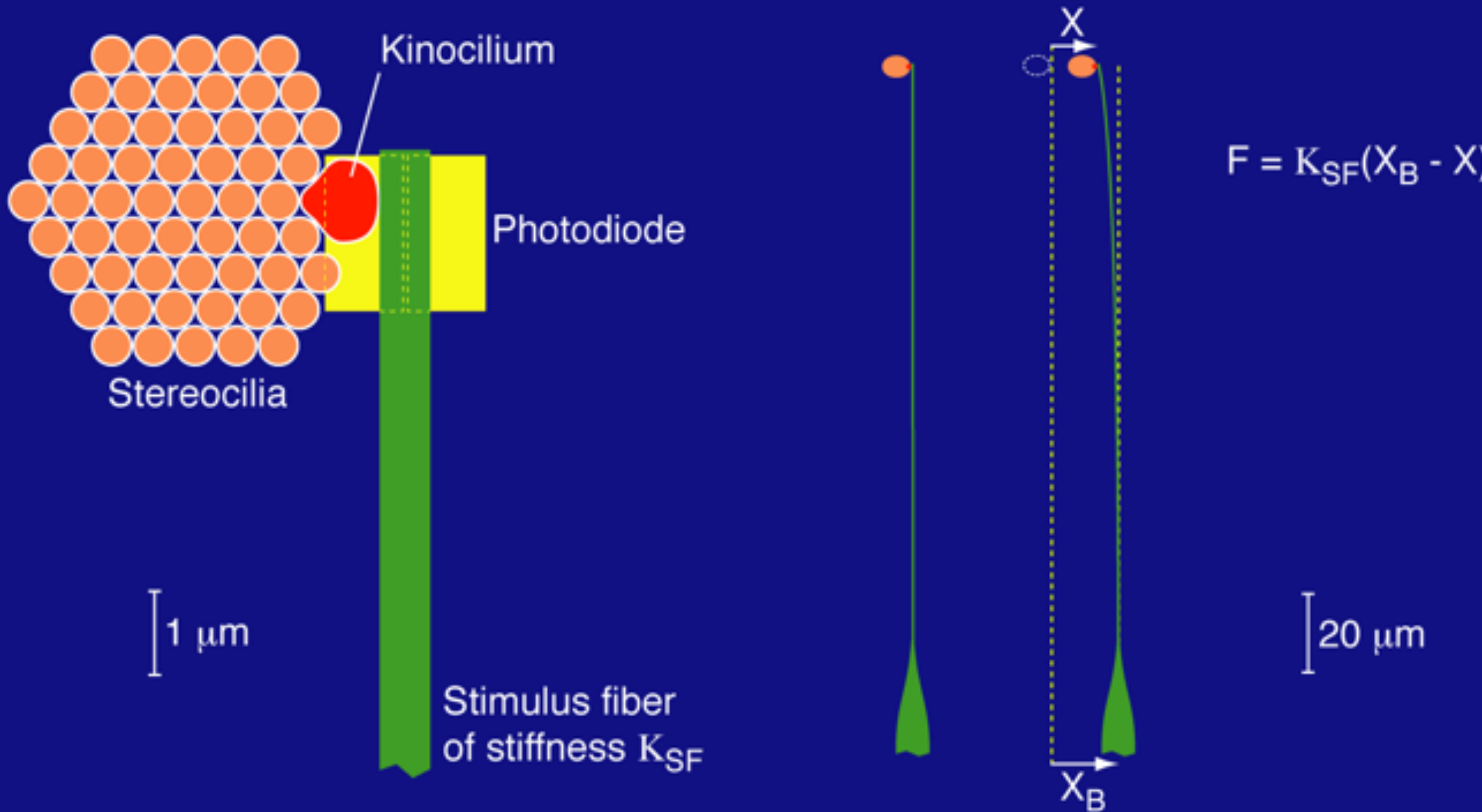

Kinocilium
Photodiode
Stereocilia
1 μm
Stimulus fiber
of stiffness K_{SF}
X
$F = K_{SF}(X_B - X)$
20 μm
X_B

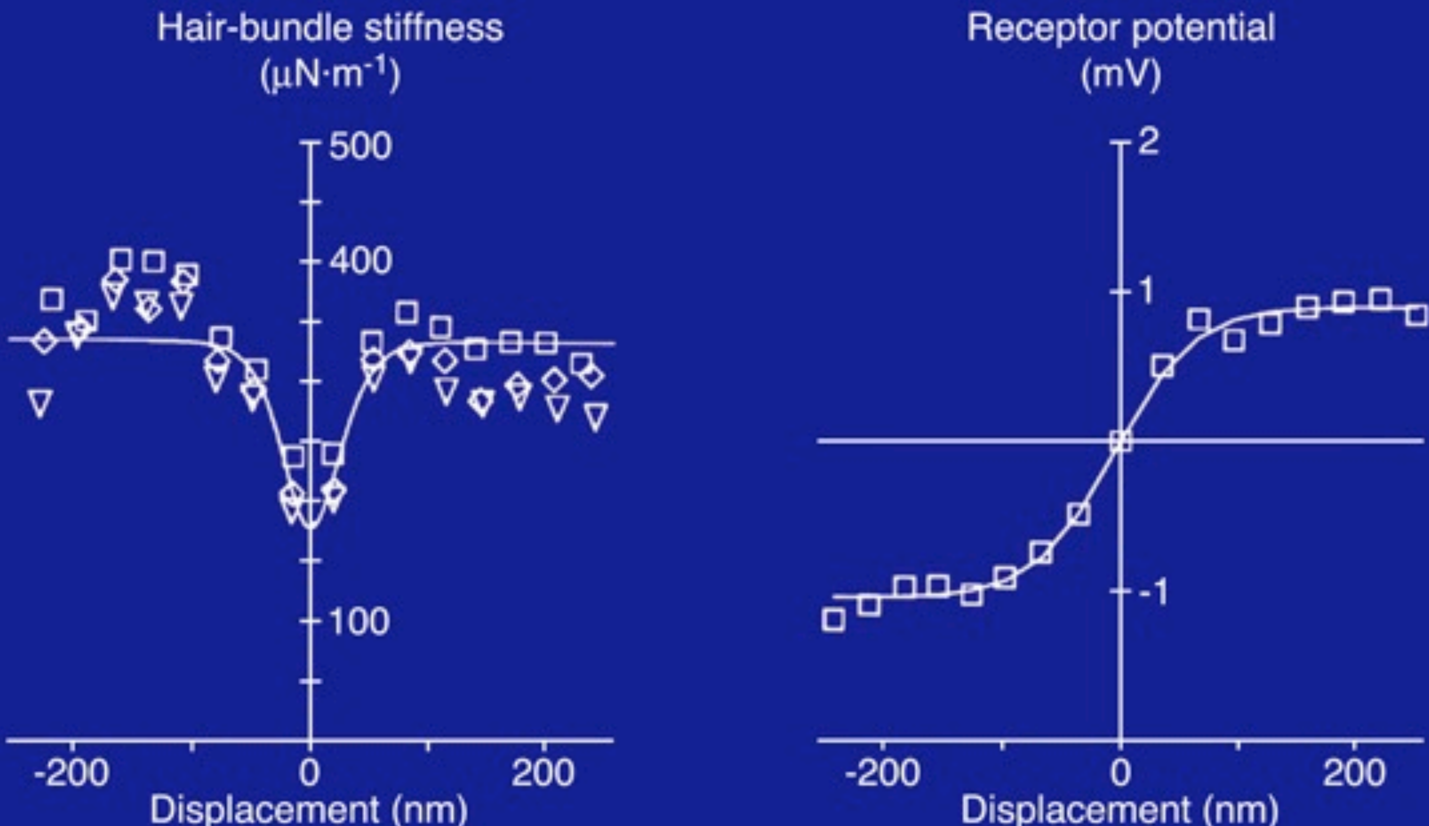

Hair-bundle stiffness
(μN·m-1)
500
400
100
-200
0
200
Displacement (nm)
Receptor potential
(mV)
2
1
-1
-200
0
200
Displacement (nm)

THE STEREOCILIARY TIP LINK

PUTATIVE COMPONENTS OF THE MECHANOELECTRICAL – TRANSDUCTION CHANNEL COMPLEX OF HAIR CELLS

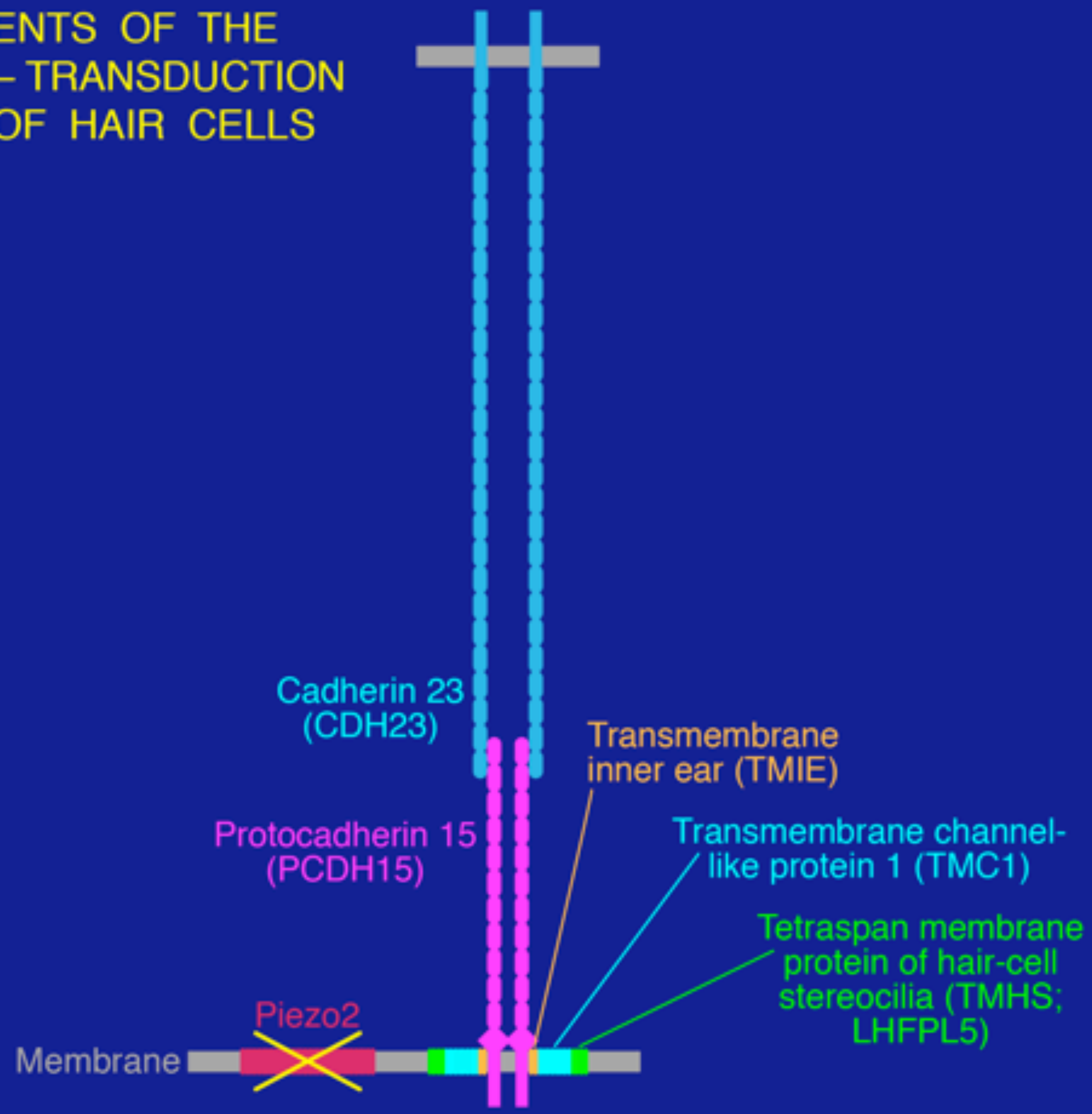

STRUCTURE OF THE TIP LINK

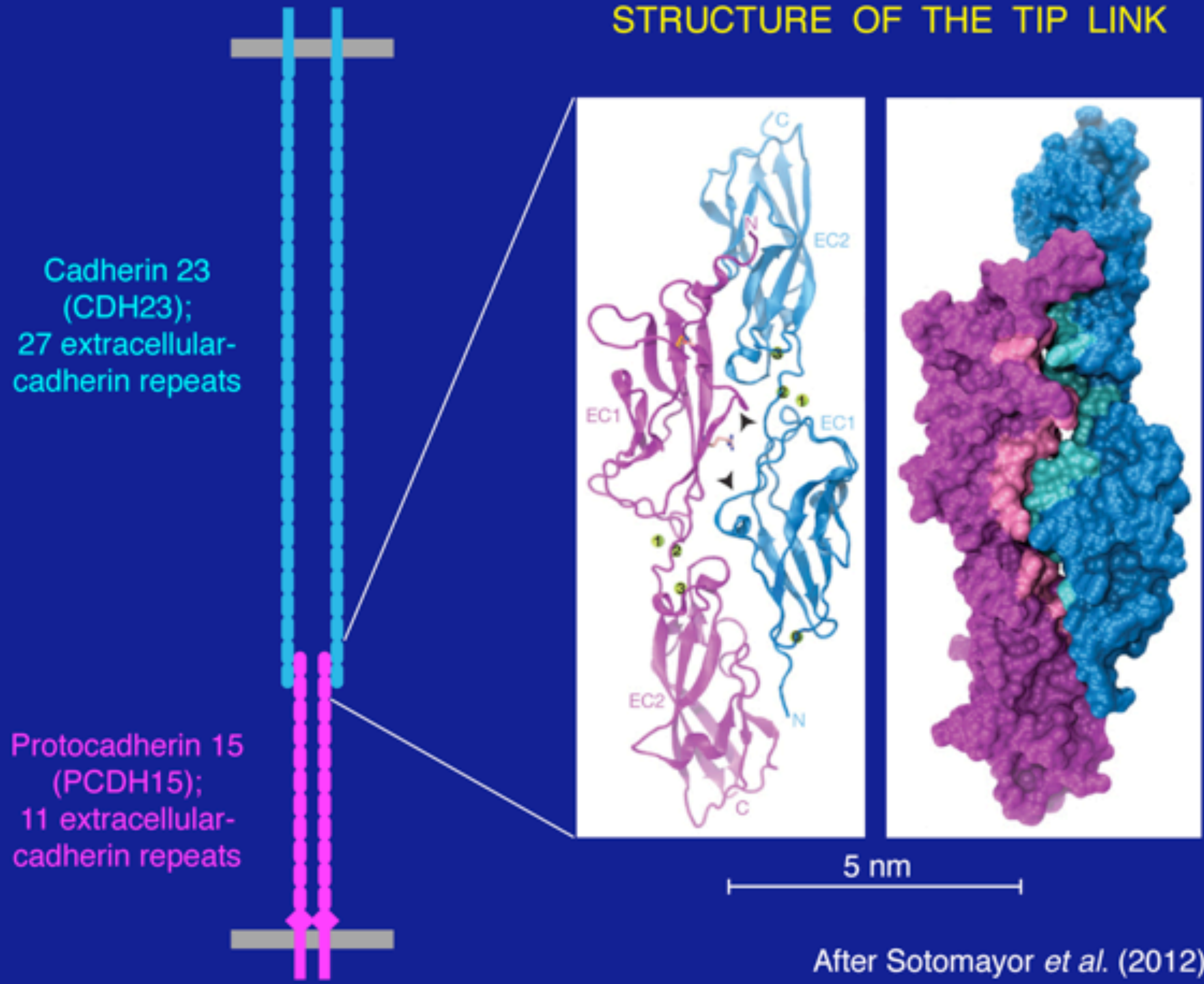

After Sotomayor *et al.* (2012)

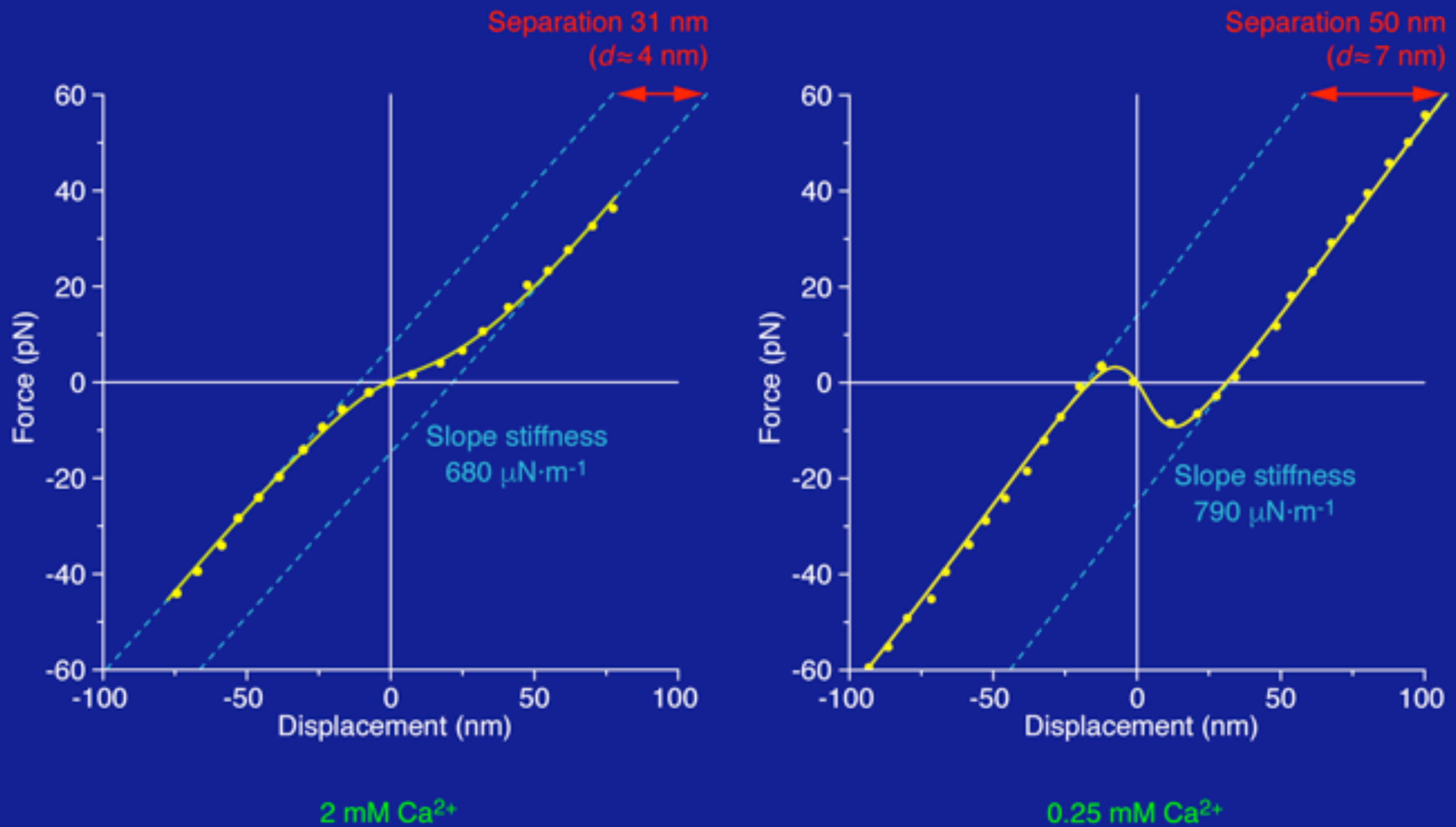

Separation 31 nm
(d≈4 nm)
Force (pN)
Displacement (nm)
Slope stiffness
680 μN·m-1
2 mM Ca2+
Separation 50 nm
(d≈7 nm)
Force (pN)
Displacement (nm)
Slope stiffness
790 μN·m-1
0.25 mM Ca2+

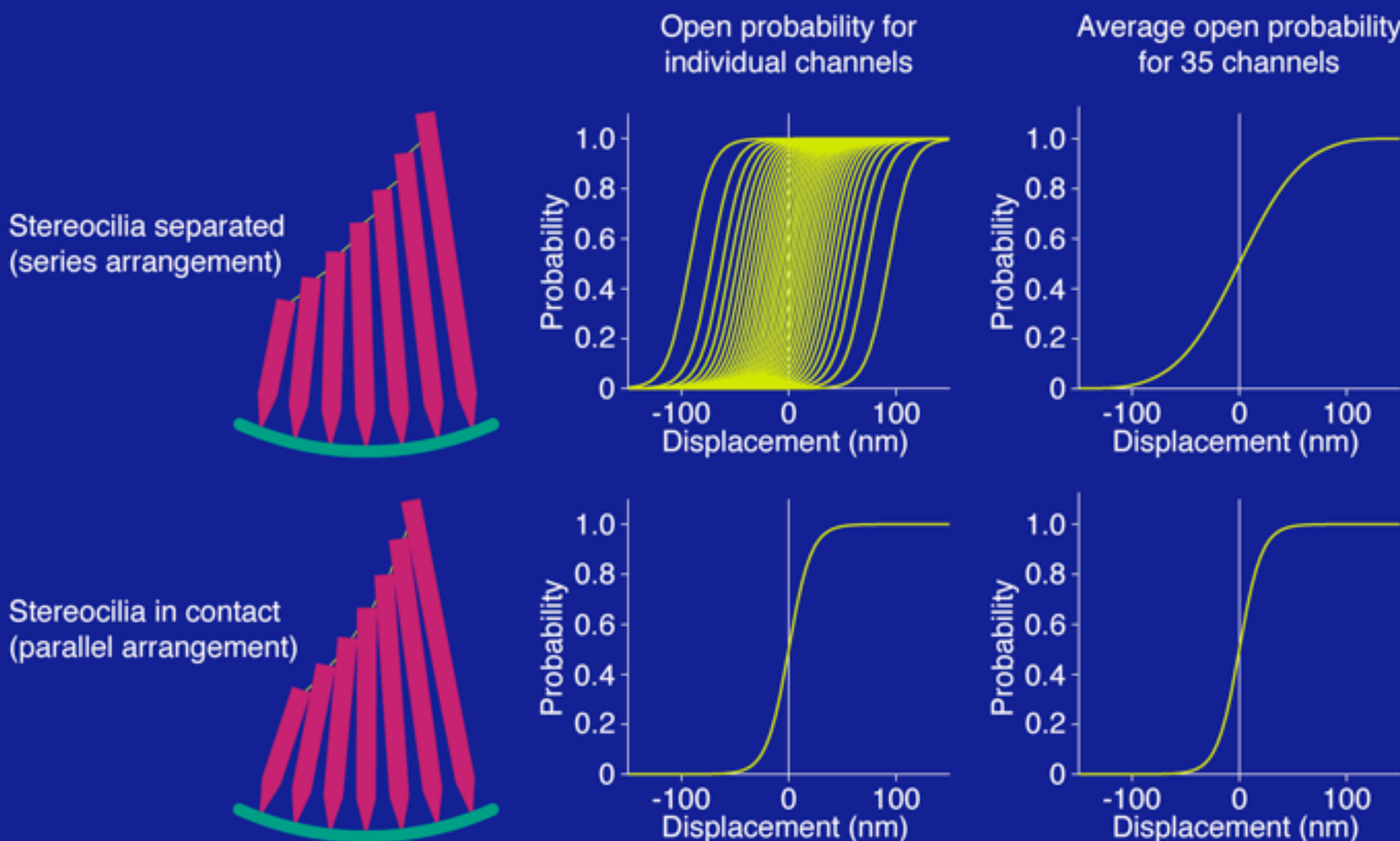
Open probability for individual channels
Average open probability for 35 channels
Stereocilia separated (series arrangement)
Stereocilia in contact (parallel arrangement)
Probability
1.0
0.8
0.6
0.4
0.2
0
-100
0
100
Displacement (nm)

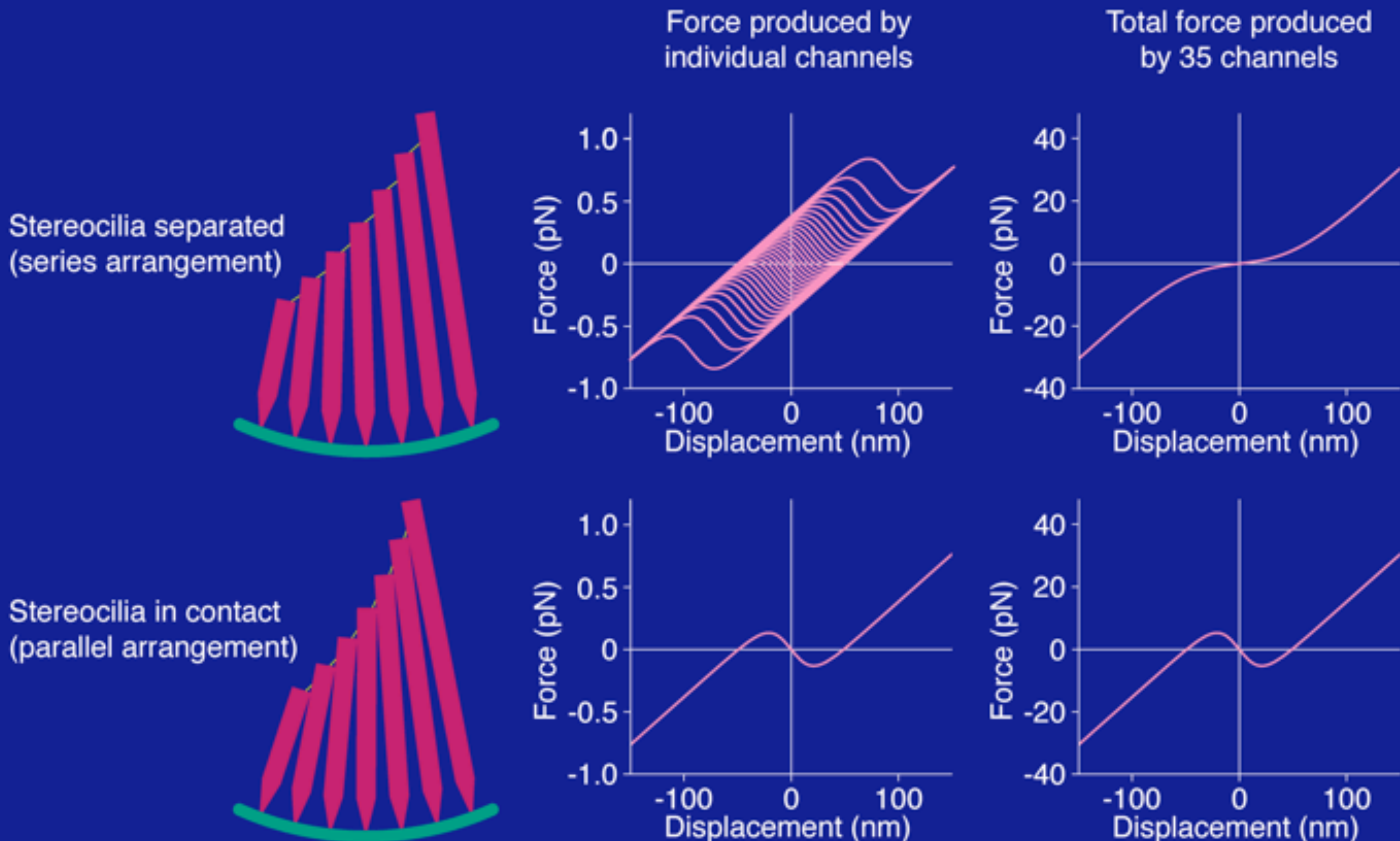

Force produced by individual channels
Total force produced by 35 channels
Stereocilia separated (series arrangement)
Stereocilia in contact (parallel arrangement)
Force (pN)
1.0
0.5
0
-0.5
-1.0
40
20
0
-20
-40
-100
0
100
Displacement (nm)

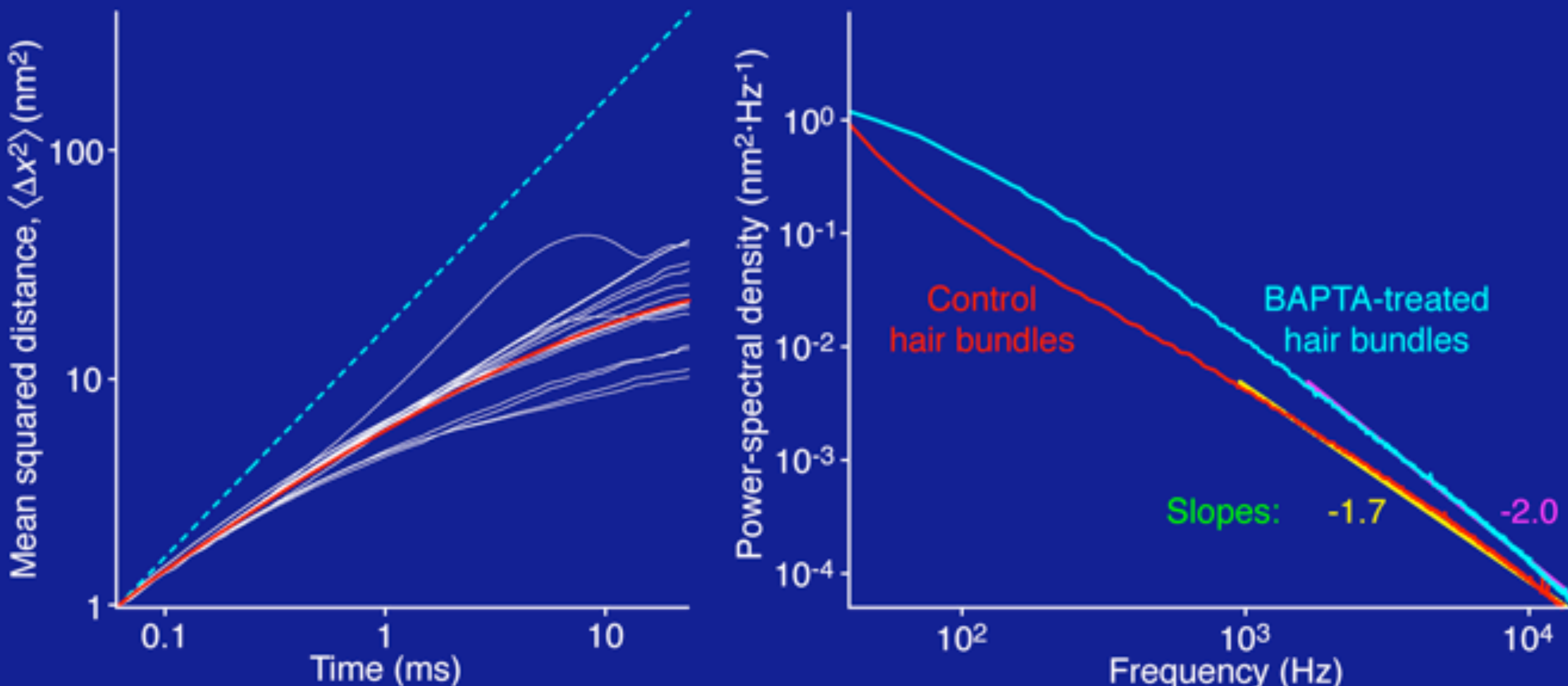

Mean squared distance, ⟨Δx²⟩ (nm²)
100
10
1
0.1
1
10
Time (ms)
Power-spectral density (nm²·Hz⁻¹)
10⁰
10⁻¹
10⁻²
10⁻³
10⁻⁴
10²
10³
10⁴
Frequency (Hz)
Control
hair bundles
BAPTA-treated
hair bundles
Slopes:
-1.7
-2.0

PARTIAL UNFOLDING OF PCDH15'S EC4 REPEAT

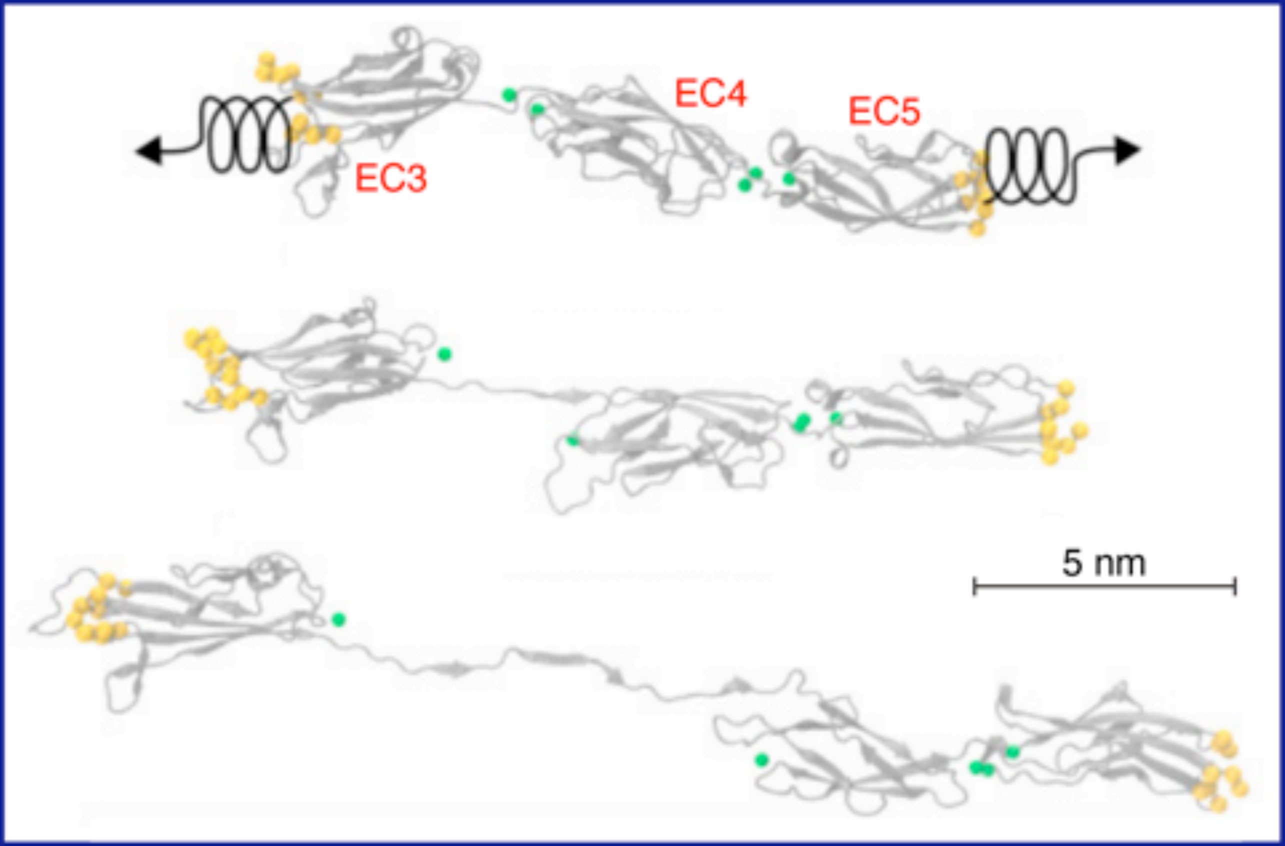

After Powers *et al.* (2017)

POSSIBLE SITES OF MECHANICAL COMPLIANCE IN THE TRANSDUCTION APPARATUS

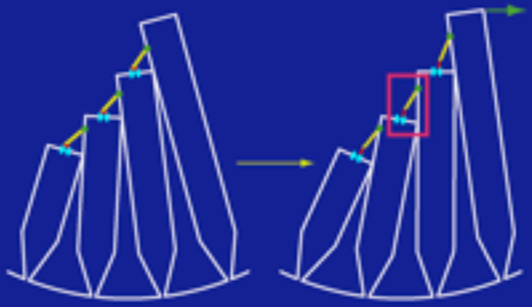

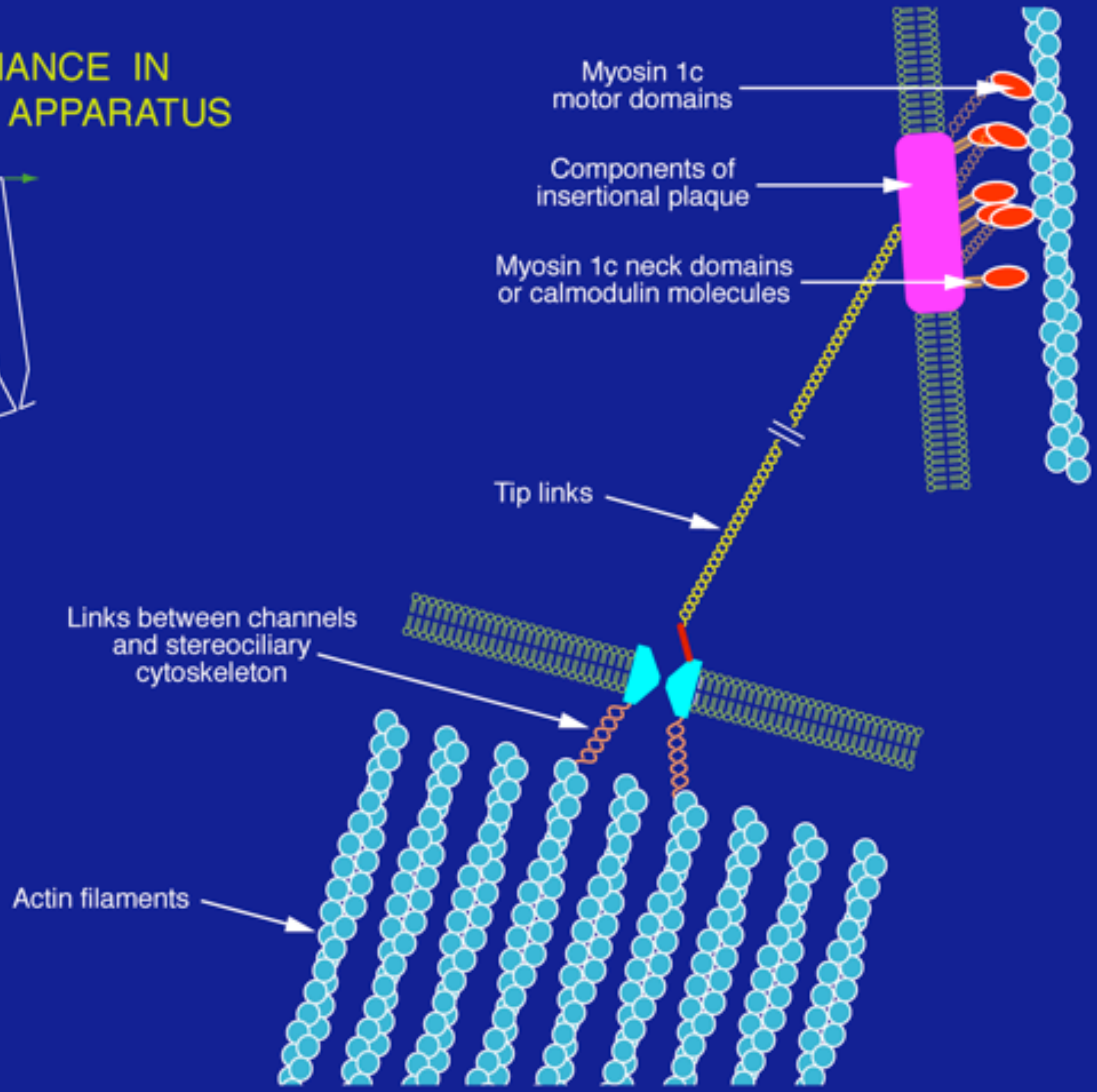

NEGATIVE HAIR–BUNDLE STIFFNESS AND THE PARALLEL ARRANGEMENT OF TRANSDUCTION CHANNELS

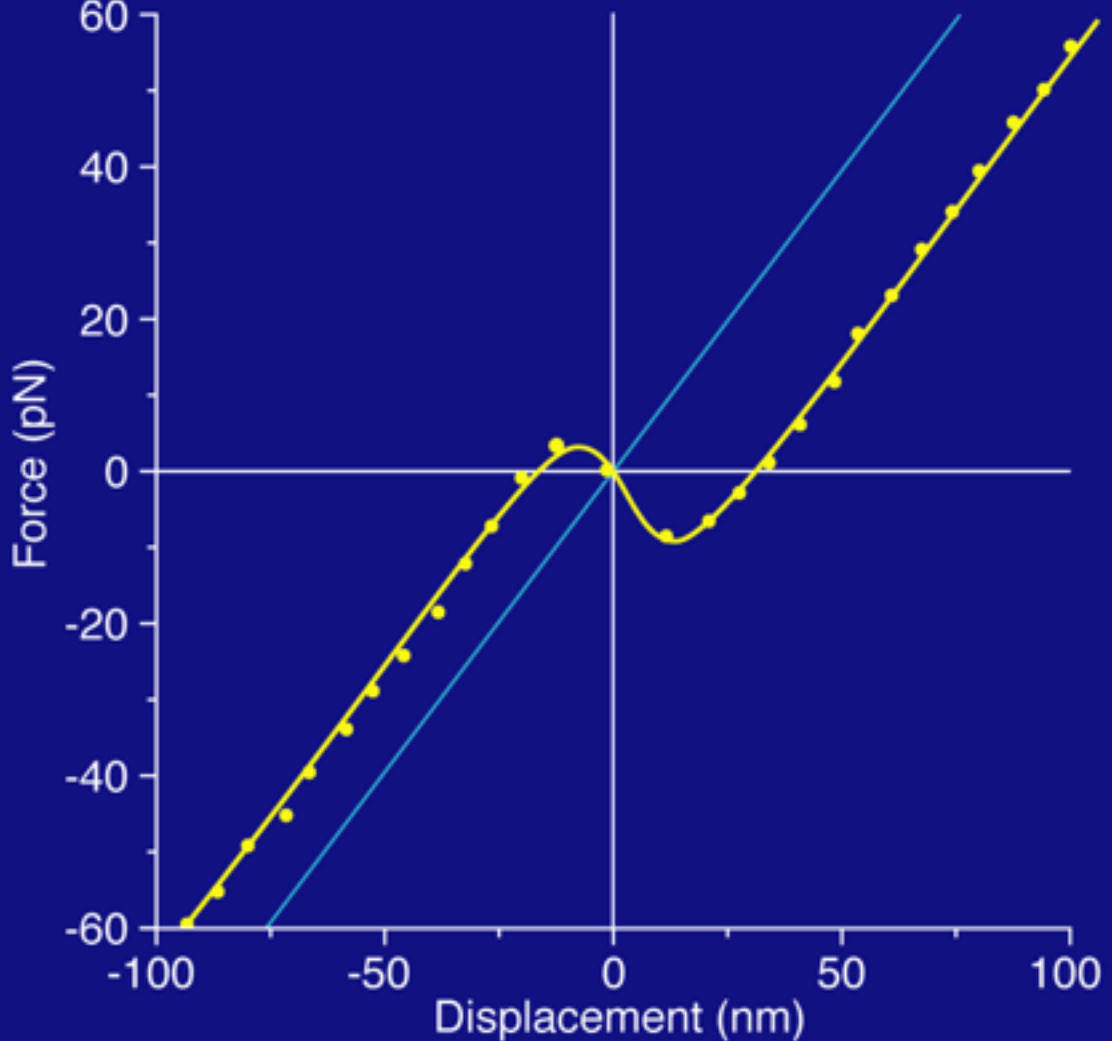

60
40
20
0
-20
-40
-60
Force (pN)
-100
-50
0
50
100
Displacement (nm)

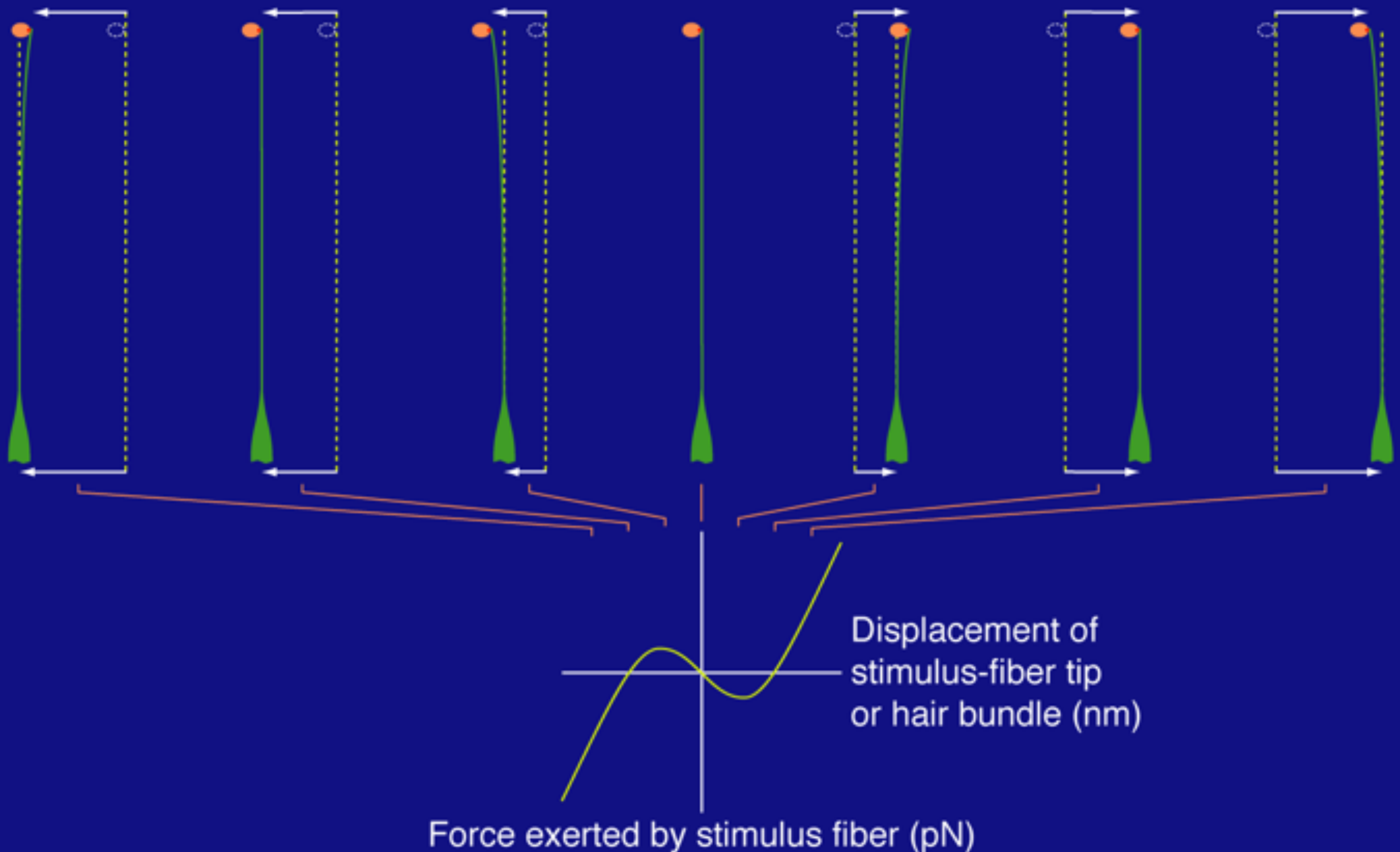

Displacement of
stimulus-fiber tip
or hair bundle (nm)
Force exerted by stimulus fiber (pN)

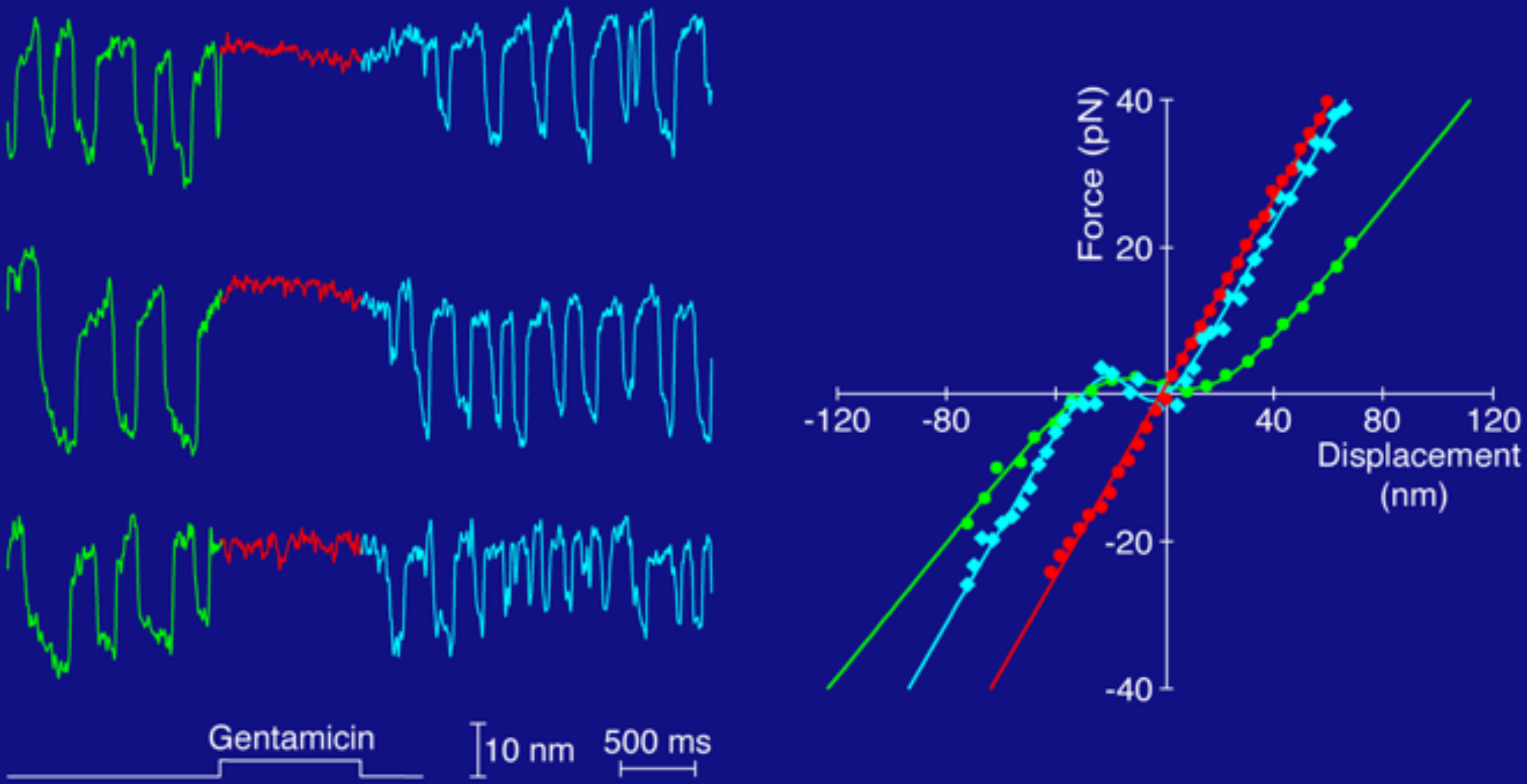

Gentamicin
10 nm
500 ms
Force (pN)
40
20
-20
-40
-120
-80
40
80
120
Displacement
(nm)

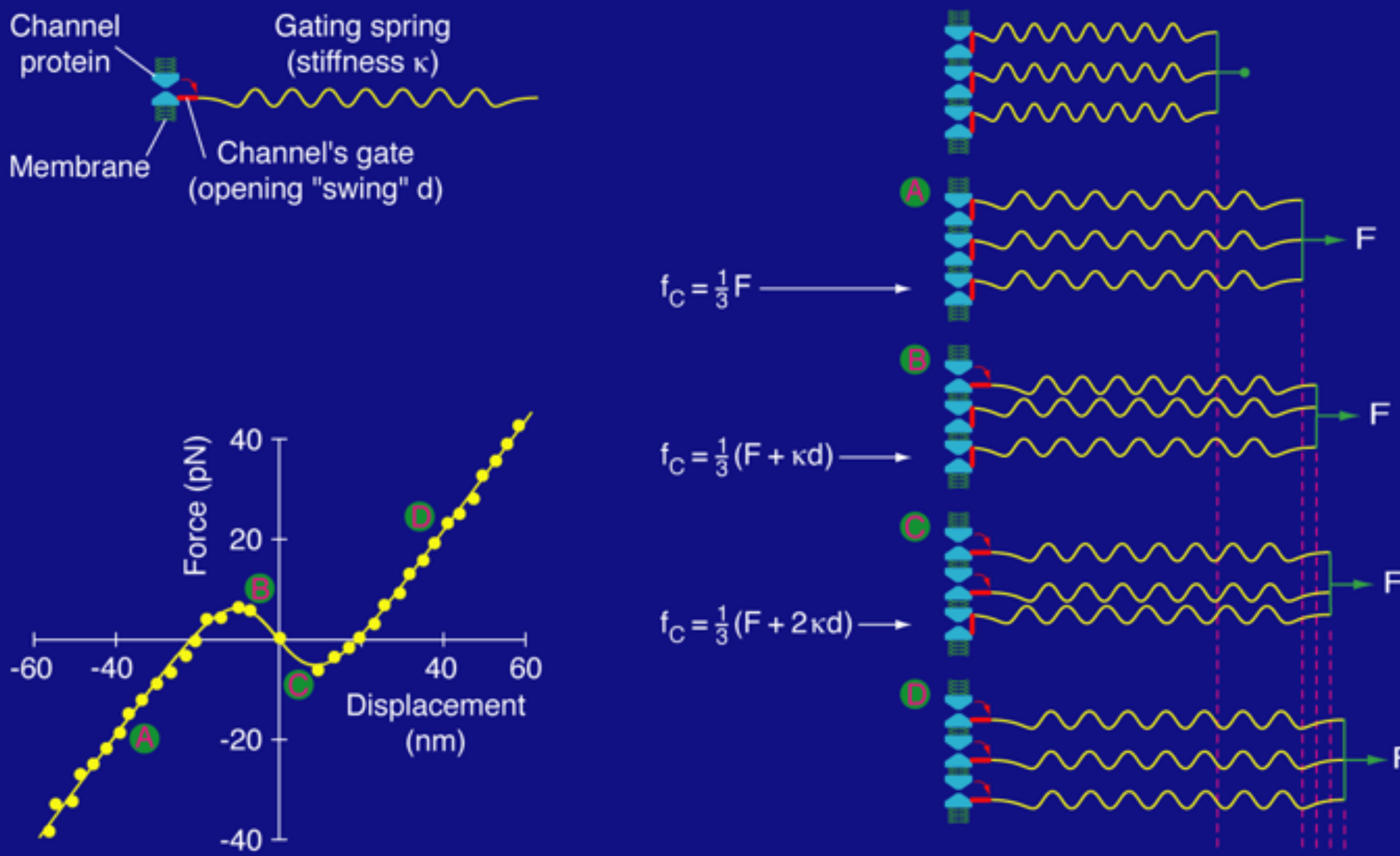
Channel protein
Gating spring (stiffness κ)
Membrane
Channel's gate (opening "swing" d)
Force (pN)
40
20
-20
-40
-60
-40
40
60
Displacement (nm)
A
B
C
D
F
$f_C = \frac{1}{3}F$
$f_C = \frac{1}{3}(F + \kappa d)$
$f_C = \frac{1}{3}(F + 2\kappa d)$

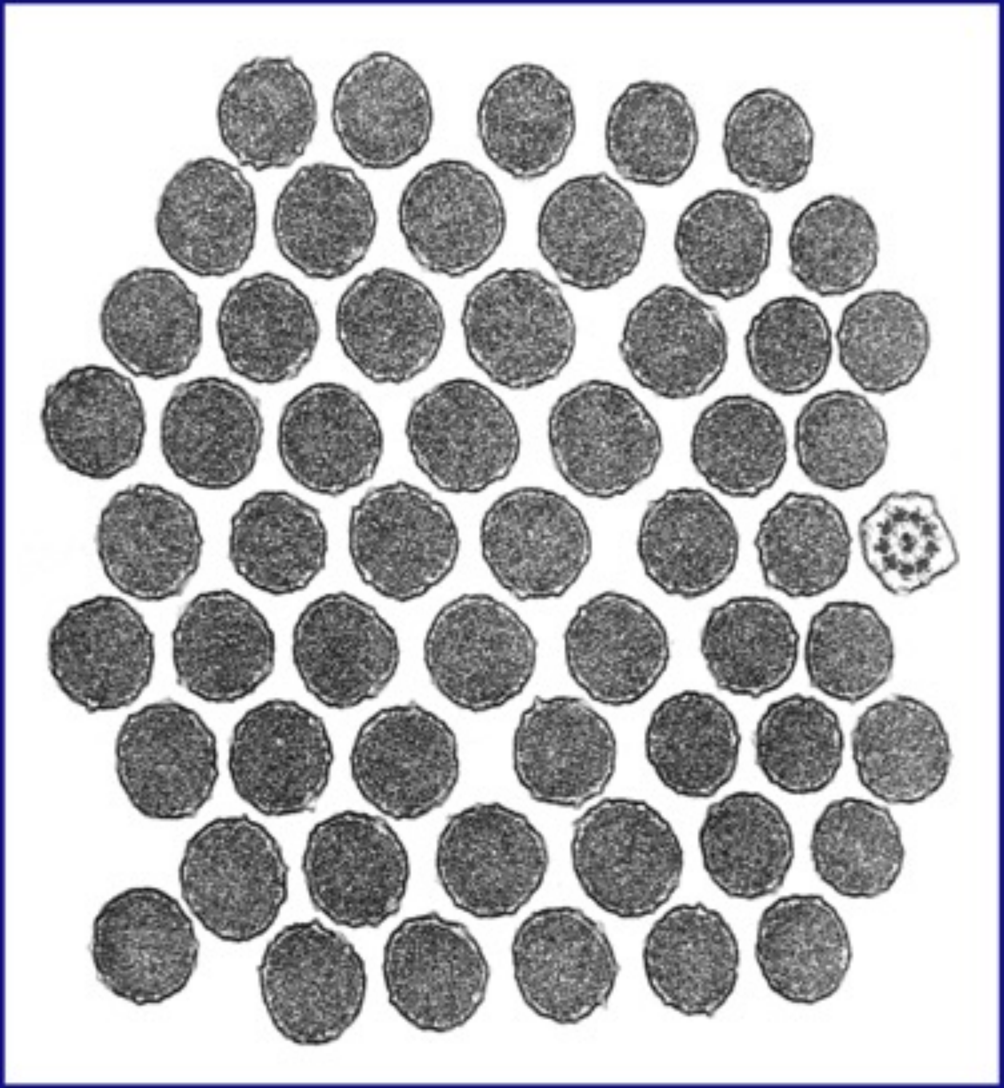

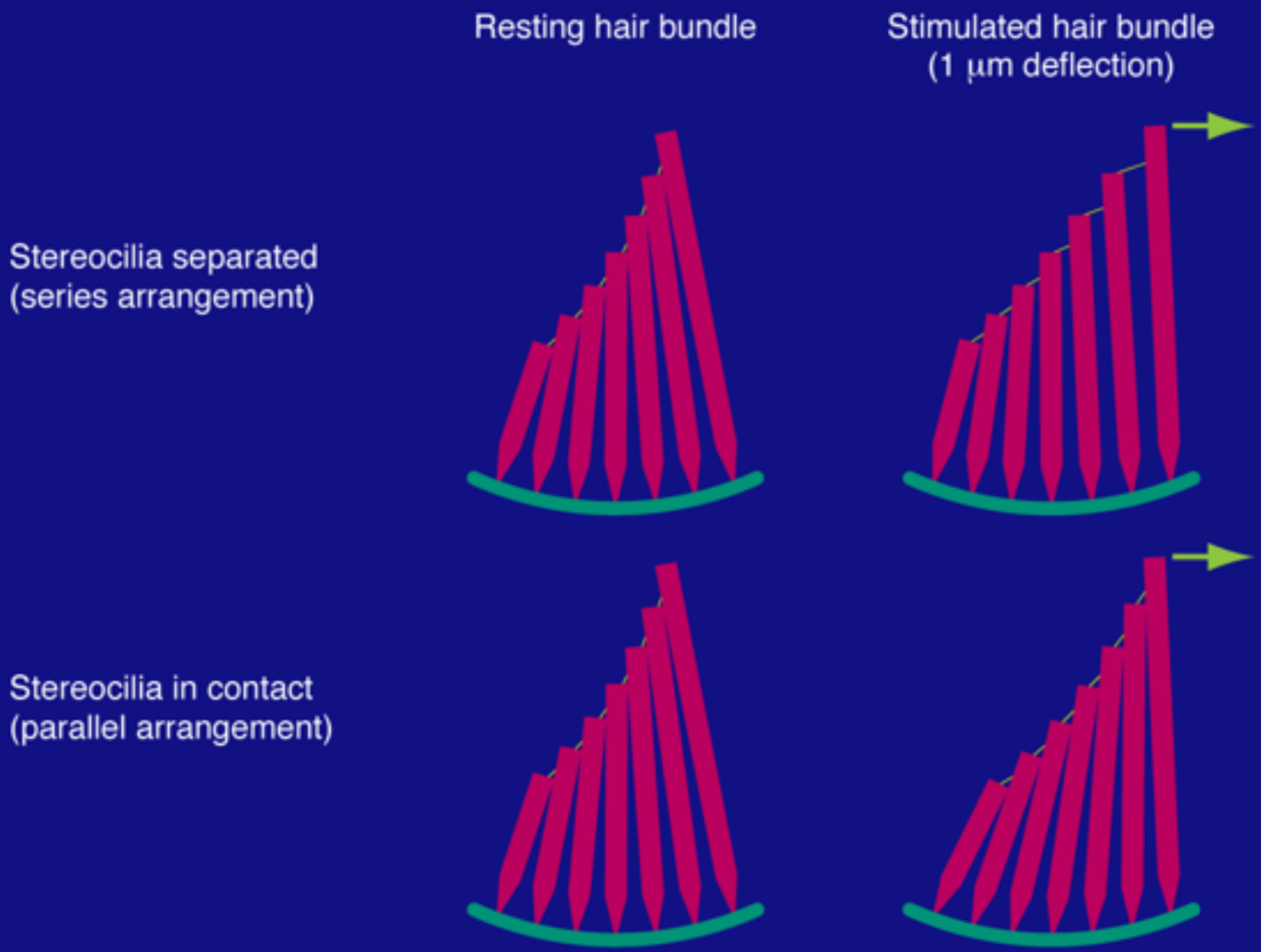
Resting hair bundle
Stimulated hair bundle (1 μm deflection)
Stereocilia separated (series arrangement)
Stereocilia in contact (parallel arrangement)

Thermal (brownian) motion
of resting hair bundle

Stereocilia separated
(series arrangement)

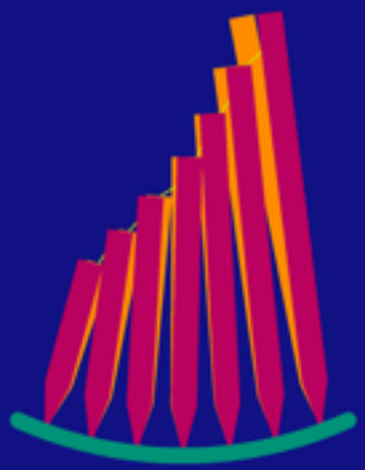

Stereocilia in contact
(parallel arrangement)

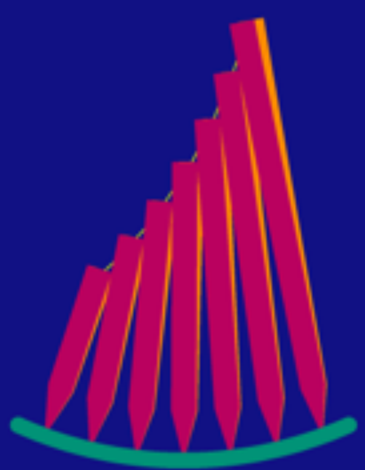

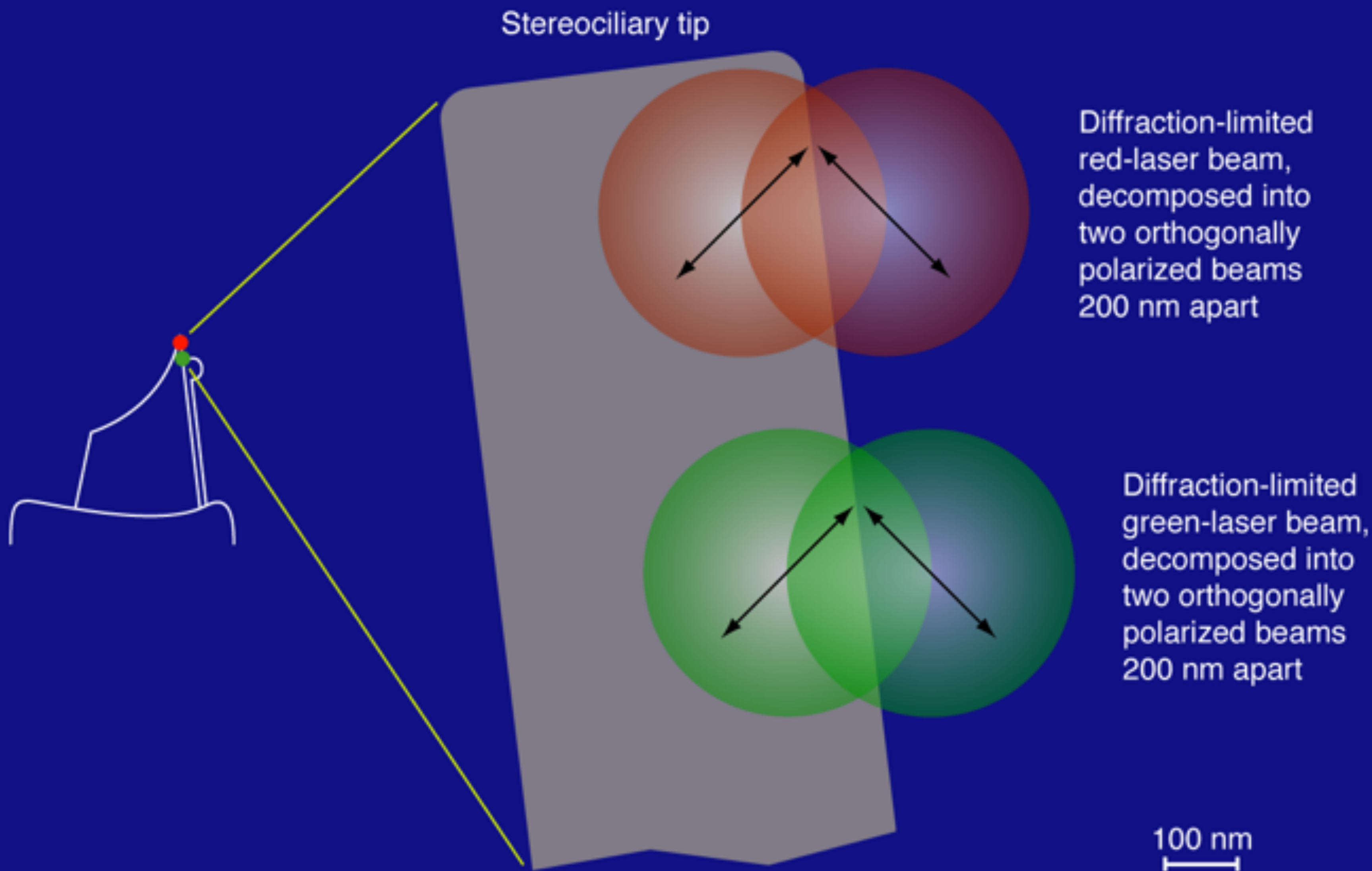
Stereociliary tip
Diffraction-limited
red-laser beam,
decomposed into
two orthogonally
polarized beams
200 nm apart
Diffraction-limited
green-laser beam,
decomposed into
two orthogonally
polarized beams
200 nm apart
100 nm

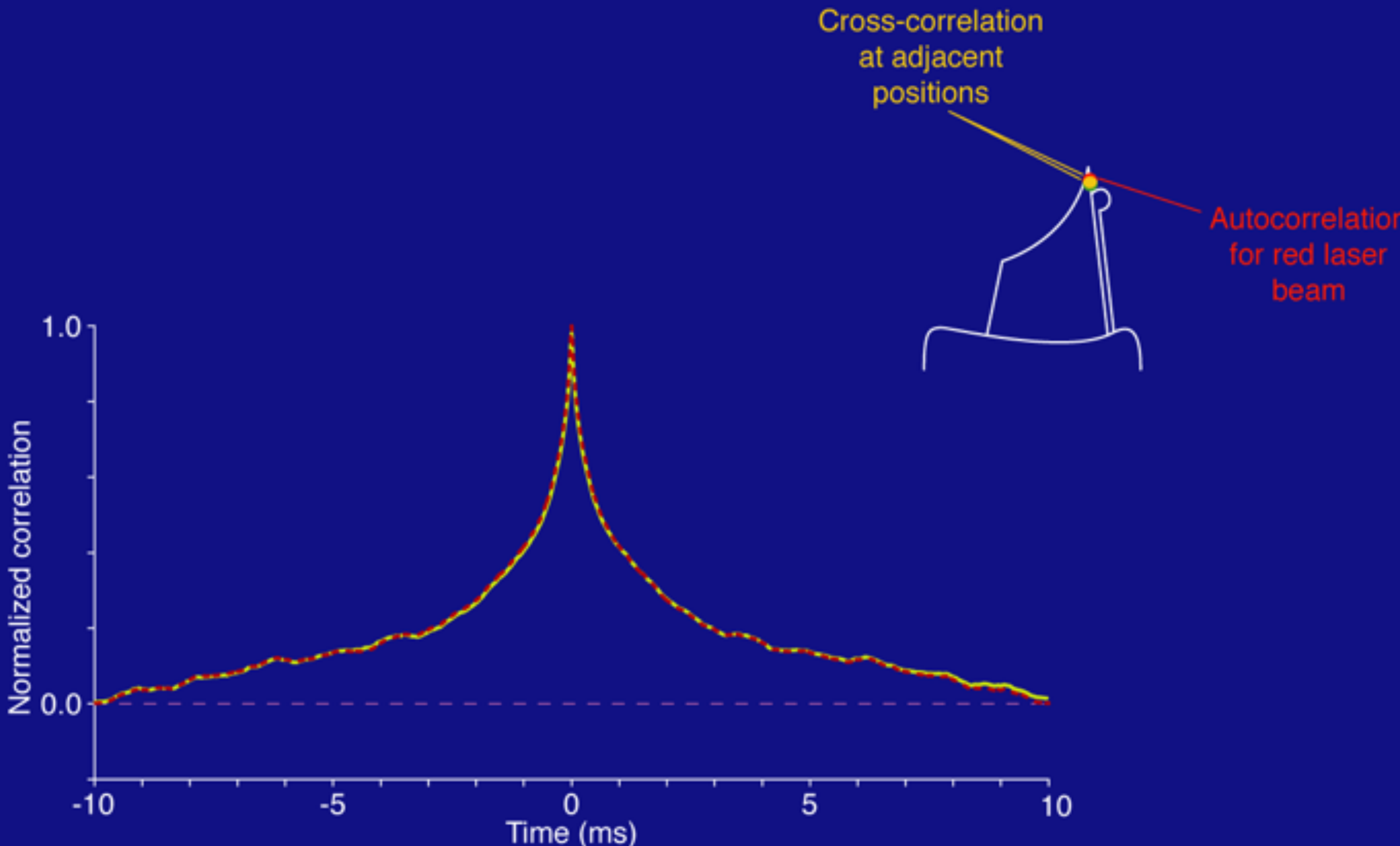

Cross-correlation
at adjacent
positions
Autocorrelation
for red laser
beam
1.0
0.0
Normalized correlation
-10
-5
0
5
10
Time (ms)

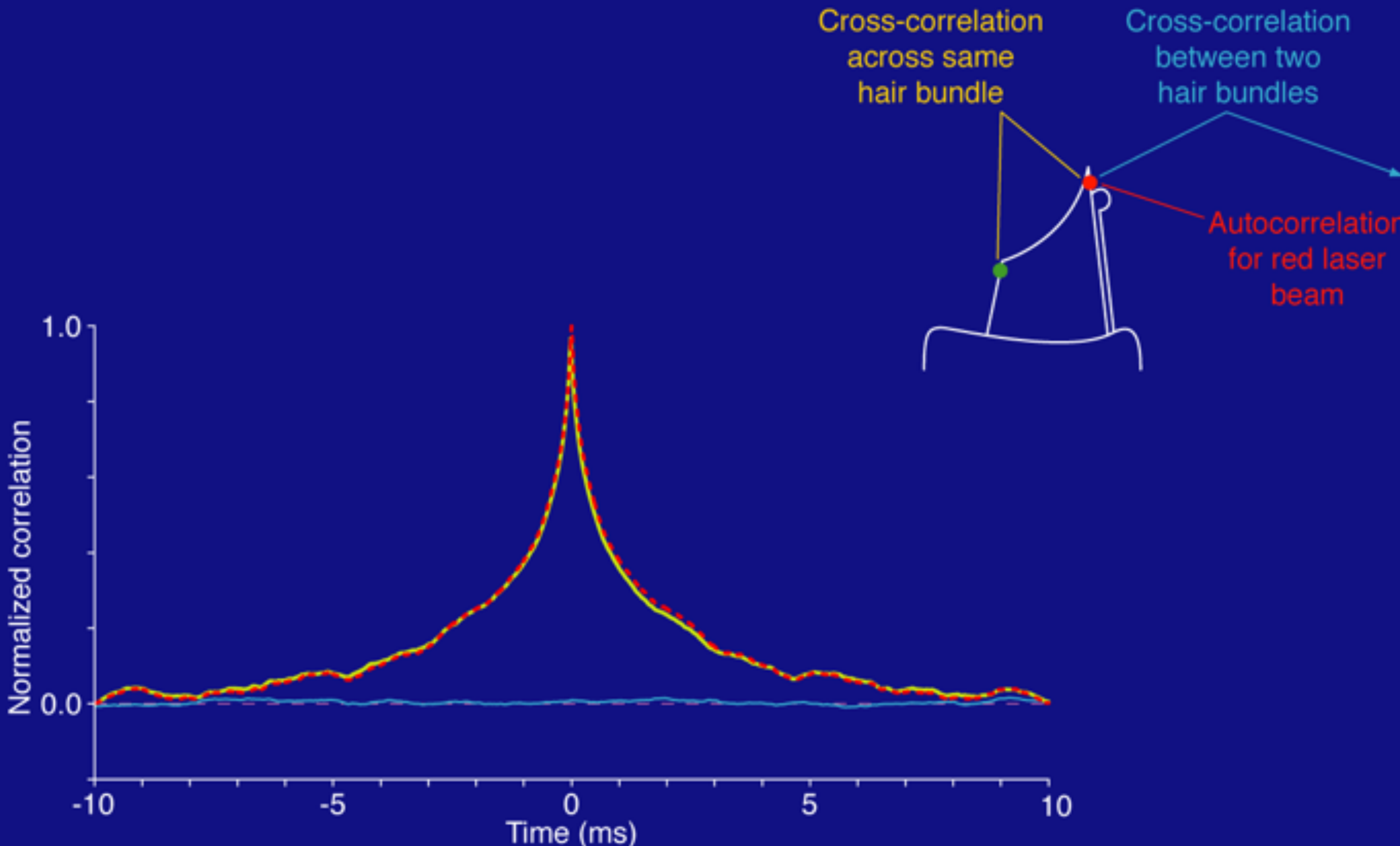
Cross-correlation across same hair bundle
Cross-correlation between two hair bundles
Autocorrelation for red laser beam
1.0
0.0
Normalized correlation
-10
-5
0
5
10
Time (ms)

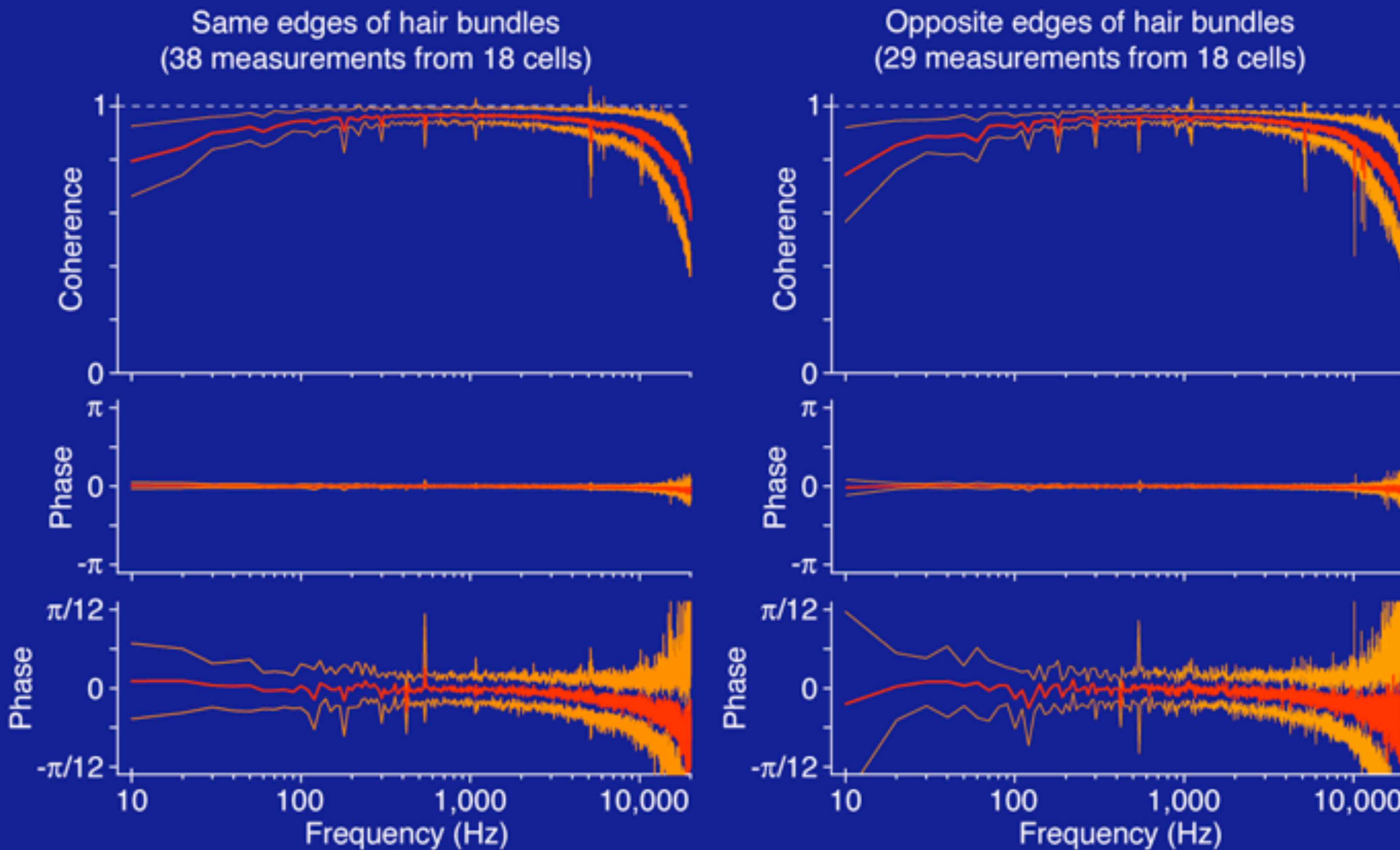

Same edges of hair bundles
(38 measurements from 18 cells)
Opposite edges of hair bundles
(29 measurements from 18 cells)
Coherence
1
0
Phase
π
0
-π
Phase
π/12
0
-π/12
10
100
1,000
10,000
Frequency (Hz)

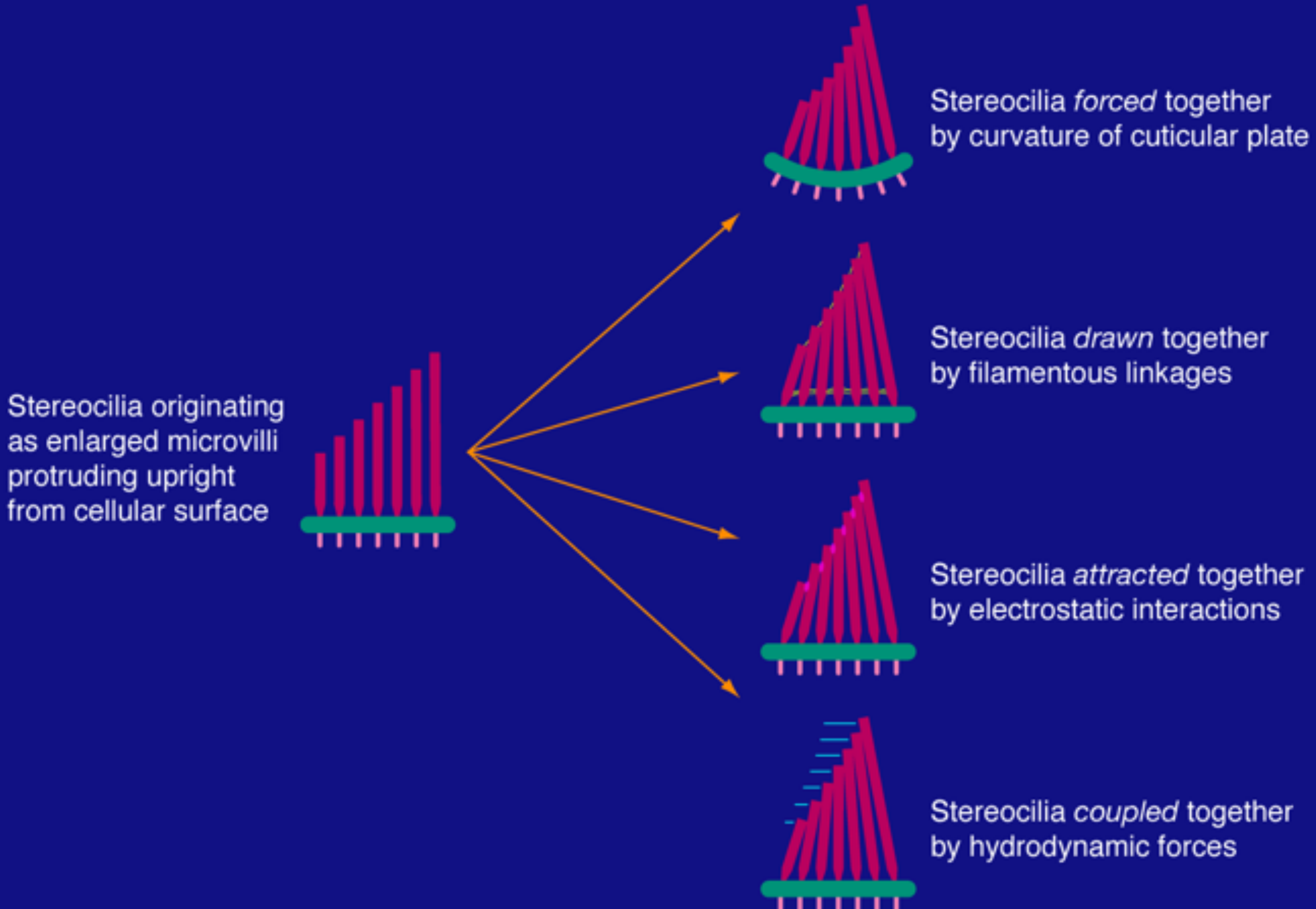

Stereocilia originating as enlarged microvilli protruding upright from cellular surface
Stereocilia *forced* together by curvature of cuticular plate
Stereocilia *drawn* together by filamentous linkages
Stereocilia *attracted* together by electrostatic interactions
Stereocilia *coupled* together by hydrodynamic forces

Finite-element modeling of hydrodynamic coupling between stereocilia

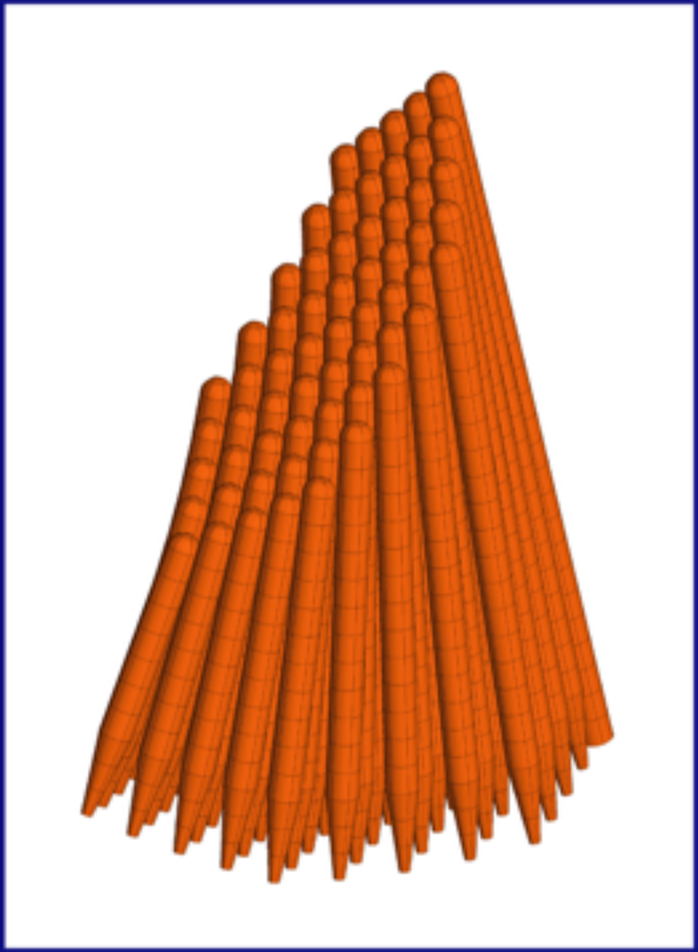

Detailed, quantitative representation of the bullfrog's saccular hair bundle and surrounding liquid

60 stereocilia and a kinocilium in a realistic array

Optional tip links, basal links, and horizontal top connectors

50,000 volume elements (voxels) of sizes adapted to local hydrodynamic conditions

200,000 nodes and 800,000 degrees of freedom

Used in solution of the Navier-Stokes equation for an incompressible liquid:

$$\rho\left(\frac{\partial \mathbf{v}}{\partial t} + \mathbf{v} \cdot \nabla \mathbf{v}\right) = -\nabla p + \mu \nabla^2 \mathbf{v}$$

for flow velocity $\boldsymbol{v}$, density ρ, pressure p, and dynamic viscosity μ

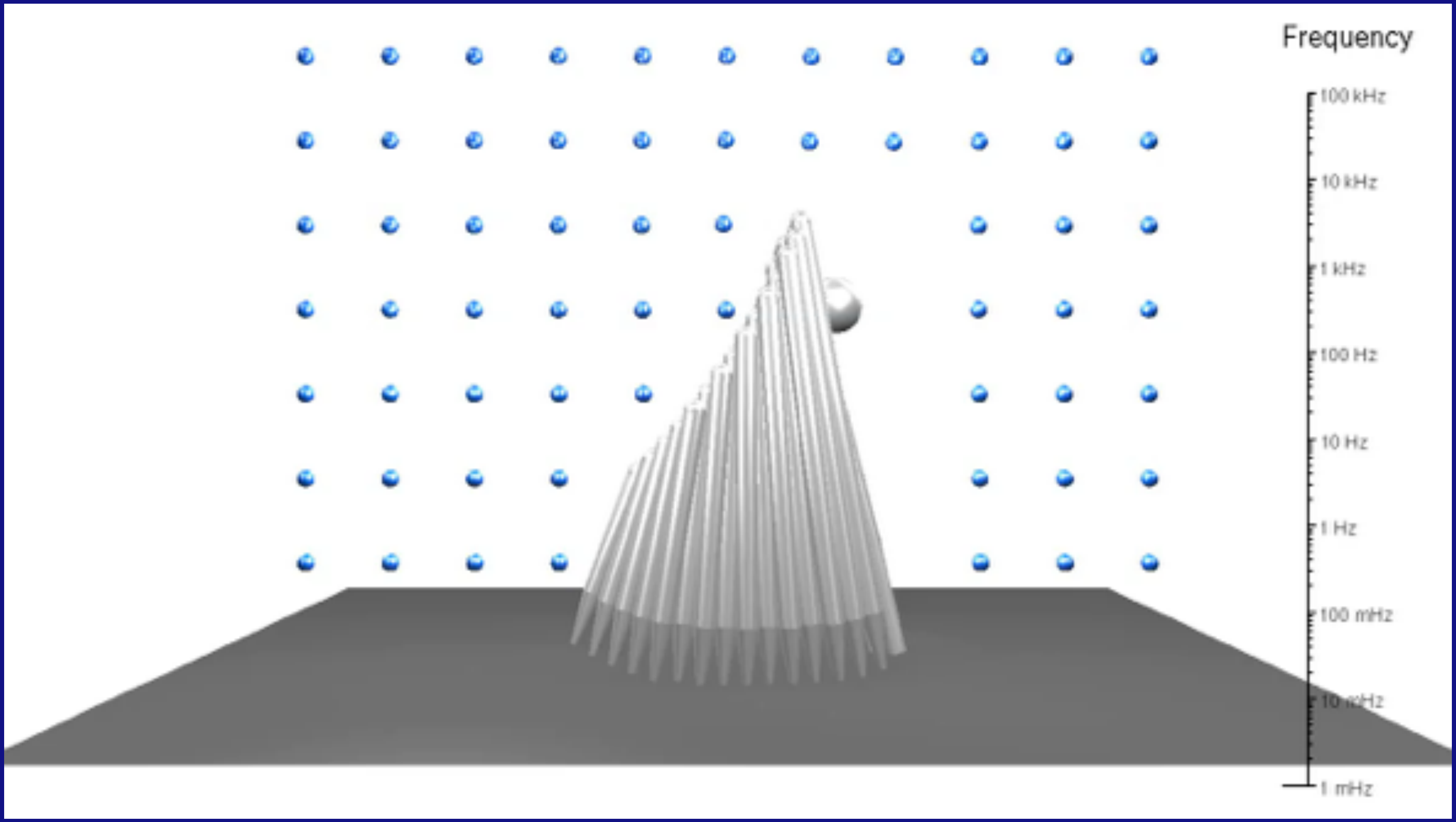
Frequency
100 kHz
10 kHz
1 kHz
100 Hz
10 Hz
1 Hz
100 mHz
10 mHz
1 mHz

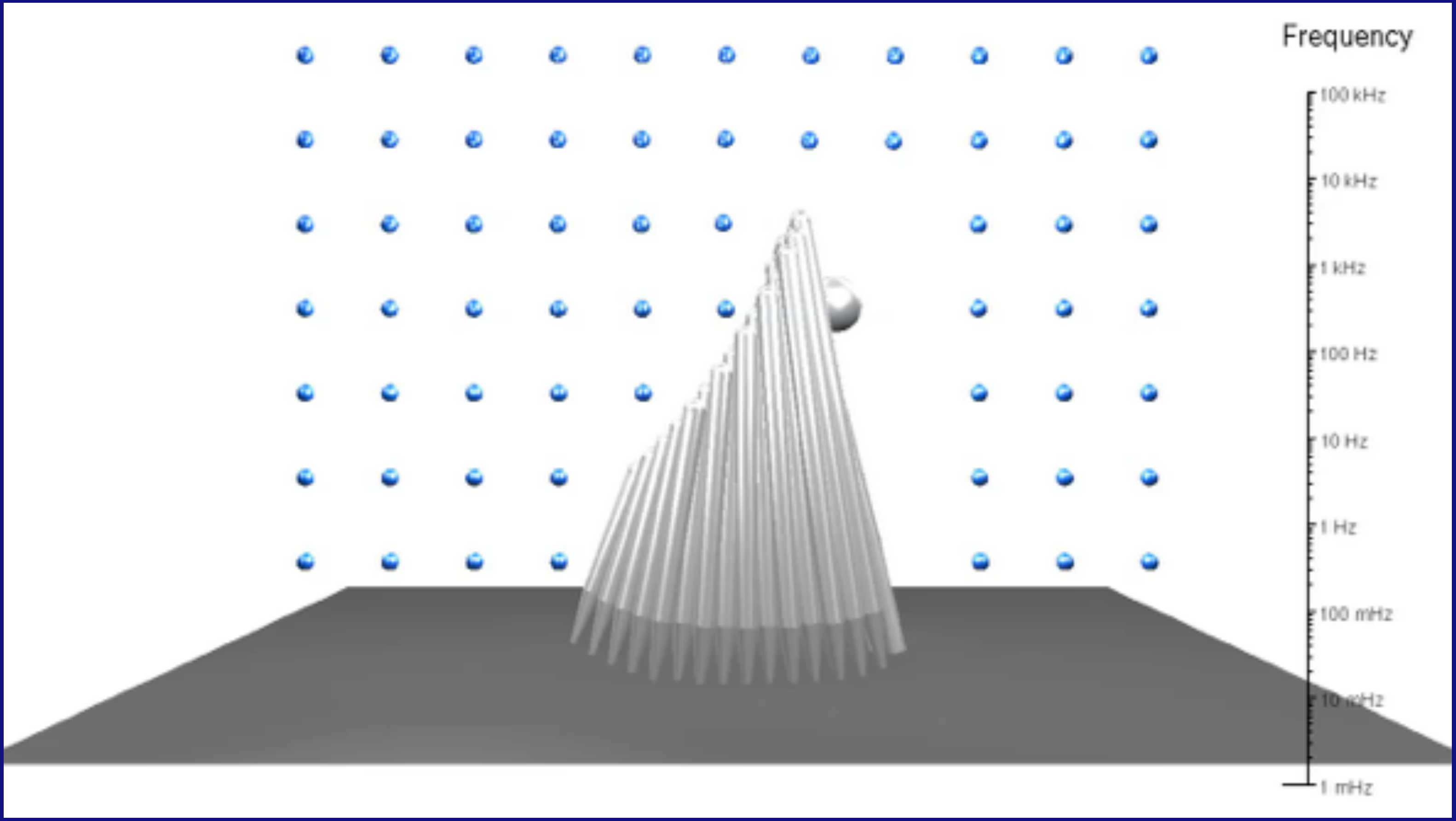

Frequency
100 kHz
10 kHz
1 kHz
100 Hz
10 Hz
1 Hz
100 mHz
10 mHz
1 mHz

Squeezing mode of
stereociliary motion
(series arrangement)

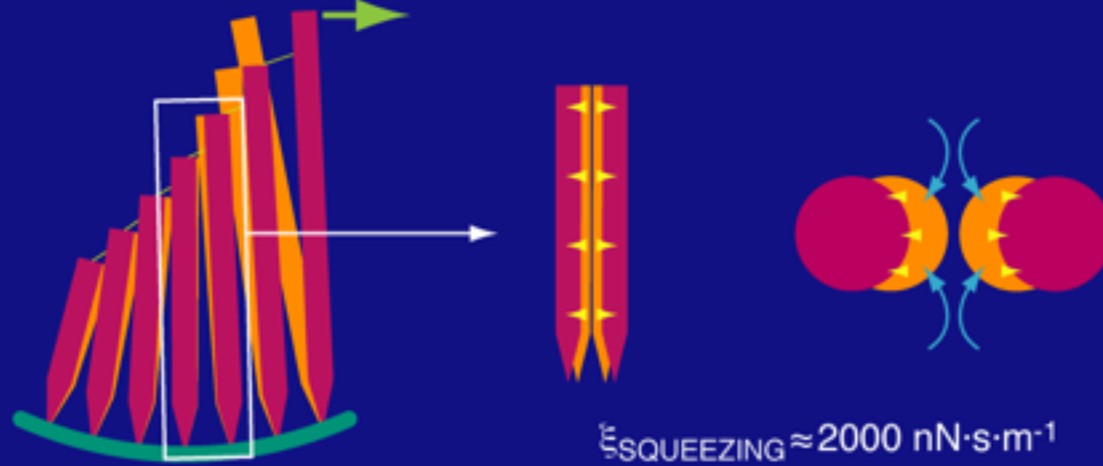

Shearing mode of
stereociliary motion
(parallel arrangement)

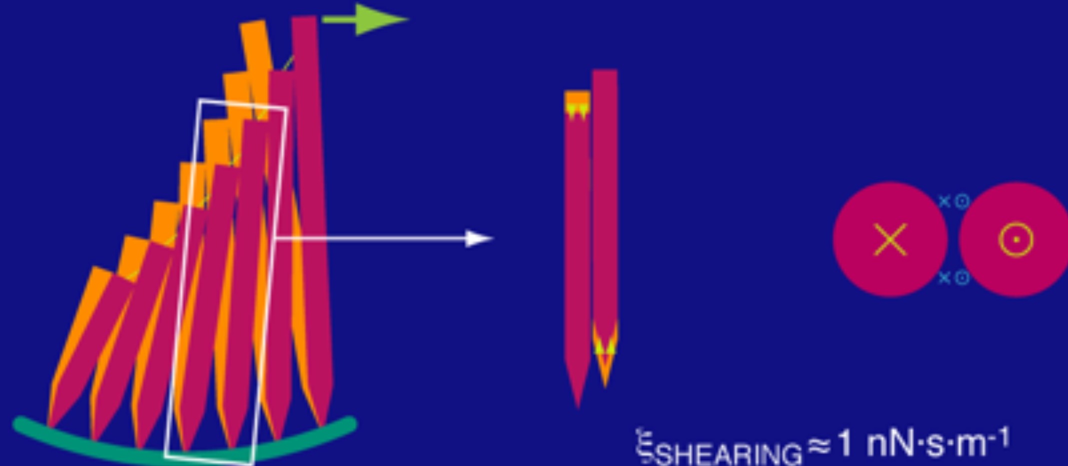

SLOW ADAPTATION

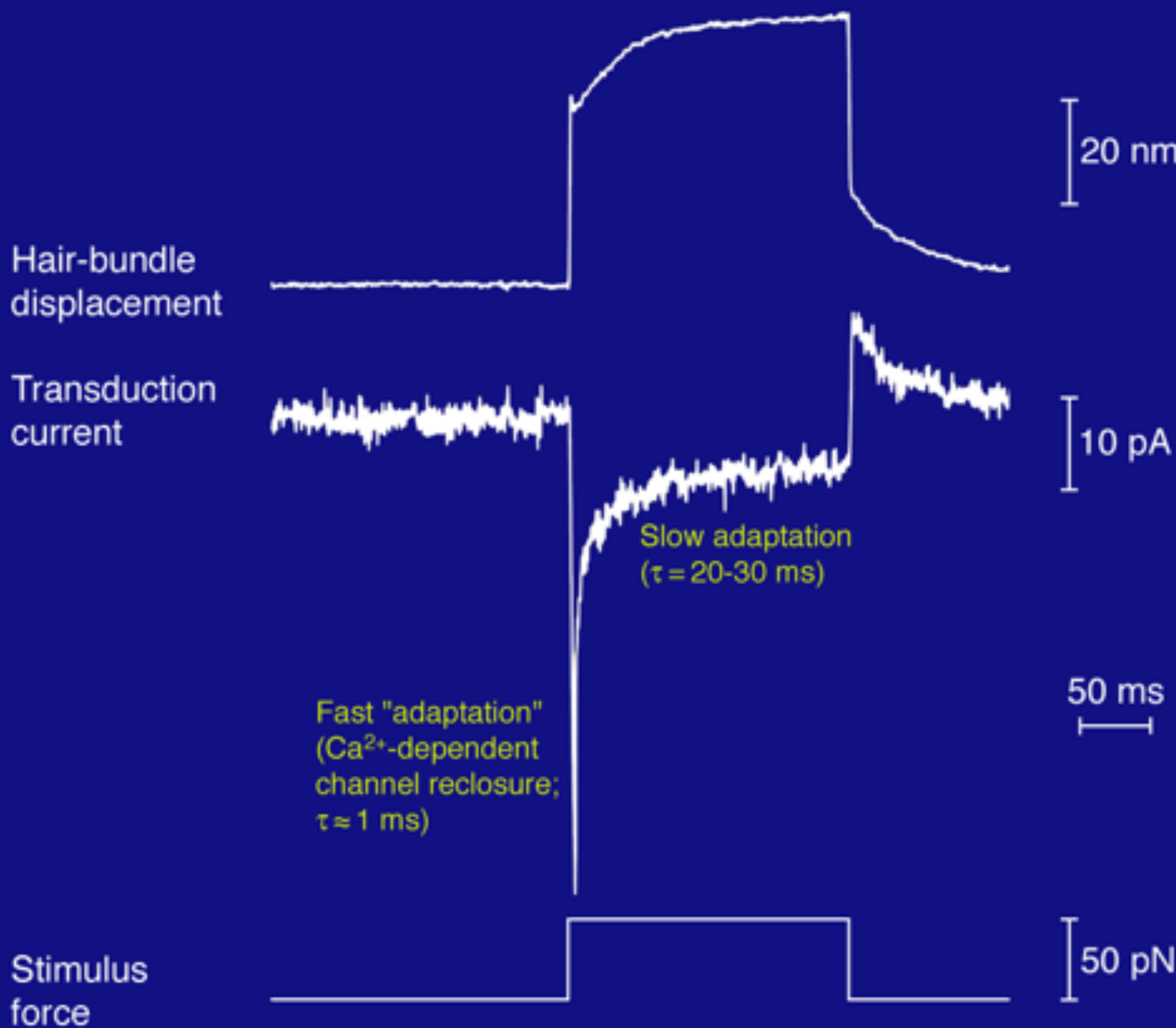

Hair-bundle displacement
Transduction current
Stimulus force
20 nm
10 pA
50 ms
50 pN
Slow adaptation
(τ = 20-30 ms)
Fast "adaptation"
(Ca2+-dependent
channel reclosure;
τ ≈ 1 ms)

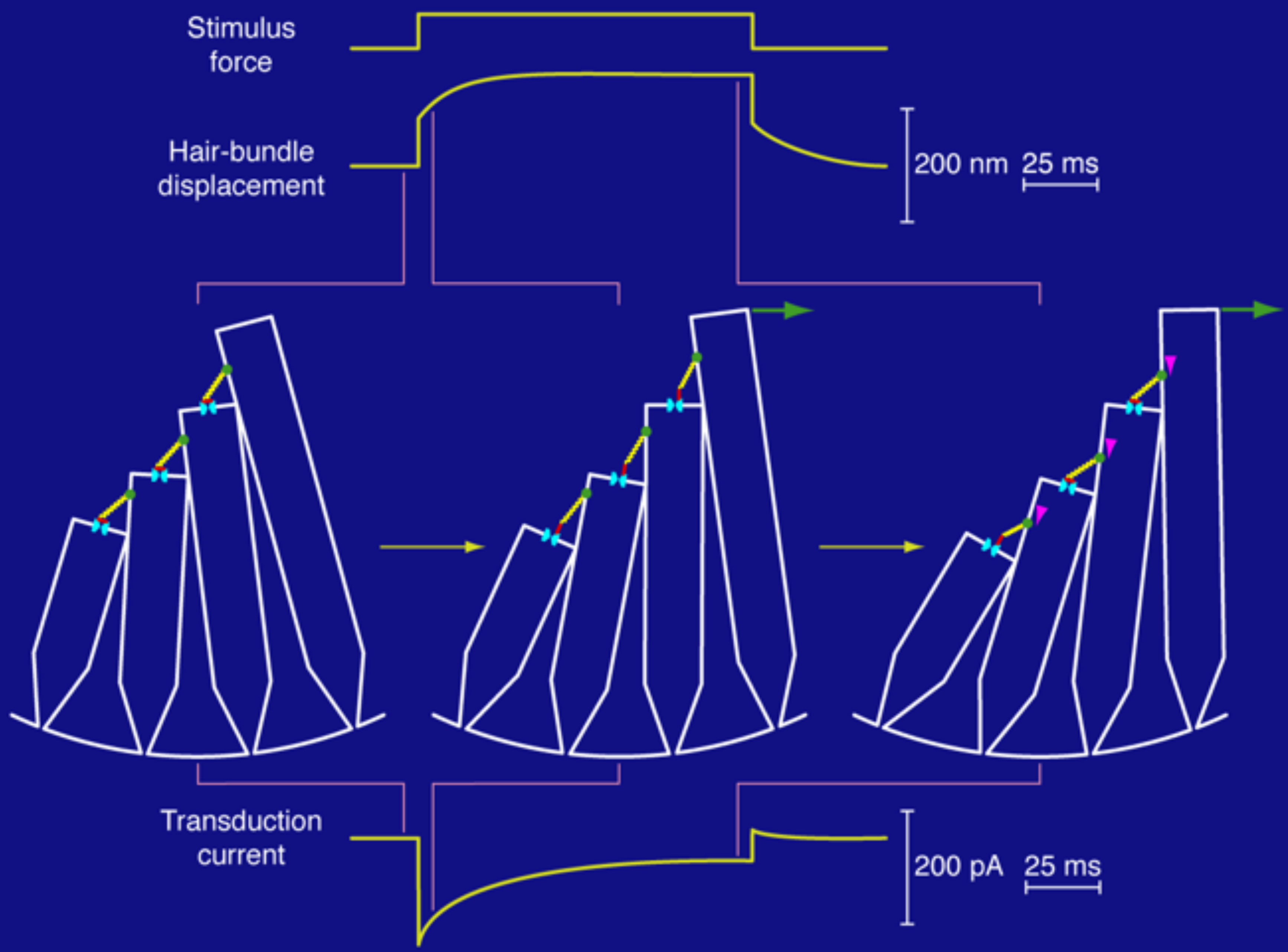
Stimulus
force
Hair-bundle
displacement
200 nm
25 ms
Transduction
current
200 pA
25 ms

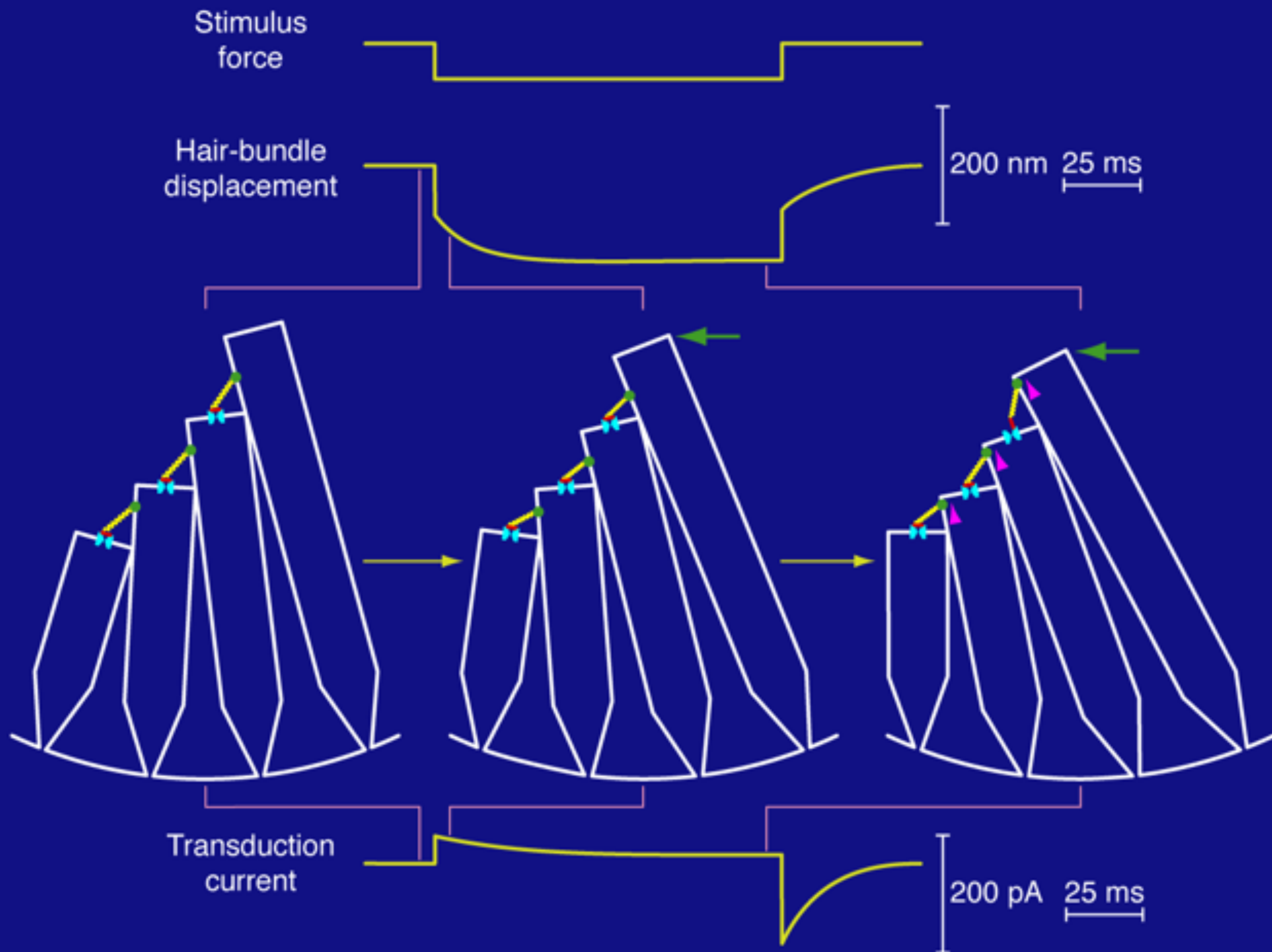
Stimulus
force
Hair-bundle
displacement
200 nm
25 ms
Transduction
current
200 pA
25 ms

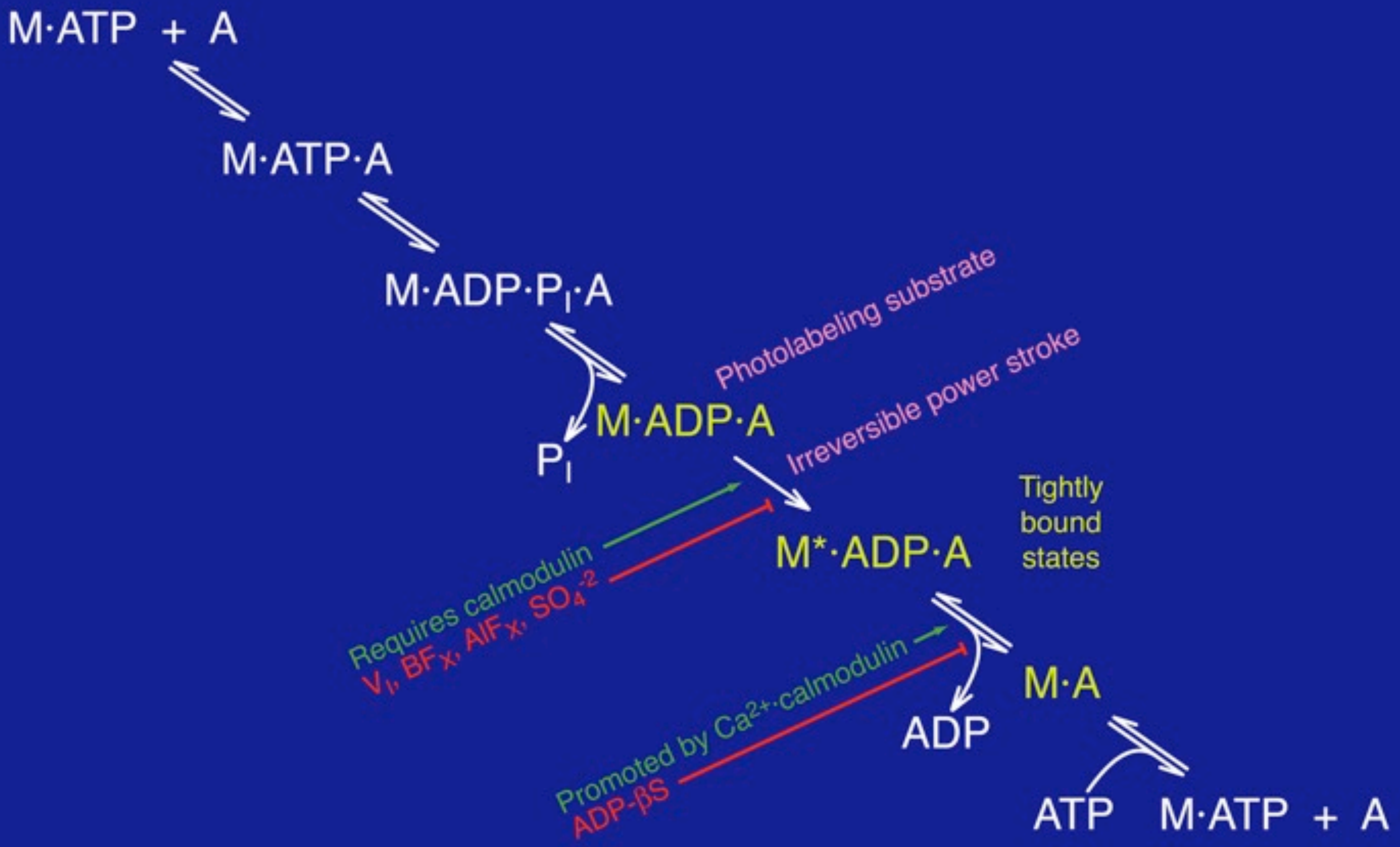

M·ATP + A
M·ATP·A
M·ADP·P$_I$·A
Photolabeling substrate
Irreversible power stroke
M·ADP·A
P$_I$
Tightly bound states
M*·ADP·A
Requires calmodulin
V$_I$, BF$_X$, AlF$_X$, SO$_4^{-2}$
M·A
ADP
Promoted by Ca^{2+}·calmodulin
ADP-βS
ATP
M·ATP + A

Myosin labeling
with[α-^{32}P]UTP
by vanadate trapping
and photo-crosslinking

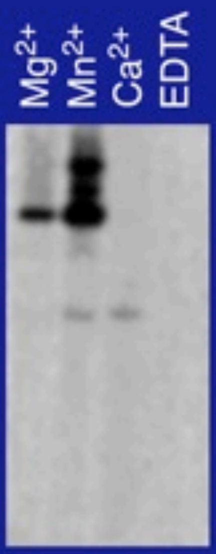

Immunoblotting
with anti-mammalian
adrenal myosin Ic

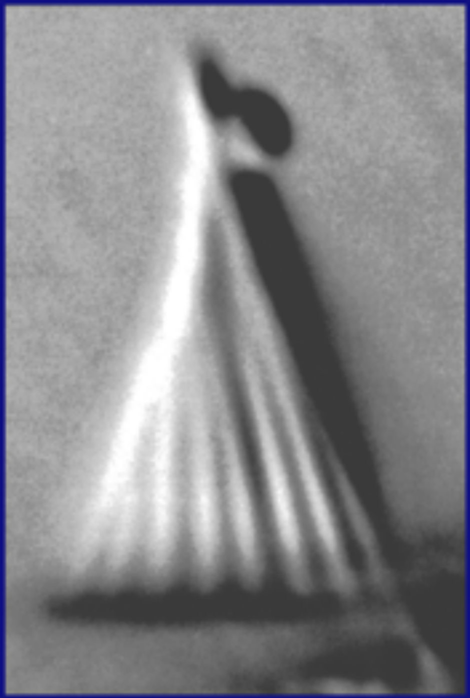

Differential-interference-
contrast microscopy

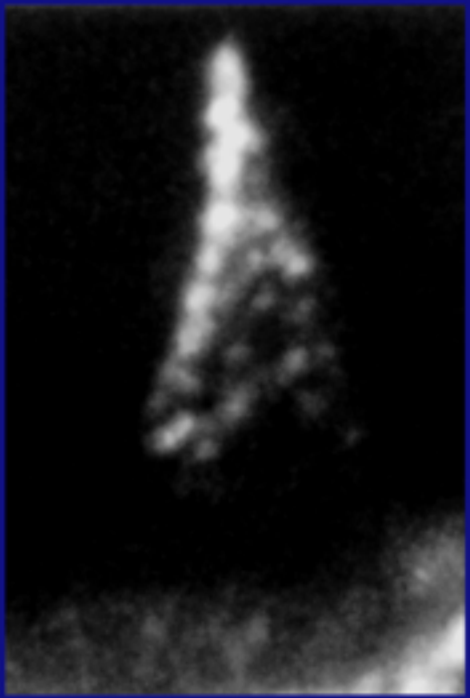

Myosin-1c
immunoreactivity

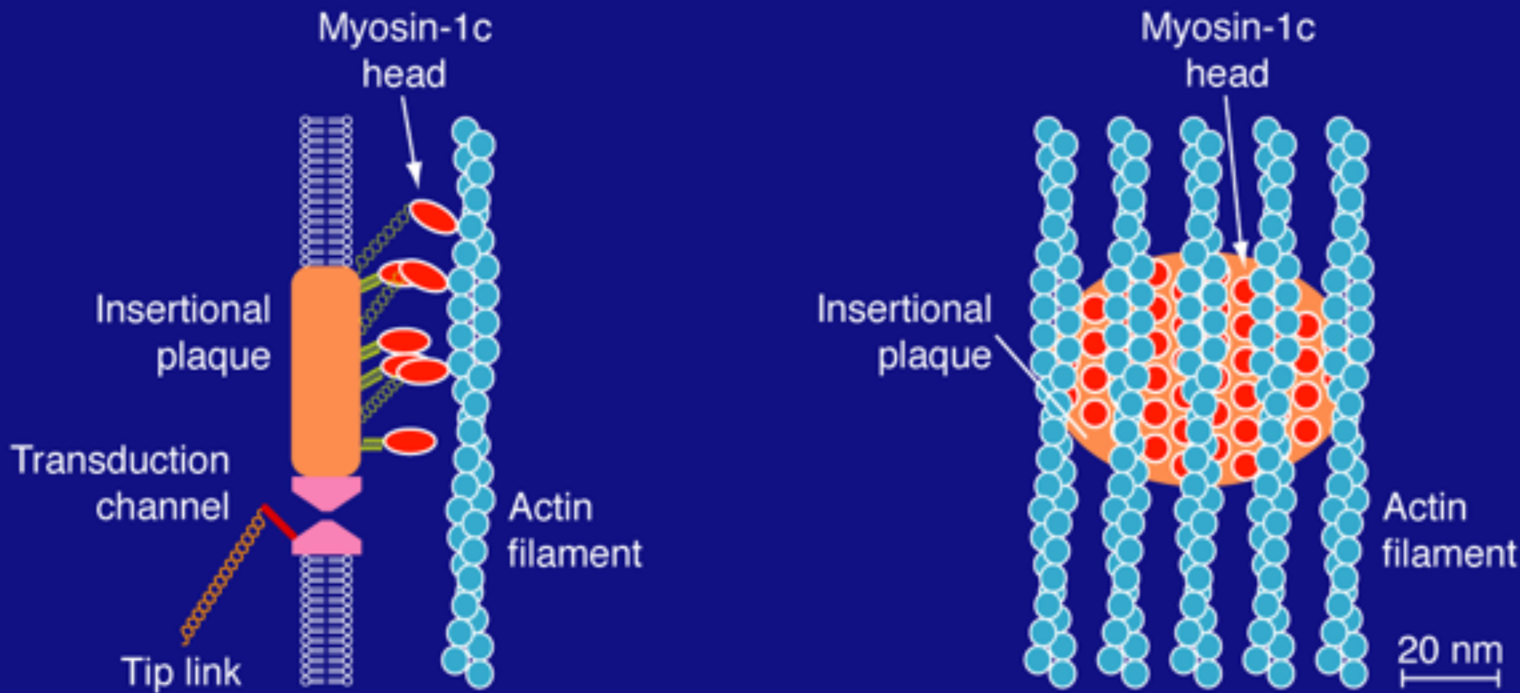
Myosin-1c head
Insertional plaque
Transduction channel
Tip link
Actin filament
Myosin-1c head
Insertional plaque
Actin filament
20 nm

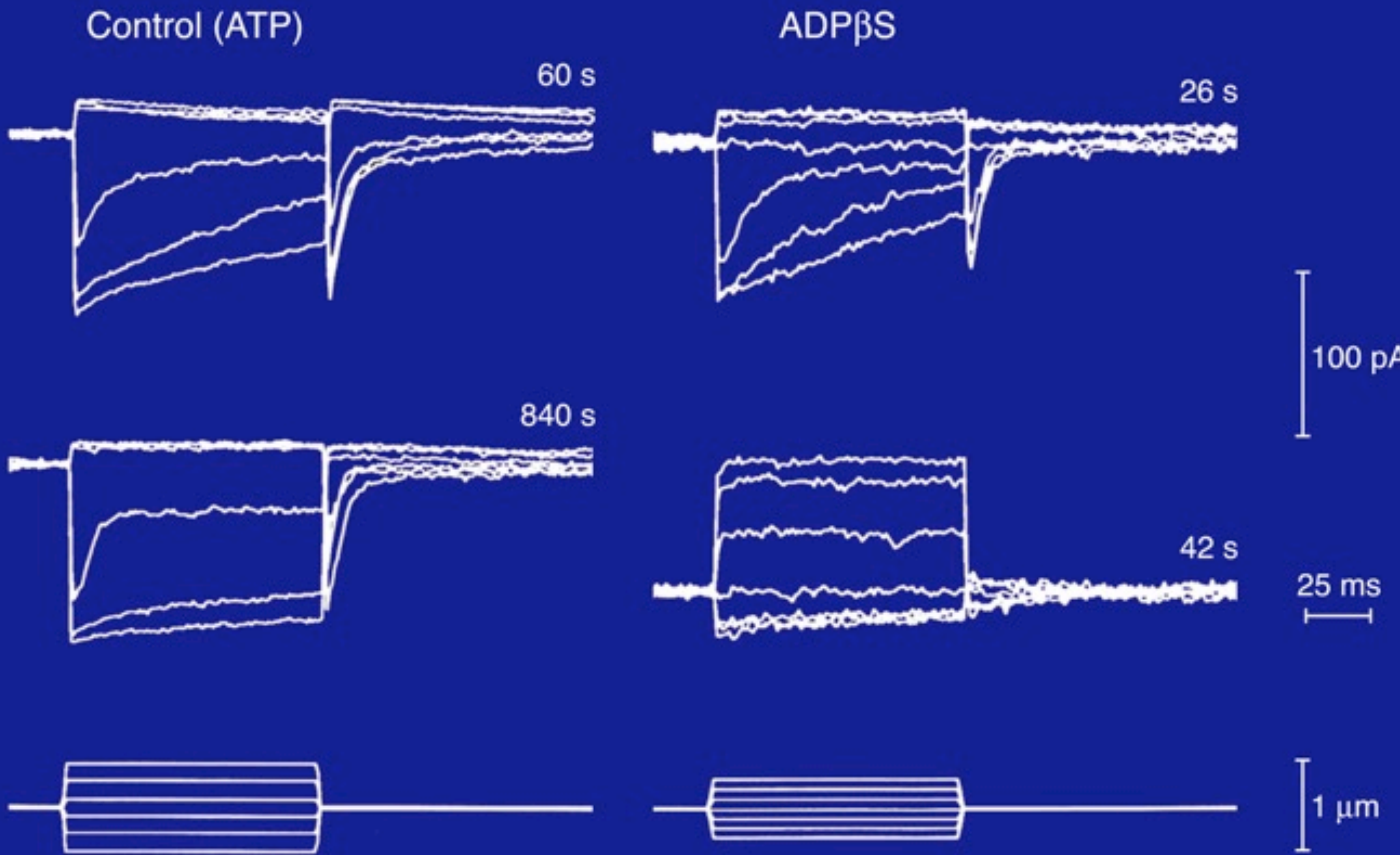
Control (ATP)
ADPβS
60 s
26 s
100 pA
840 s
42 s
25 ms
1 μm

Site-directed mutagenesis of transgenic myosin-1c to permit binding of a blocker

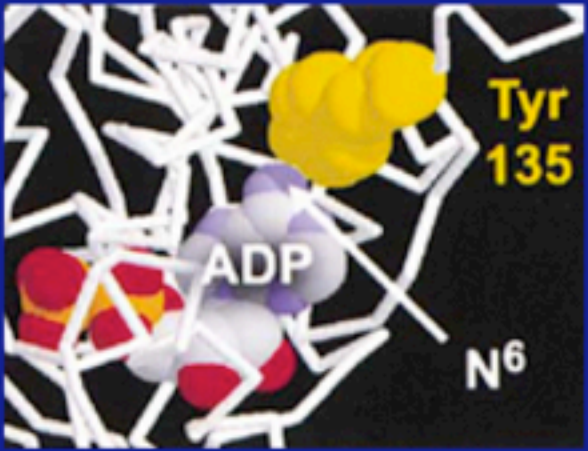

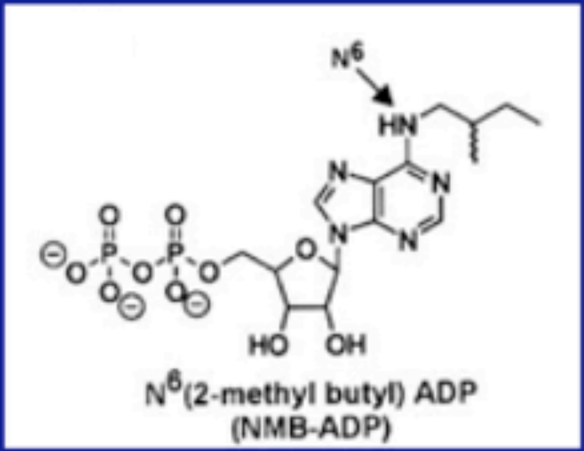

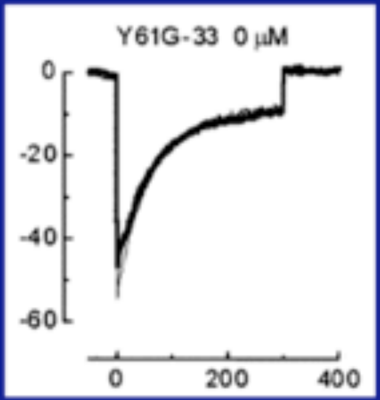

Mutant myosin-1c
with ordinary ATP

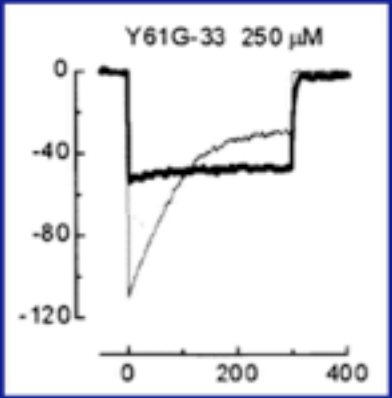

Mutant myosin-1c
with ADP analog

After Holt *et al.*, 2002

HAIR – BUNDLE OSCILLATION

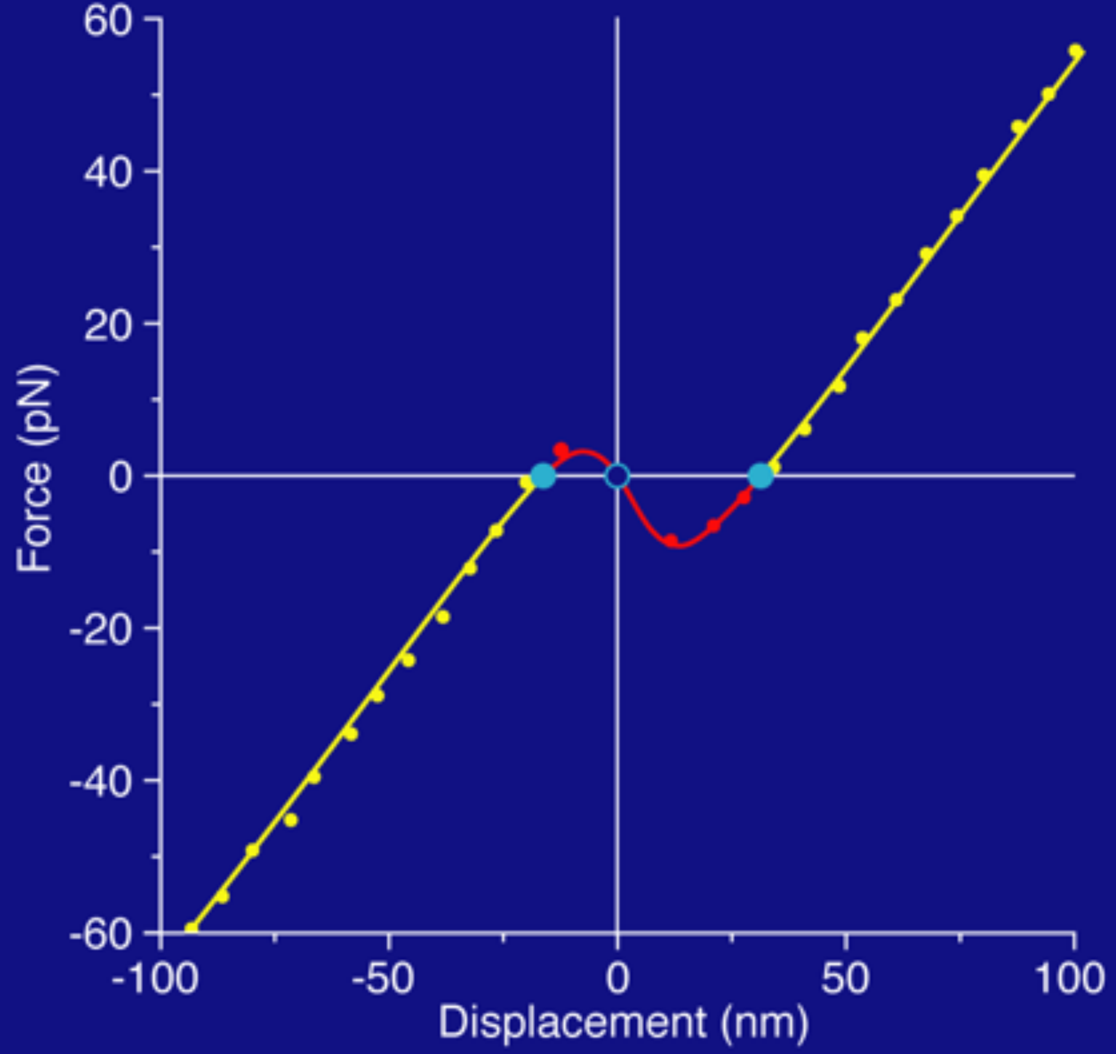
60
40
20
0
-20
-40
-60
Force (pN)
-100
-50
0
50
100
Displacement (nm)

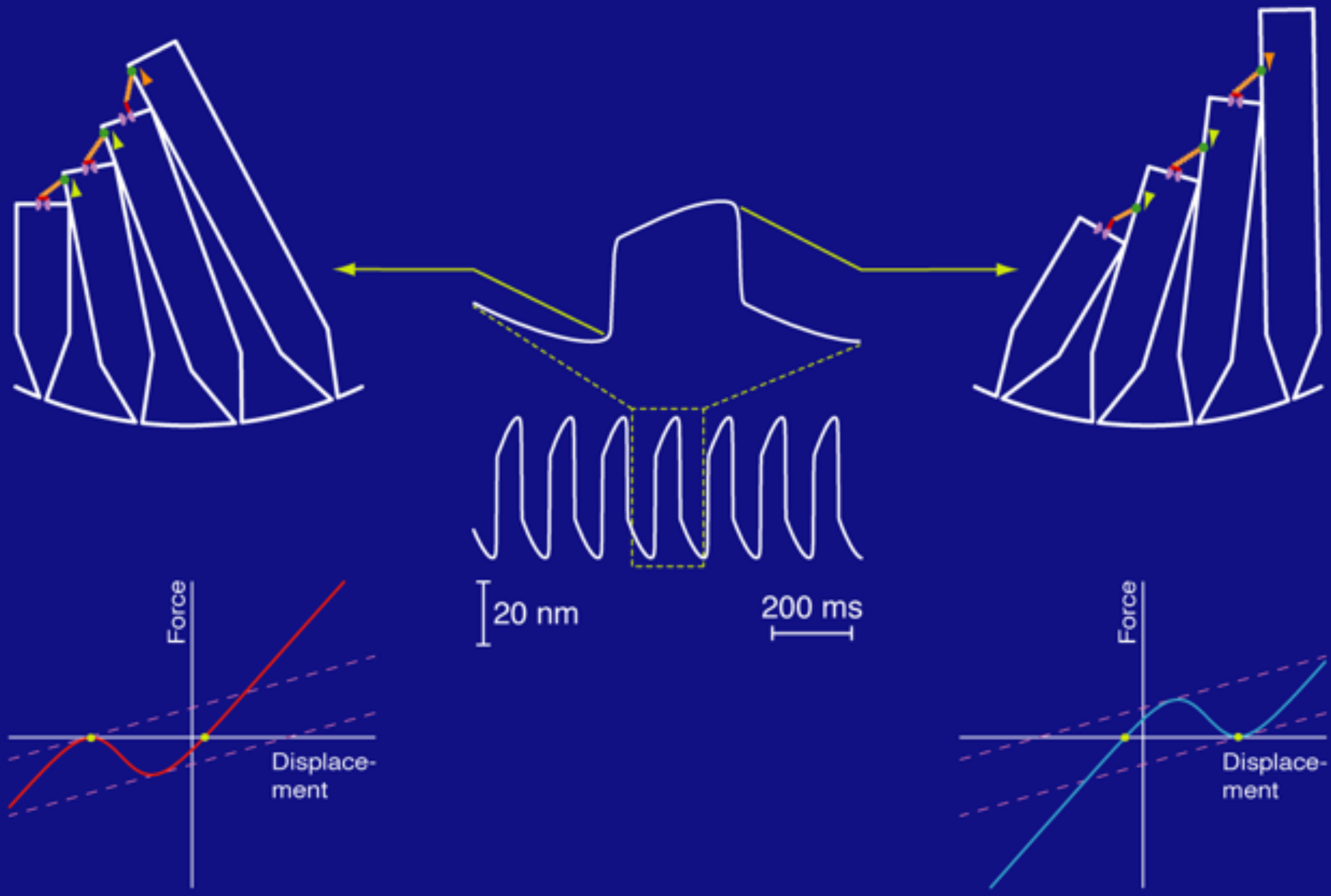

20 nm
200 ms
Force
Displace-
ment
Force
Displace-
ment

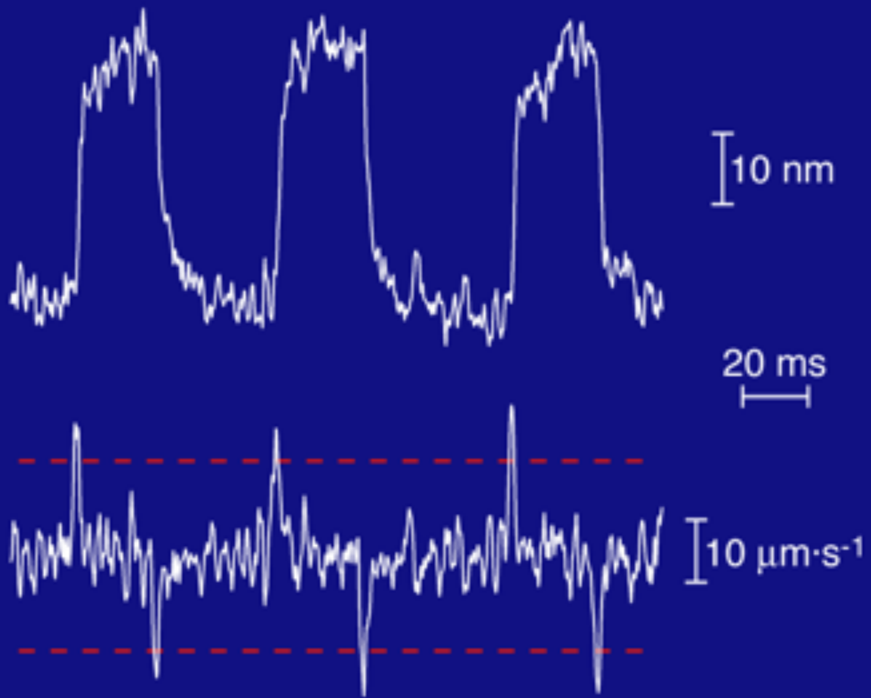

10 nm
20 ms
10 µm·s-1

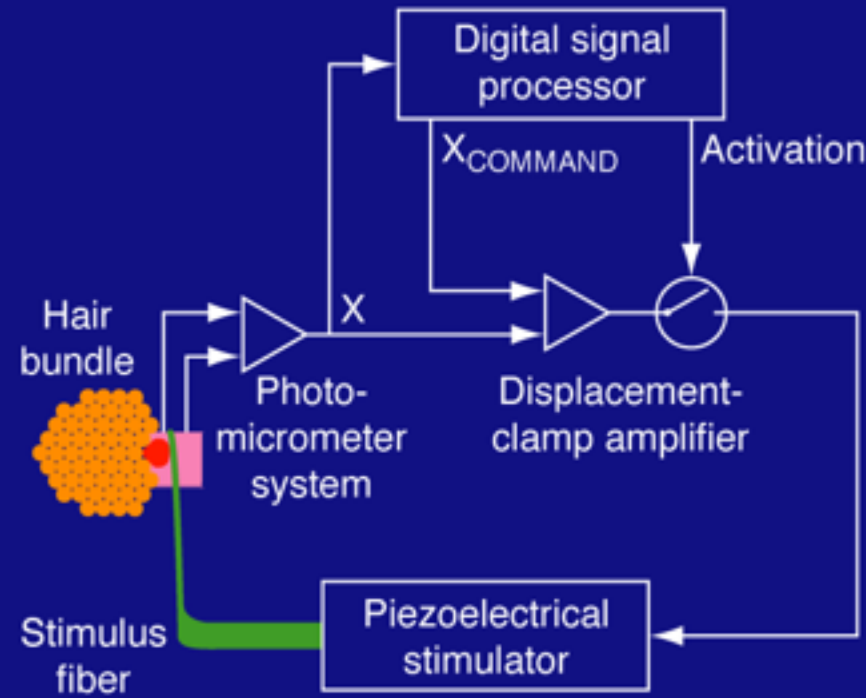

Digital signal processor
XCOMMAND
Activation
X
Hair bundle
Photo-micrometer system
Displacement-clamp amplifier
Stimulus fiber
Piezoelectrical stimulator

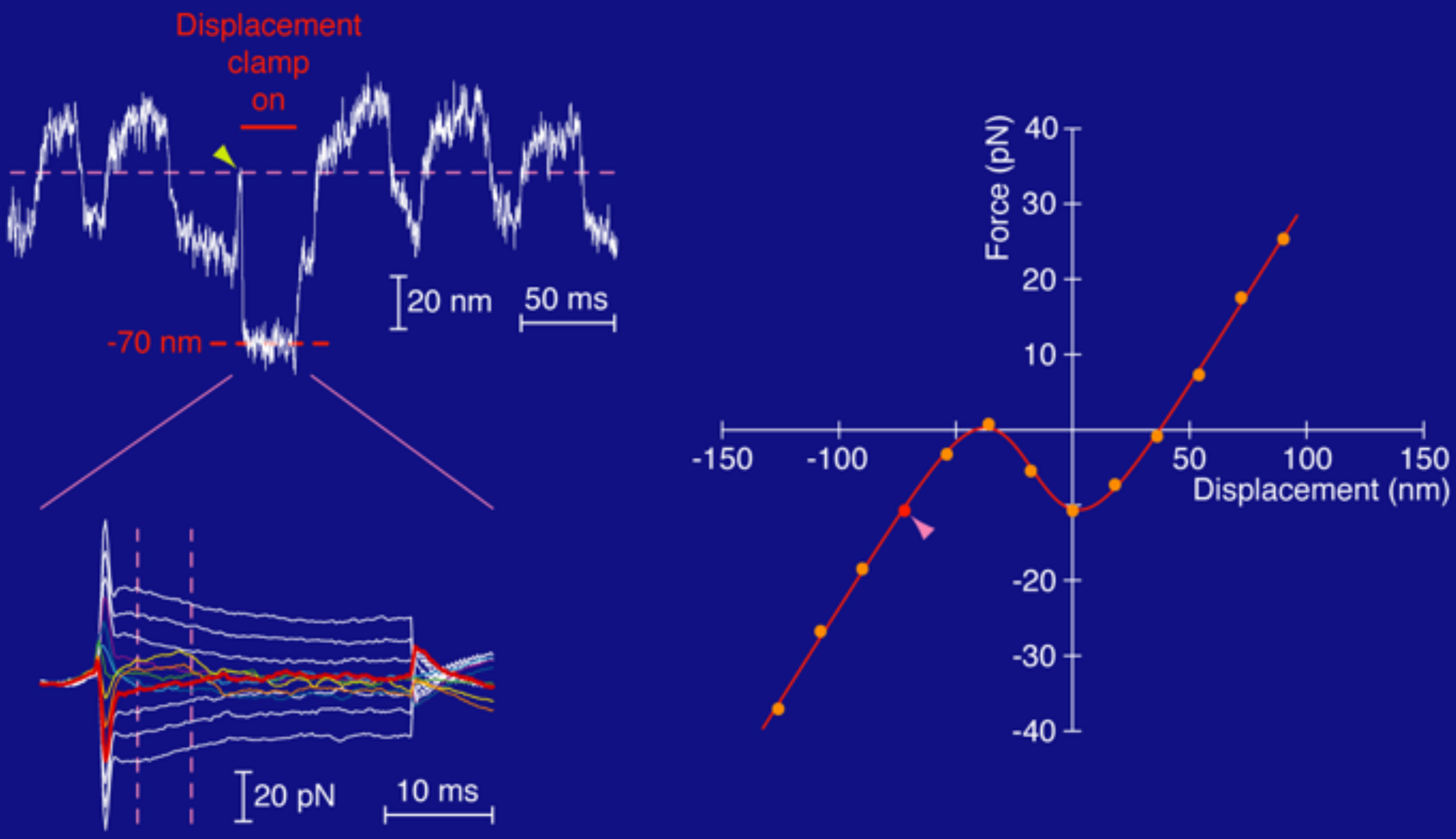

Displacement
clamp
on
20 nm
50 ms
-70 nm
20 pN
10 ms
Force (pN)
40
30
20
10
-20
-30
-40
-150
-100
50
100
150
Displacement (nm)

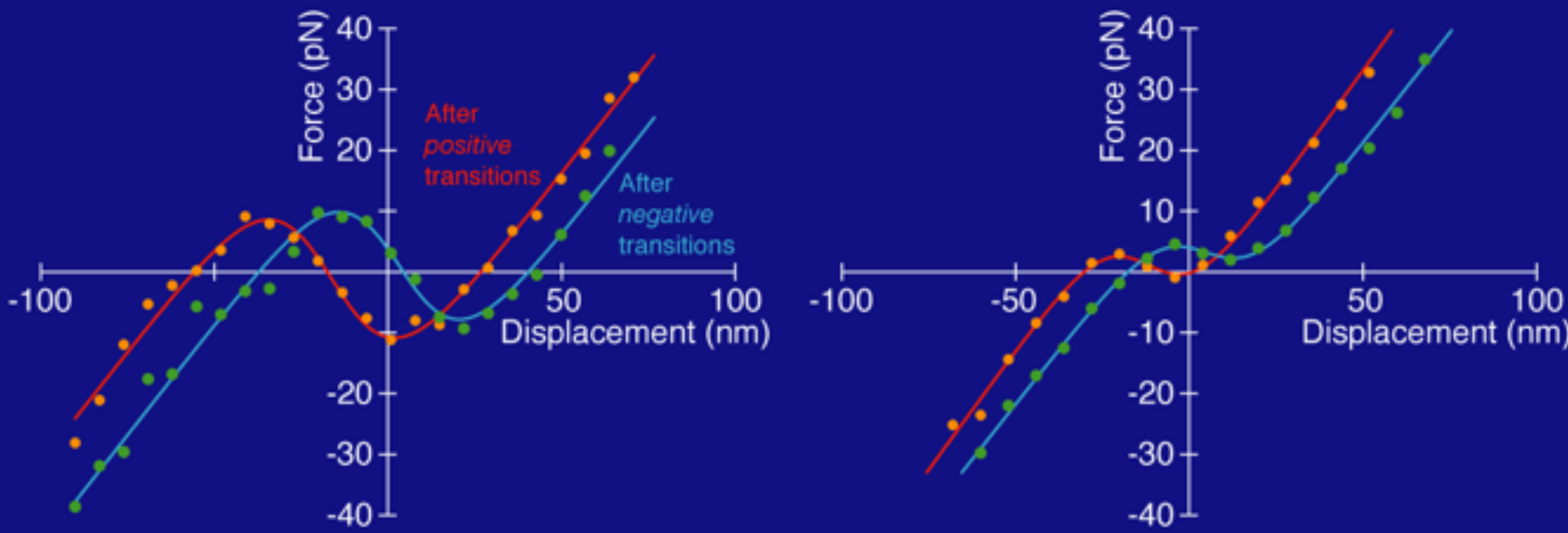
Force (pN)
40
30
20
-20
-30
-40
-100
50
100
Displacement (nm)
After
positive
transitions
After
negative
transitions
Force (pN)
40
30
20
10
-10
-20
-30
-40
-100
-50
50
100
Displacement (nm)

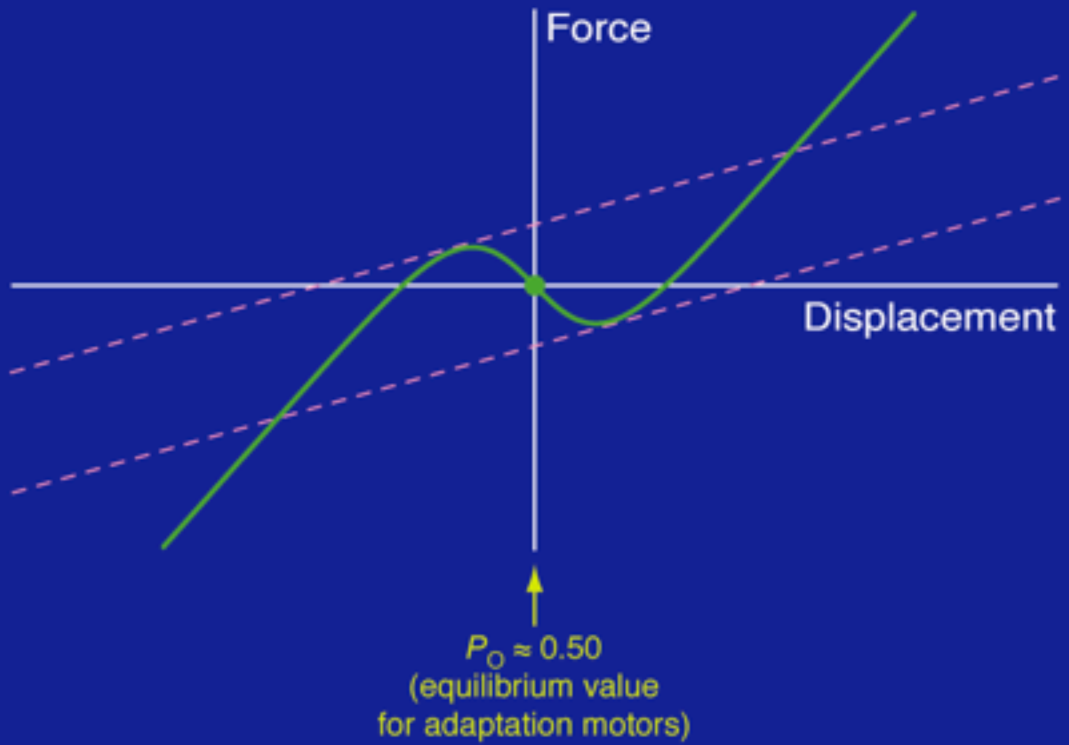

Force
Displacement
$P_O \approx 0.50$
(equilibrium value
for adaptation motors)

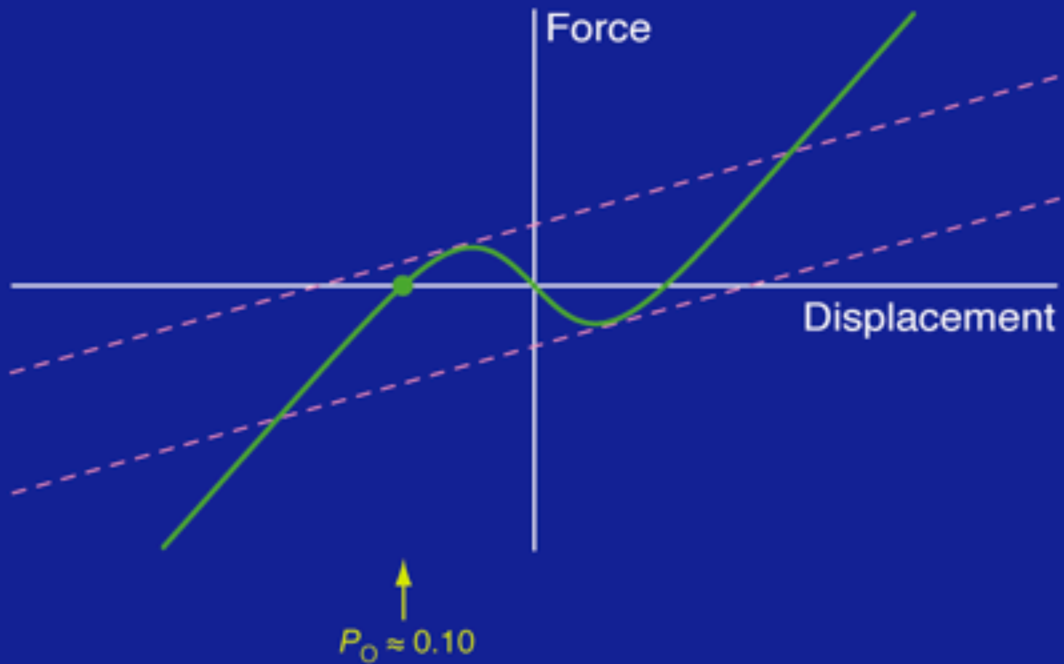
Force
Displacement
$P_O \approx 0.10$

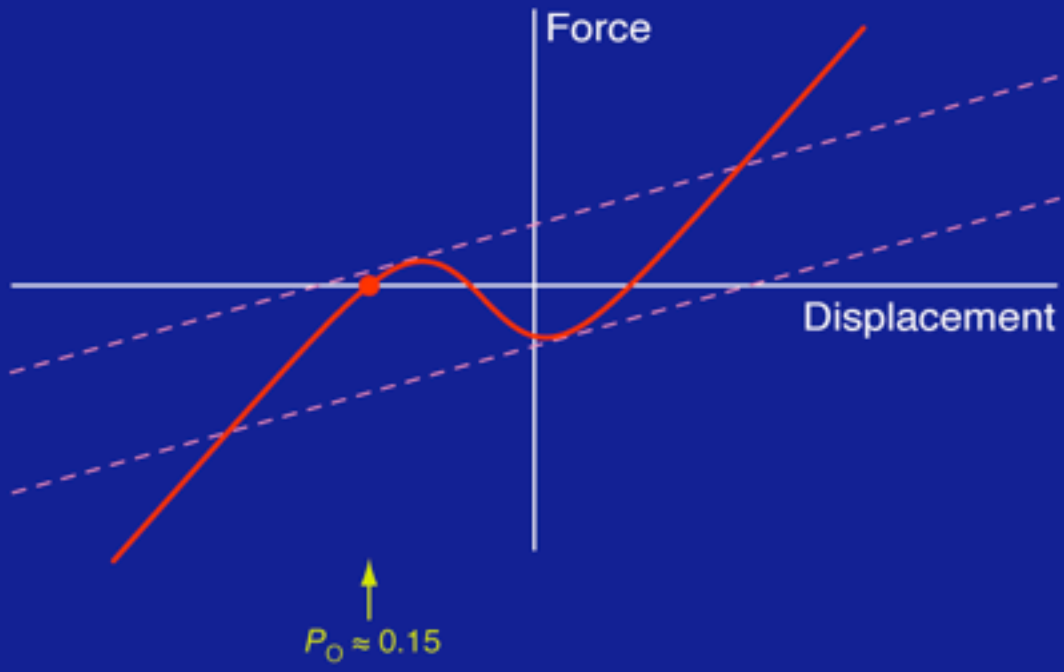

Force
Displacement
$P_O \approx 0.15$

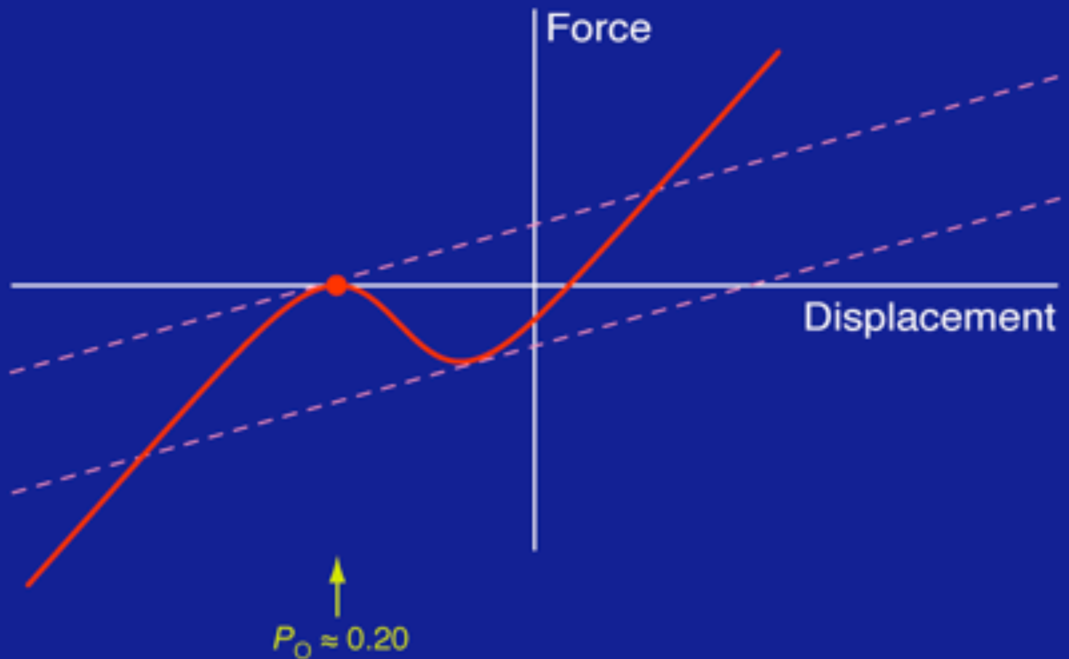

Force
Displacement
$P_O \approx 0.20$

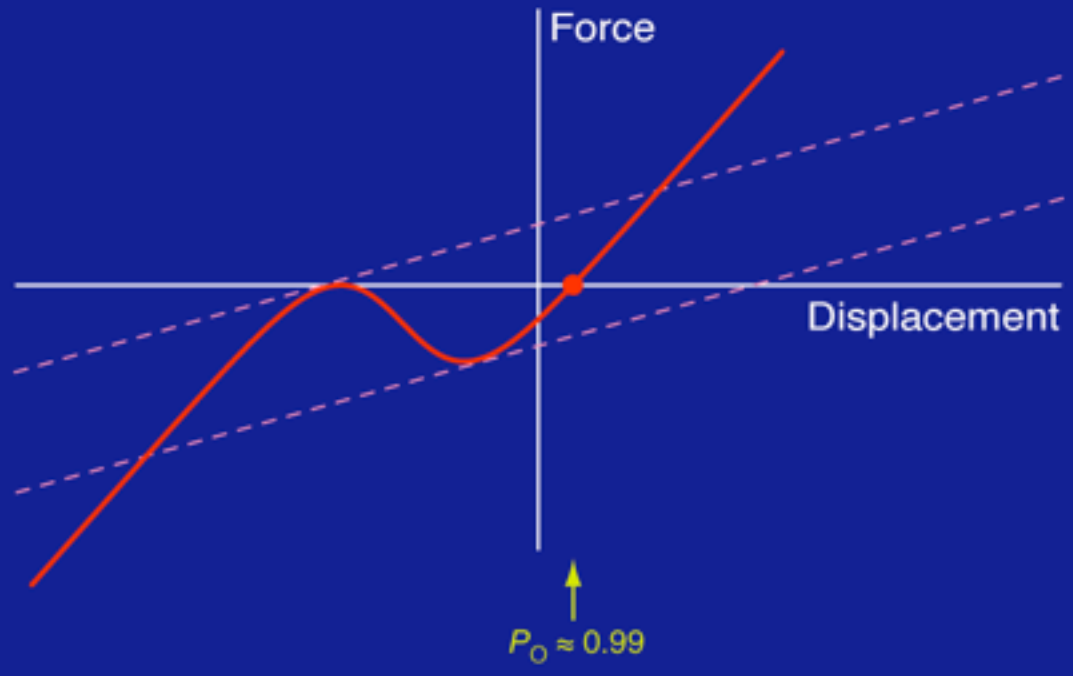
Force
Displacement
$P_O \approx 0.99$

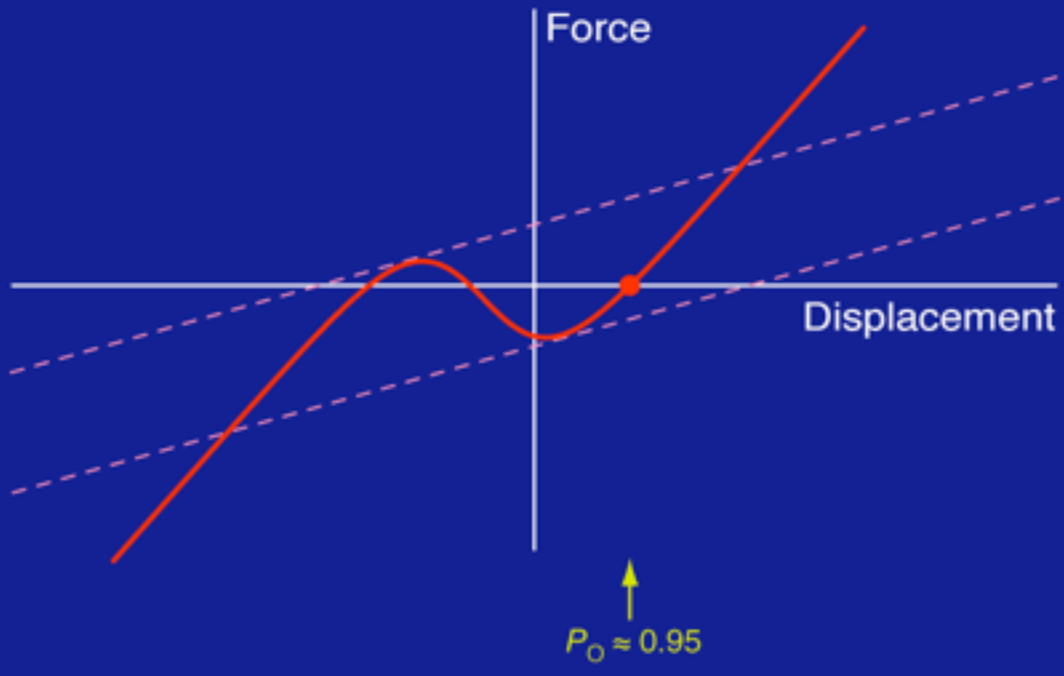
Force
Displacement
$P_O \approx 0.95$

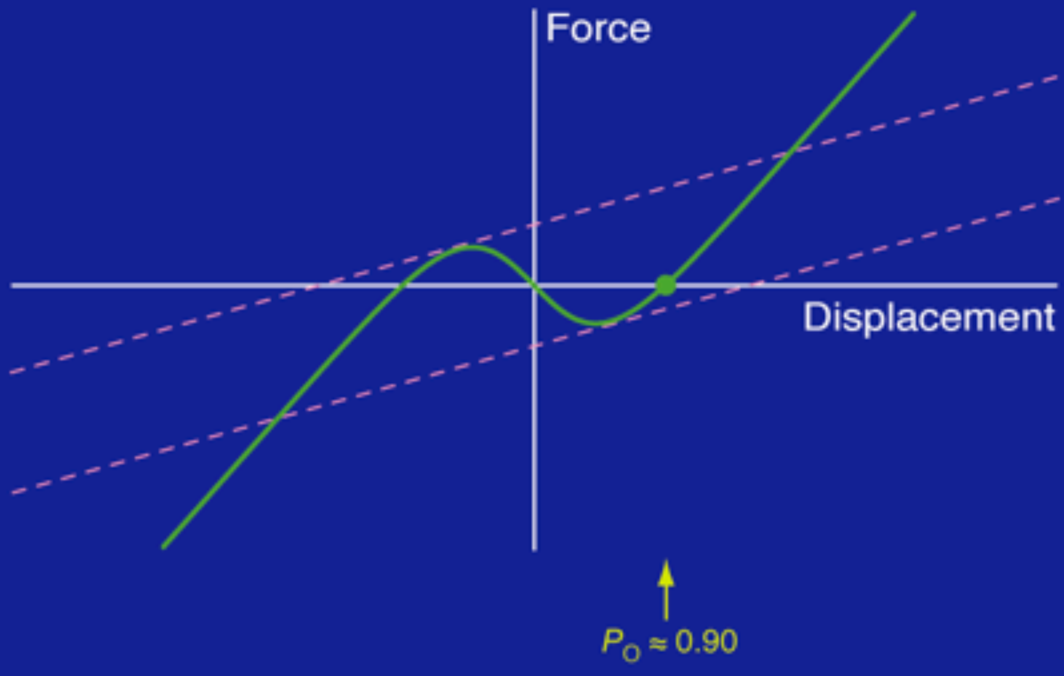
Force
Displacement
$P_O \approx 0.90$

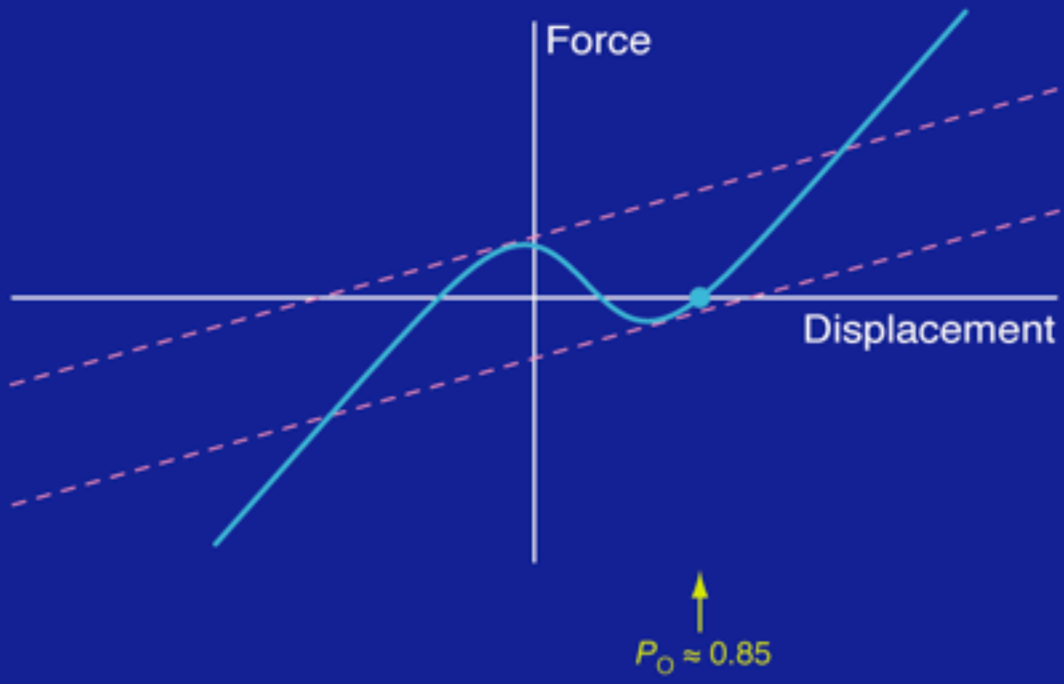
Force
Displacement
$P_O \approx 0.85$

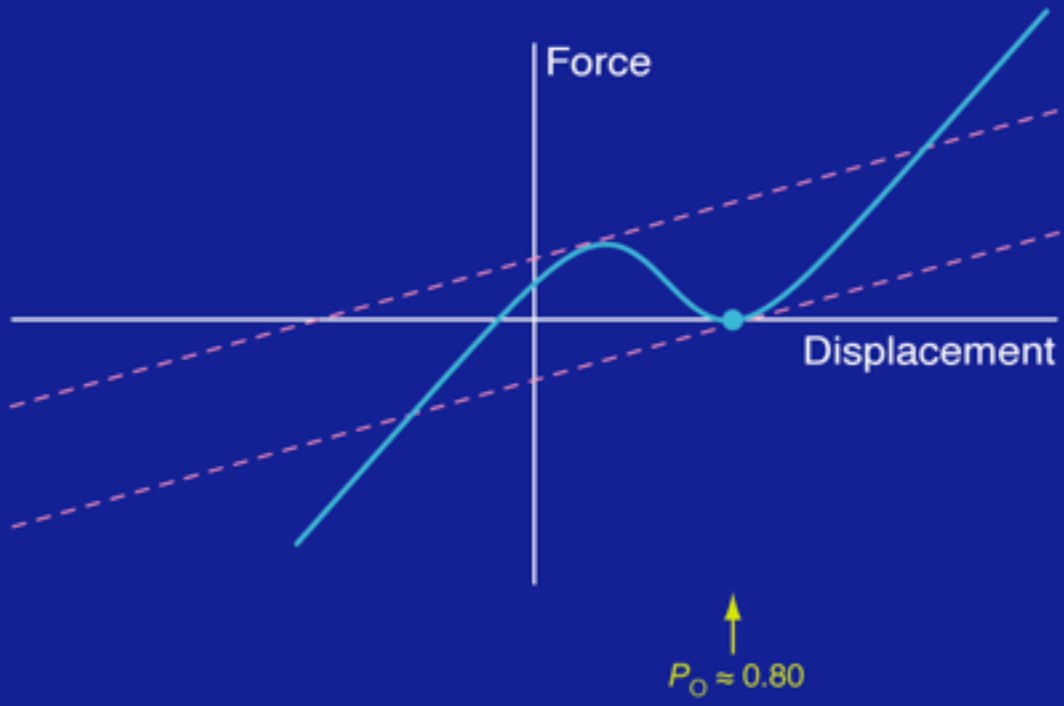

Force
Displacement
$P_O \approx 0.80$

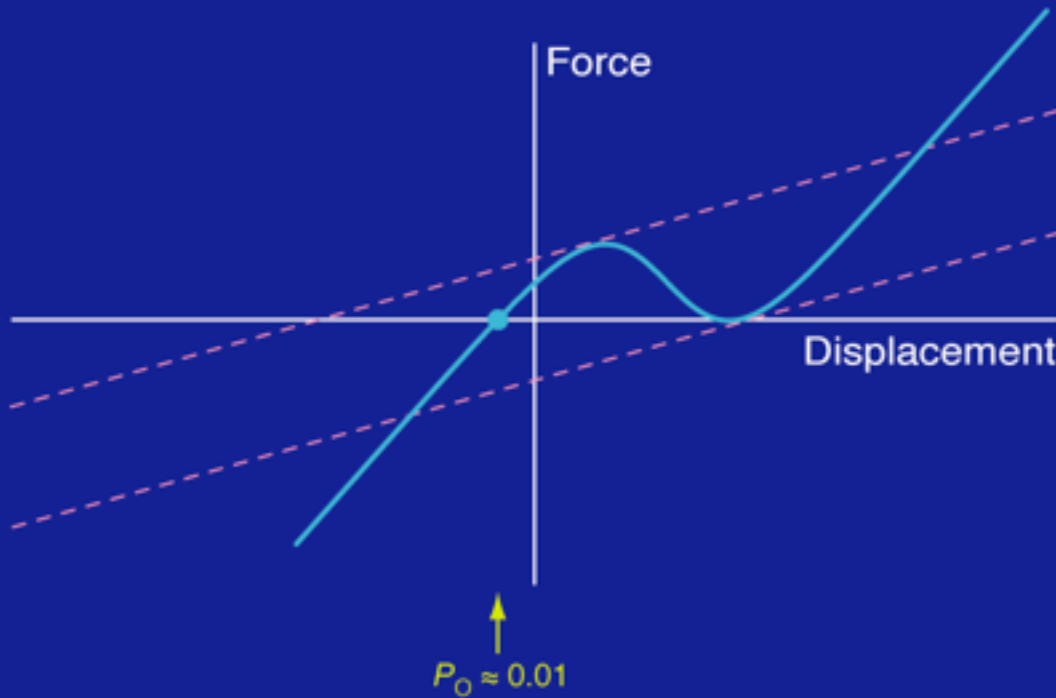
Force
Displacement
$P_O \approx 0.01$

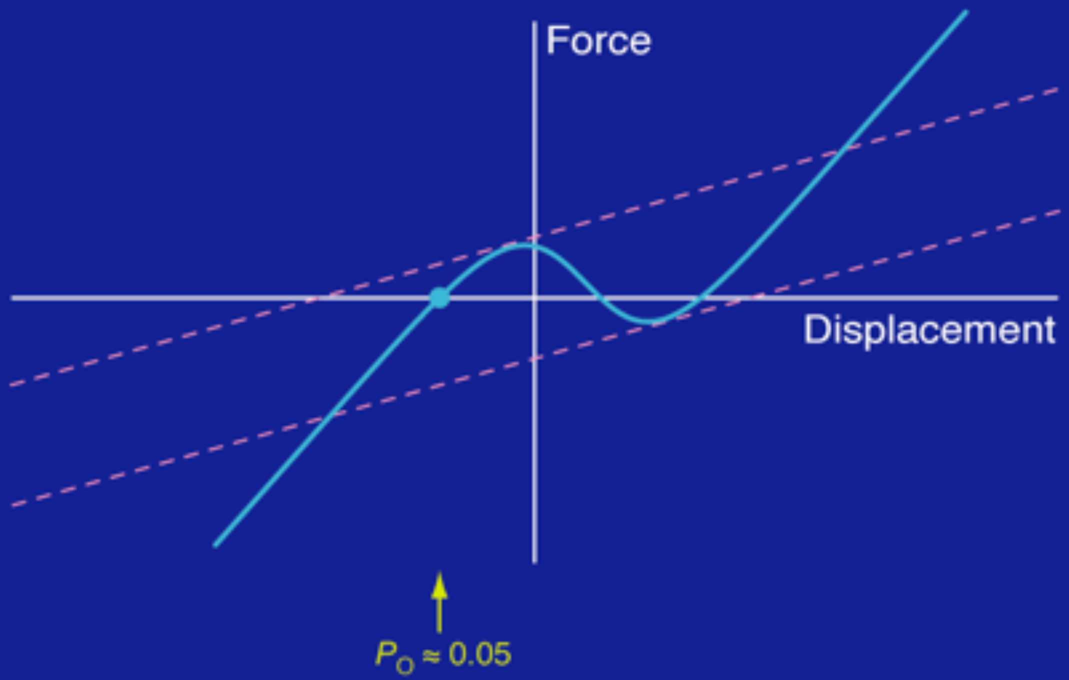
Force
Displacement
$P_O \approx 0.05$

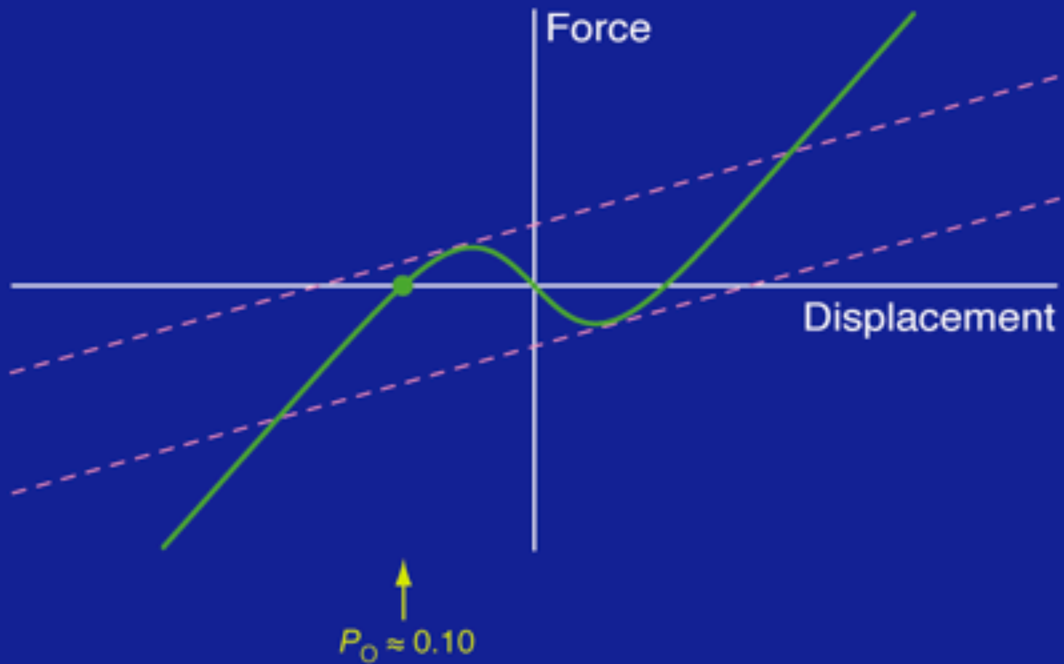
Force
Displacement
$P_O \approx 0.10$

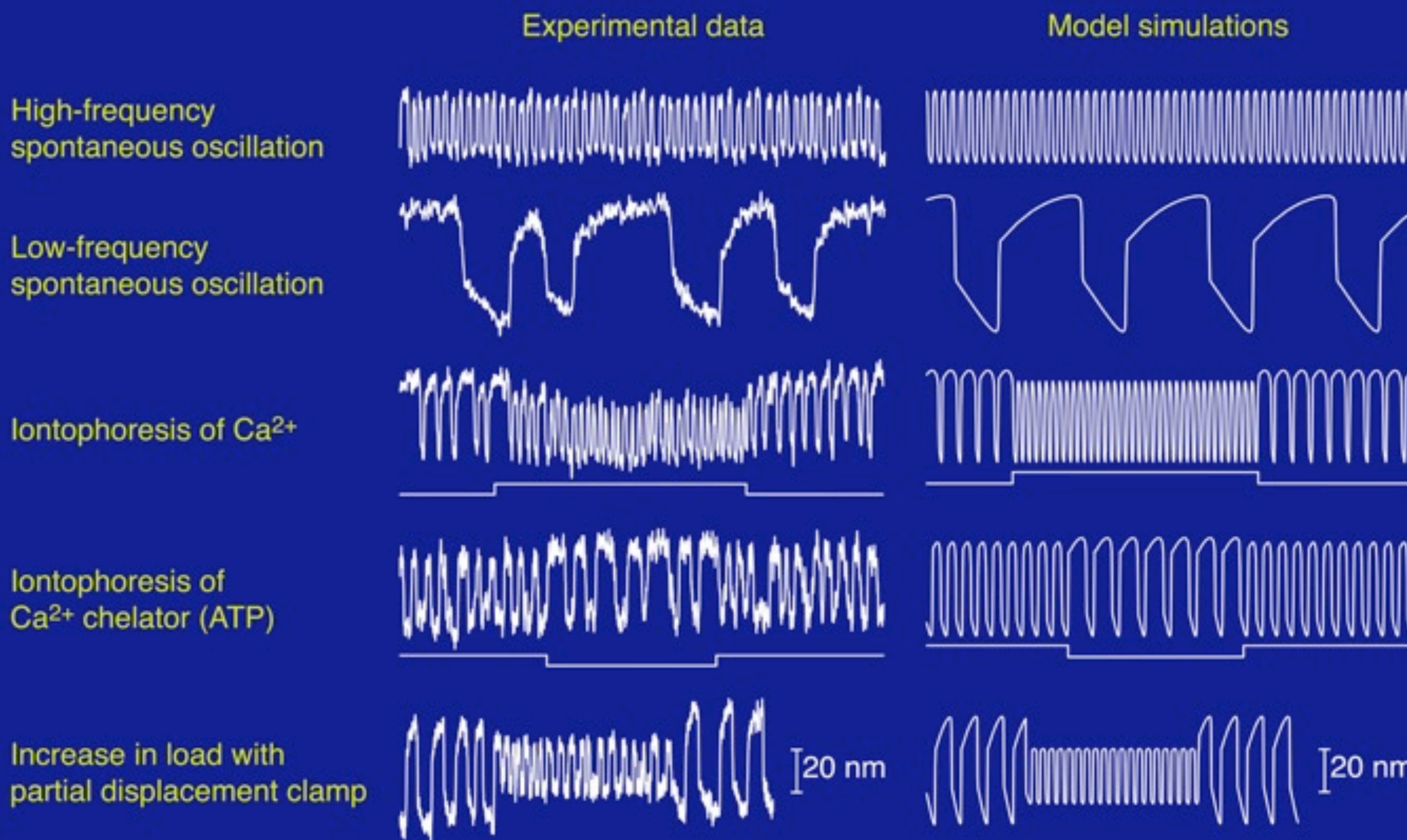
Experimental data
Model simulations
High-frequency spontaneous oscillation
Low-frequency spontaneous oscillation
Iontophoresis of Ca2+
Iontophoresis of Ca2+ chelator (ATP)
Increase in load with partial displacement clamp
20 nm
20 nm

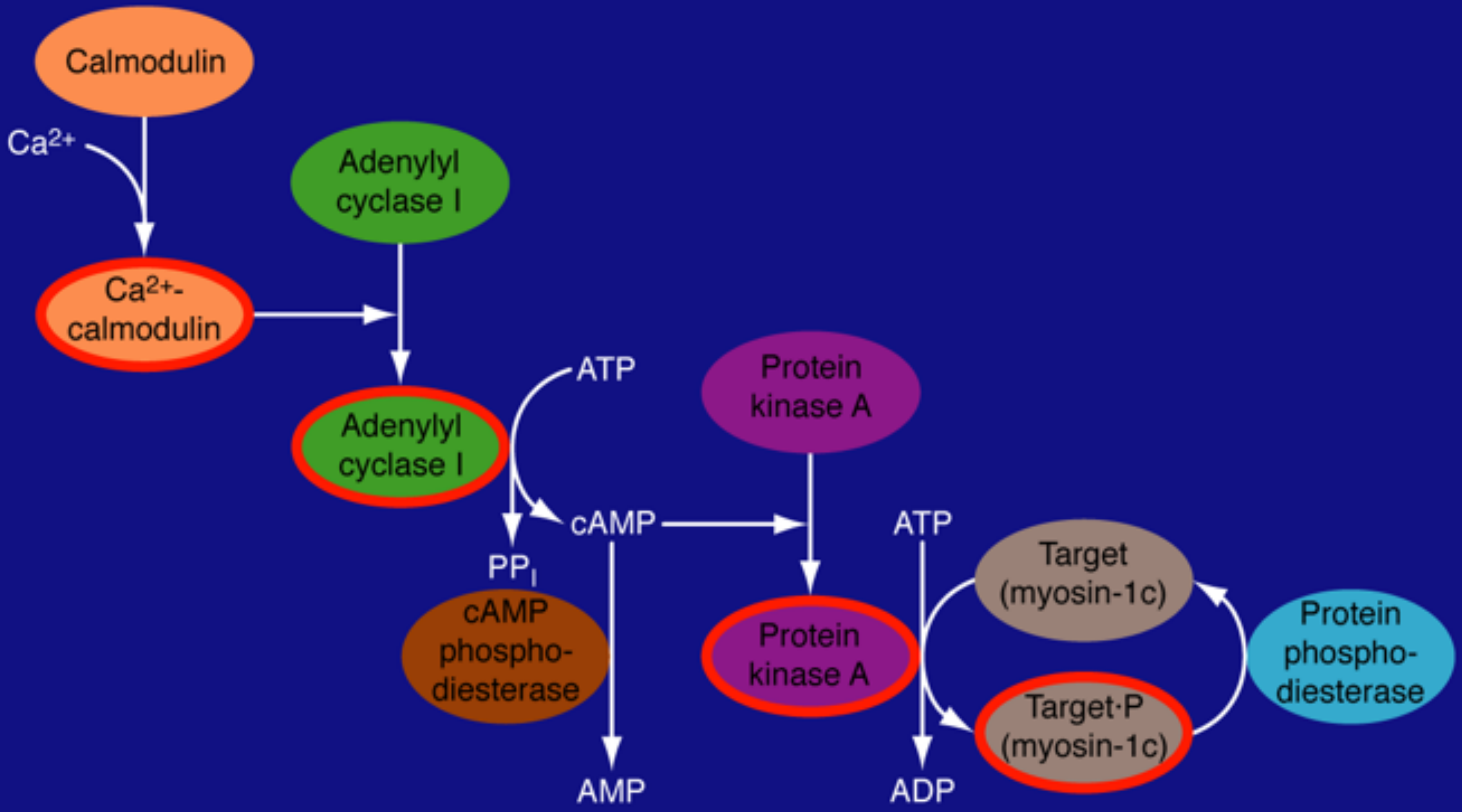

Calmodulin
Ca2+
Ca2+-calmodulin
Adenylyl cyclase I
Adenylyl cyclase I
ATP
PPi
cAMP
cAMP phospho-diesterase
AMP
Protein kinase A
Protein kinase A
ATP
ADP
Target (myosin-1c)
Target·P (myosin-1c)
Protein phospho-diesterase

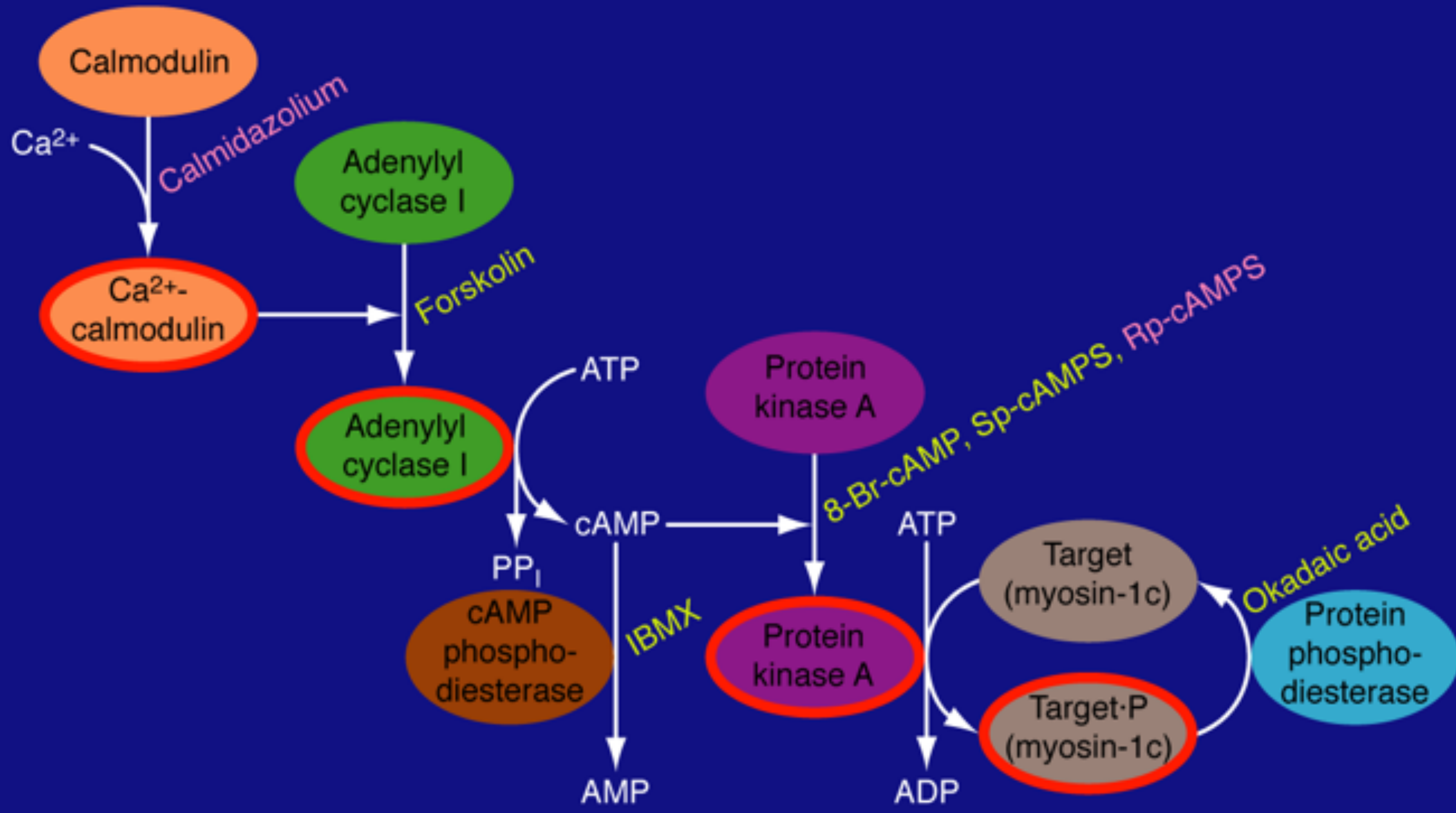
Calmodulin
Ca2+
Calmidazolium
Adenylyl cyclase I
Ca2+-calmodulin
Forskolin
ATP
Adenylyl cyclase I
Protein kinase A
8-Br-cAMP, Sp-cAMPS, Rp-cAMPS
cAMP
PPi
cAMP phospho-diesterase
IBMX
AMP
Protein kinase A
ATP
ADP
Target (myosin-1c)
Okadaic acid
Protein phospho-diesterase
Target·P (myosin-1c)

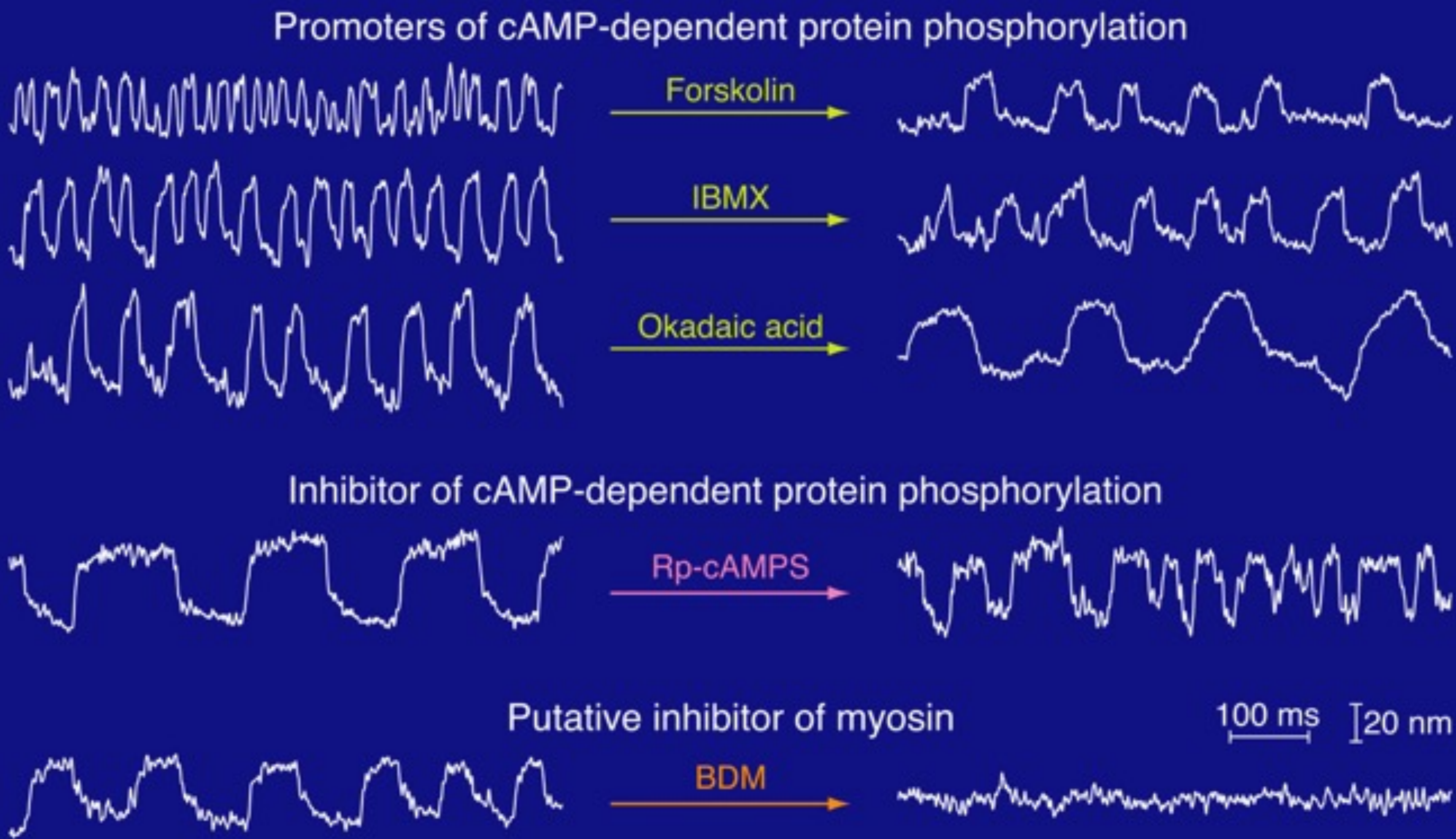

Promoters of cAMP-dependent protein phosphorylation
Forskolin
IBMX
Okadaic acid
Inhibitor of cAMP-dependent protein phosphorylation
Rp-cAMPS
Putative inhibitor of myosin
100 ms
20 nm
BDM

FAST ADAPTATION

(Ca^{2+}–DEPENDENT CHANNEL RECLOSURE)

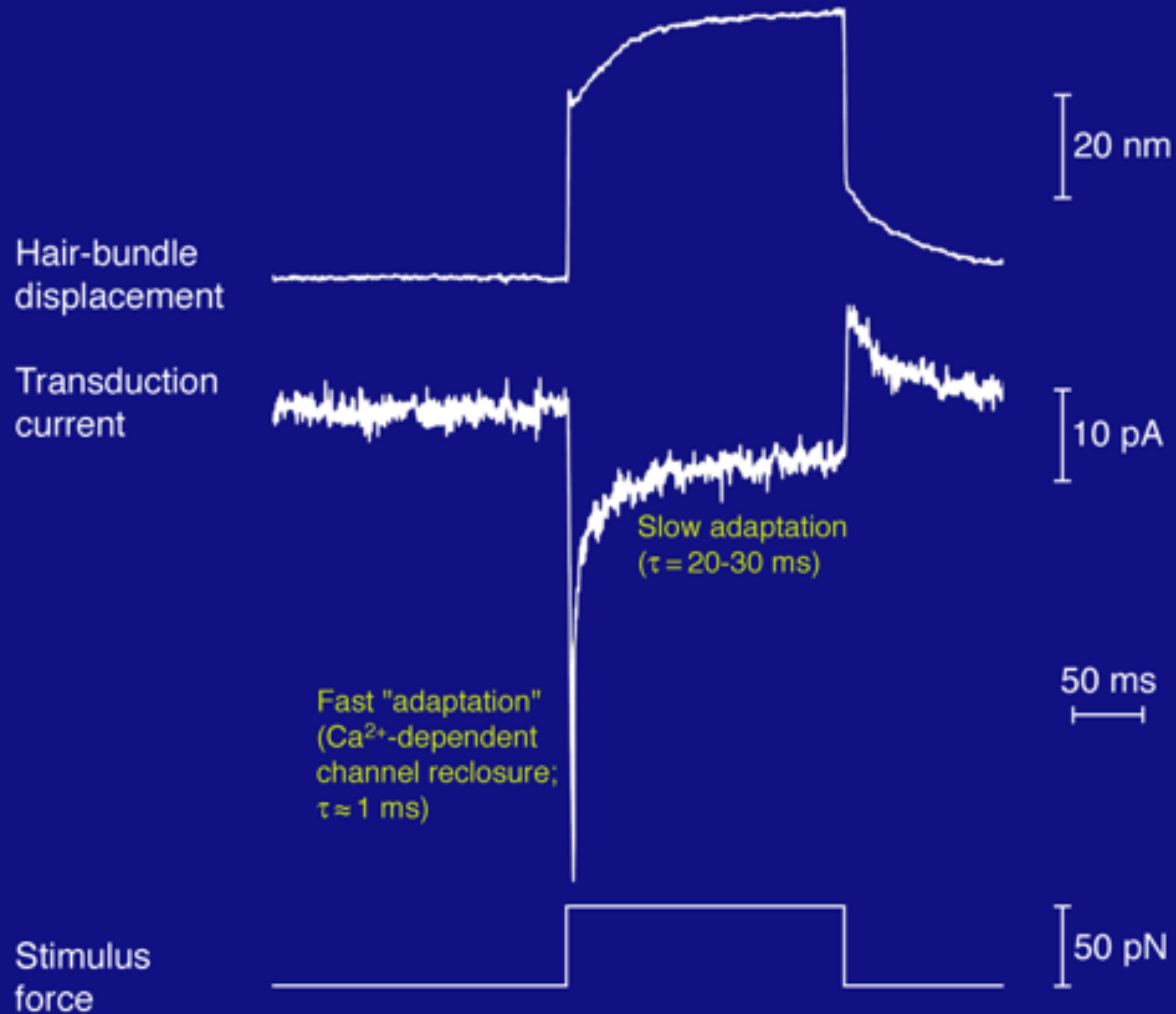

Hair-bundle displacement
Transduction current
Stimulus force
20 nm
10 pA
50 ms
50 pN
Slow adaptation
(τ = 20-30 ms)
Fast "adaptation"
(Ca2+-dependent
channel reclosure;
τ ≈ 1 ms)

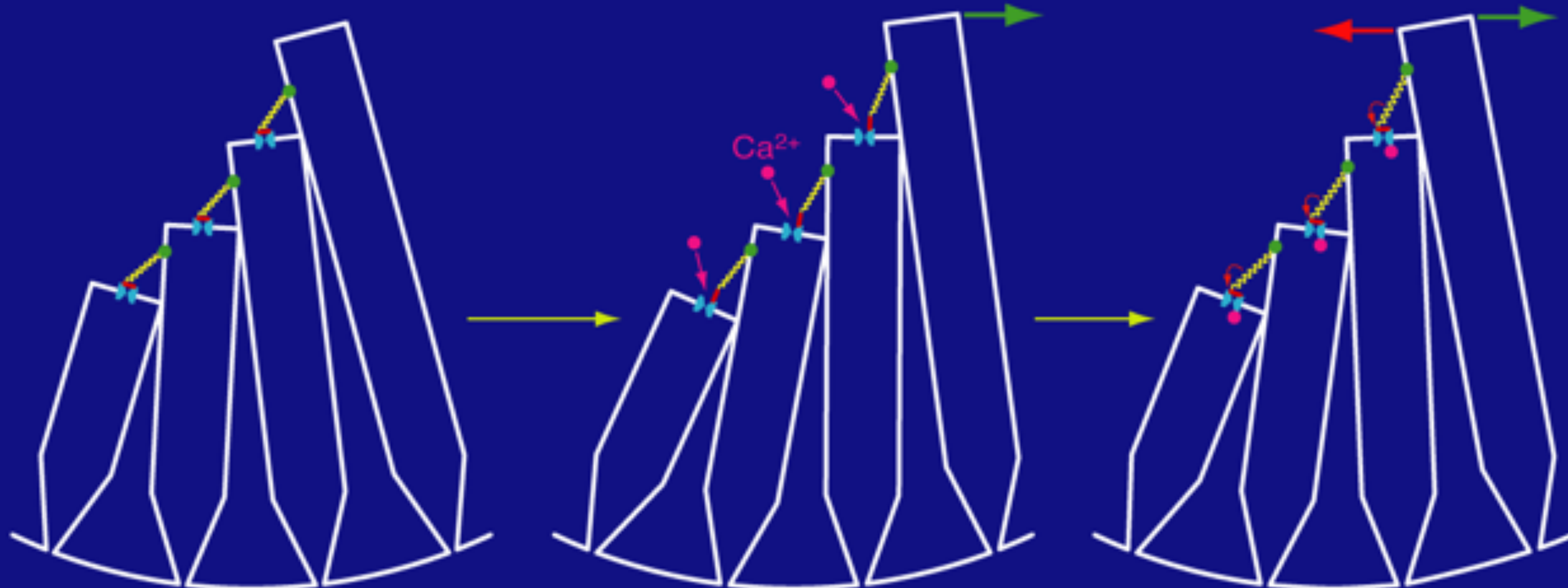
Ca²⁺

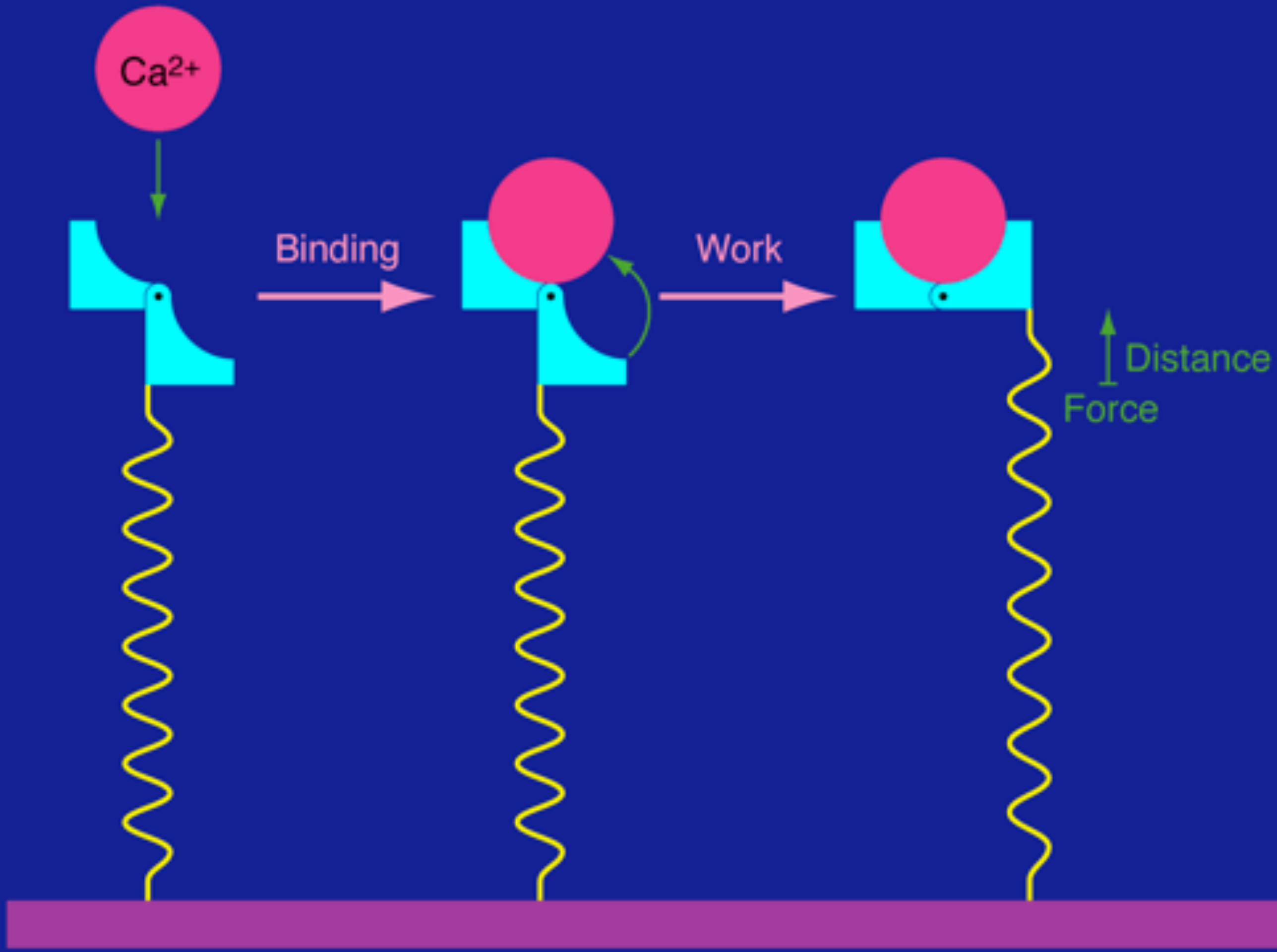

Ca2+
Binding
Work
Distance
Force

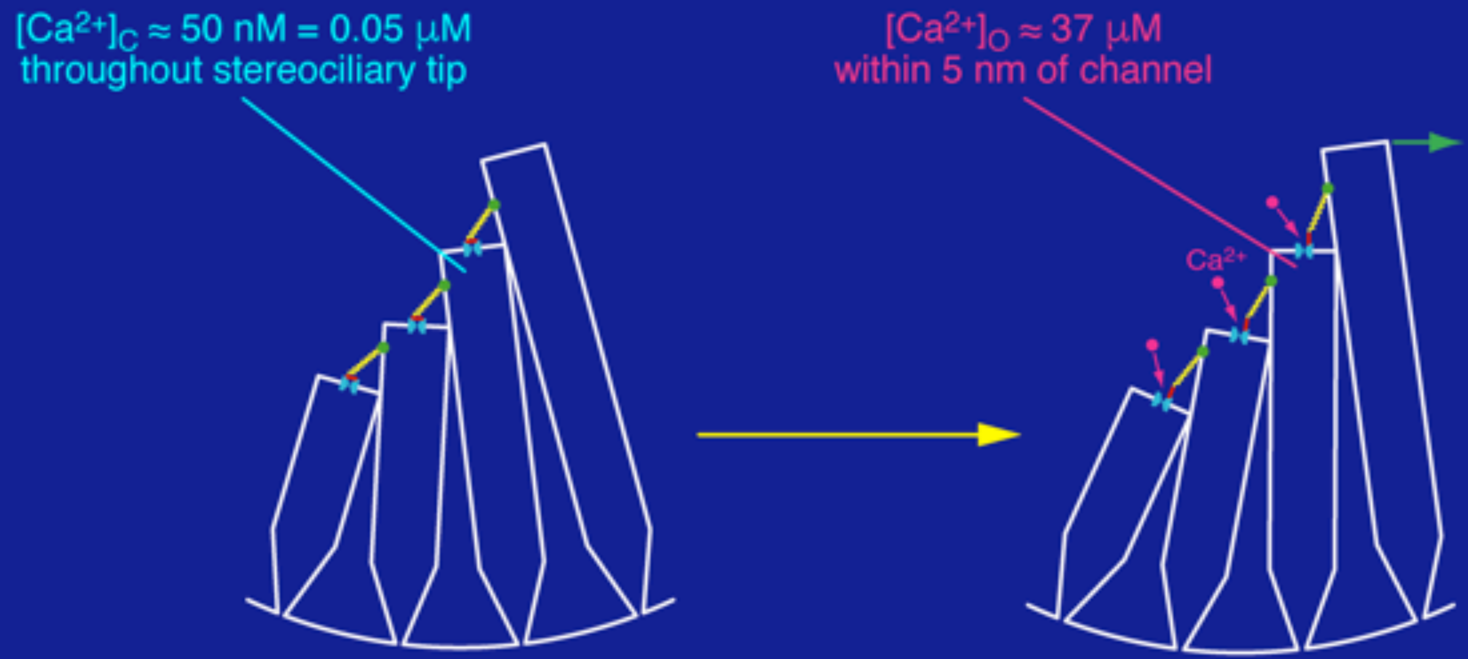

From the change in intracellular Ca^{2+} concentration,

$$\Delta G = kT \cdot \ln\left(\frac{[Ca^{2+}]_O}{[Ca^{2+}]_C}\right) = kT \cdot \ln\left(\frac{37\ \mu M}{0.05\ \mu M}\right) \approx 27\ zJ \approx 7 \cdot kT$$

POSSIBLE SITES OF Ca^{2+} – DEPENDENT CHANNEL RECLOSURE (FAST ADAPTATION)

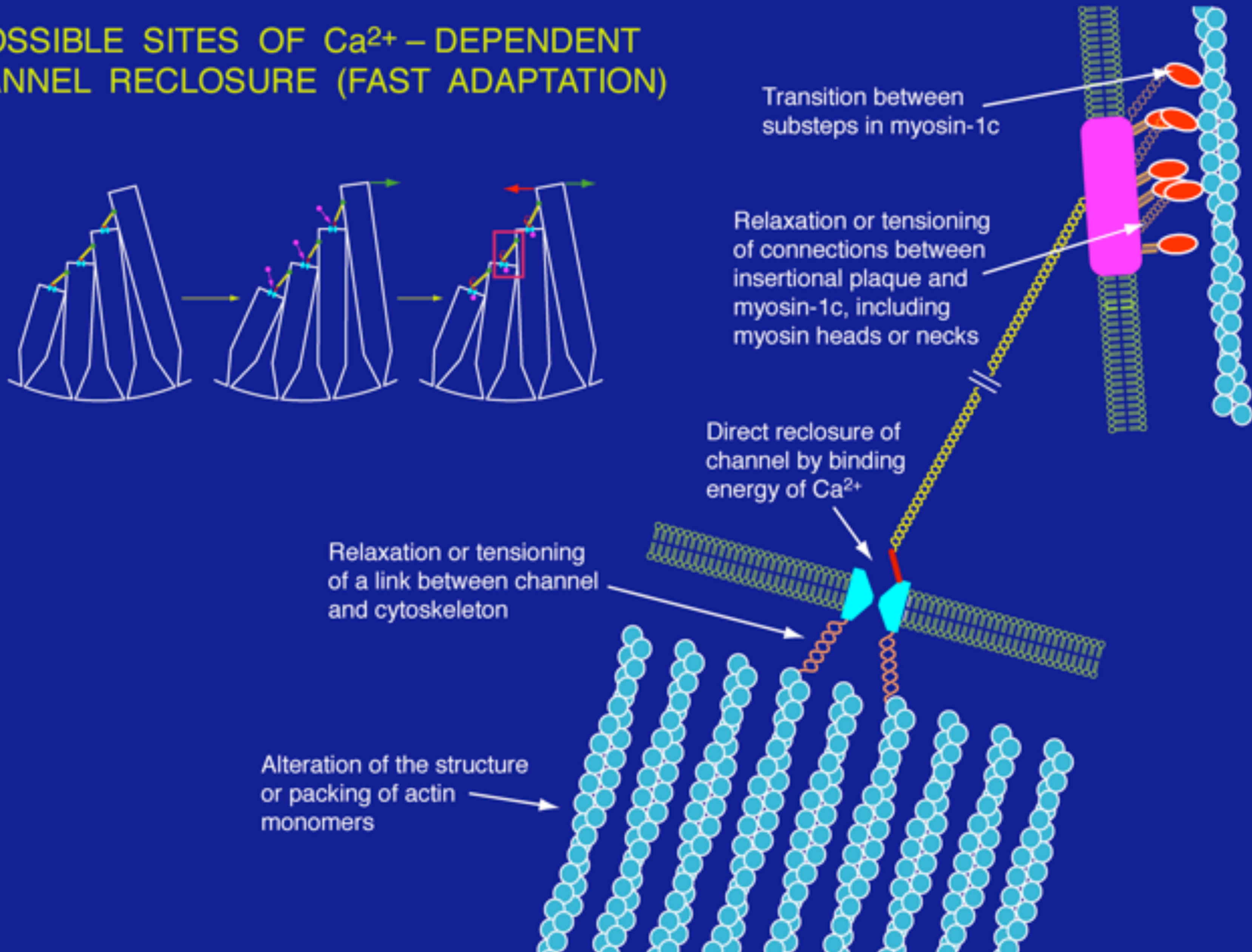

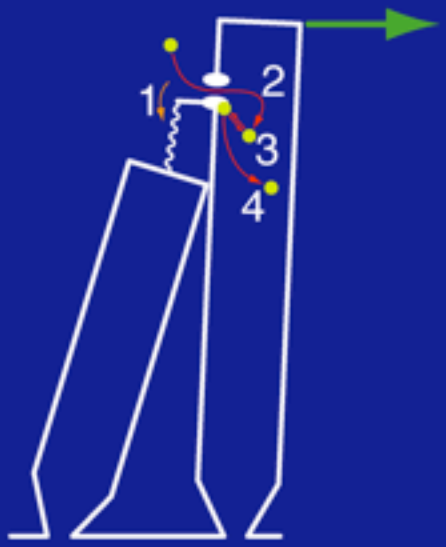

OVERALL RESPONSE

$$f_{CUTOFF} \approx \frac{1}{2\pi\tau_{LIMITING}} \approx 15\ \text{kHz}$$

1. TRANSDUCTION-CHANNEL GATING

(stimulation at ±15 nm or 60 dB SPL, temperature 37 ˚C)

$$\tau \approx \frac{1}{k_{OPENING} + k_{CLOSING}} \approx 10\ \mu s$$

2. Ca^{2+} DIFFUSION TO BINDING SITE

(located 5 nm from channel's pore, –100 pA transduction current)

$$\tau \approx \frac{x^2}{2D} \approx 0.02\ \mu s \quad \text{or} \quad [Ca^{2+}] \approx \frac{-f\gamma(V_M - E_T)}{2\pi zFDr}\,\text{erfc}\frac{r}{\sqrt{4D\tau}},\ \tau \approx 0.05\ \mu s$$

3. Ca^{2+} BINDING TO REGULATORY SITE

(Ca^{2+} concentration of 20 μM, diffusion-limited binding)

$$\tau \approx \frac{1}{k_{BINDING} \cdot [Ca^{2+}]} \approx 10\ \mu s$$

4. Ca^{2+} RELEASE TO REPRIME SYSTEM

(dissociation constant of 20 μM)

$$\tau \approx \frac{1}{k_{UNBINDING}} \approx \frac{1}{k_{BINDING} \cdot K_D} \approx 10\ \mu s$$

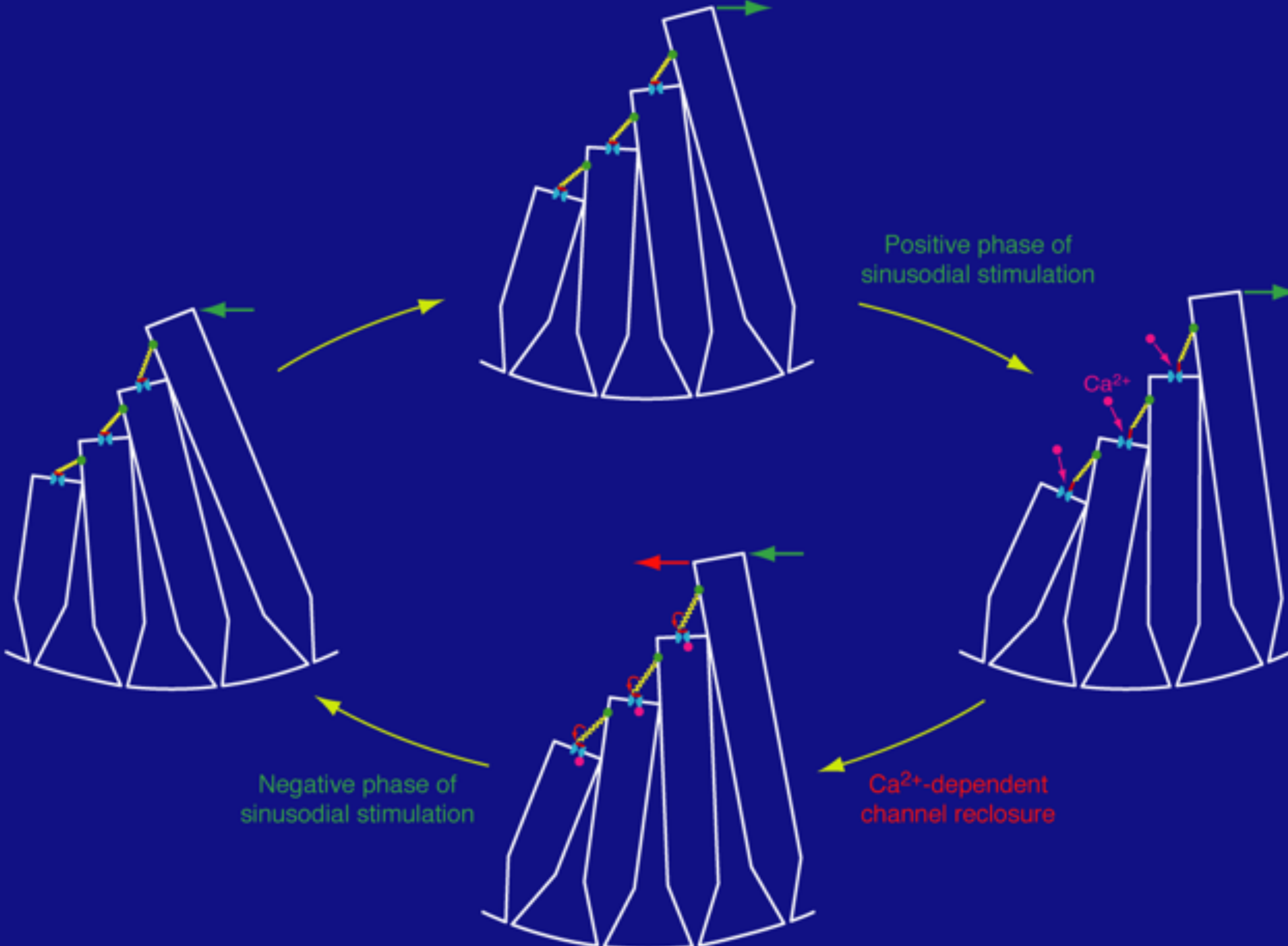
Positive phase of
sinusodial stimulation
Ca2+
Ca2+-dependent
channel reclosure
Negative phase of
sinusodial stimulation

HAIR – BUNDLE STIMULATION BY ULTRAVIOLET LIGHT

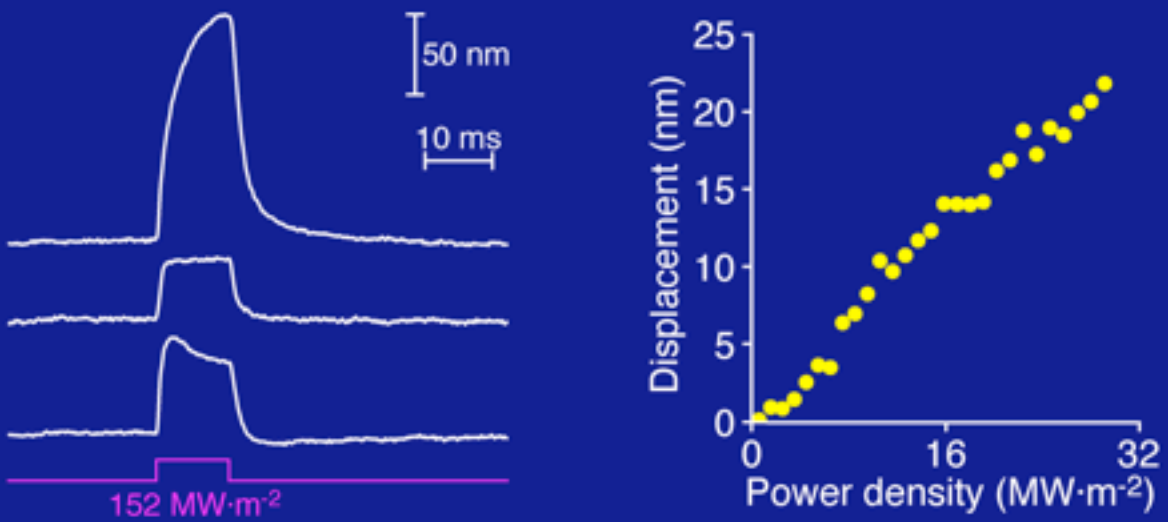

ADAPTATION OF RESPONSE TO ULTRAVIOLET LIGHT

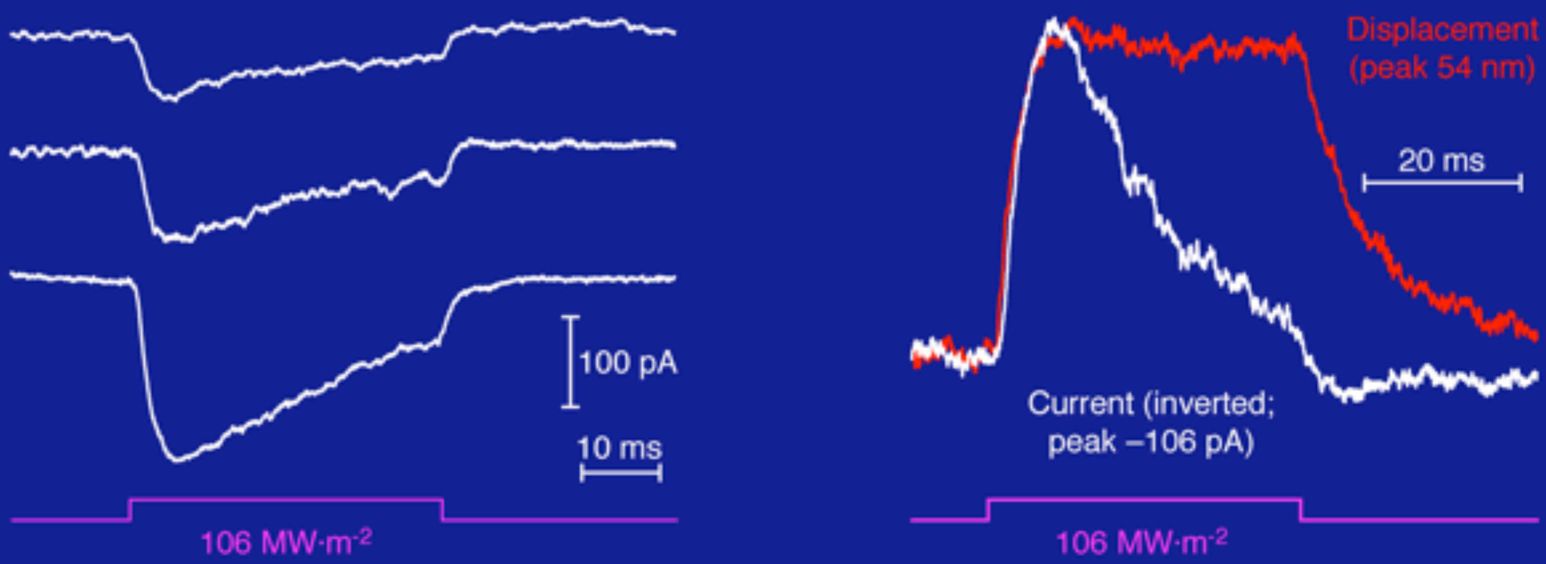

ULTRAVIOLET – *VERSUS* INFRARED – LIGHT STIMULATION